SILICA MONOLAYER SOLID ACID CATALYST PREPARED BY CHEMICAL VAPOR DEPOSITION METHOD

（化学蒸着法で調製したシリカモノレイヤー固体酸触媒）

NAONOBU KATADA

①

SILICA MONOLAYER SOLID ACID CATALYST PREPARED BY CHEMICAL VAPOR DEPOSITION METHOD

NAONOBU KATADA

Preface

This thesis presents the studies on **silica monolayer solid acid catalyst prepared by chemical vapor deposition method**. The studies have been carried out under the direction of Professor Yuichi Murakami at Department of Synthetic Chemistry, School of Engineering, Nagoya University during 1987 - 1990, and have been continued under the suggestion of Professor Miki Niwa at Department of Materials Science, Faculty of Engineering, Tottori University during 1992 - 1995.

Preparation, mechanism of formation, structure, functions, origin of functions and applications of the silica monolayer catalysts loaded on several metal oxides are investigated, and related with each other to lead a complete understanding of these novel materials. These investigations also give information about generation of catalytic functions generally observed on combined oxide, which has recently become important to protect the global environment.

The author wishes to express his faithful gratitude to Honorary Professor Yuichi Murakami for his helpful suggestions, fruitful discussion and continual encouragement. The author would like to make a grateful acknowledgment to Professor Miki Niwa in Tottori University for his profound interest, constructive suggestions and helpful encouragement throughout the studies. The author also would like to express his sincere gratefulness to Professor Tadashi Hattori for his careful advice, fruitful suggestions and kind helpfulness to write up this thesis. A grateful acknowledgment is made to Associate Professor Jong-Ho Kim in Tottori University for his instructive advice and cooperation.

The author extends his faithful gratefulness to Professor Yusuke Izumi for his fruitful advice especially for understanding the principle of acid-base chemistry. The author also expresses his grateful acknowledgment for Professor Kosuke Shobatake for the kind comments from the view point of physical chemists. Faithful thanks are also expressed for Associate Professor Kazuo Urabe and Assistant Professor Atsushi Satsuma for their constructive discussion and helpful suggestions.

The author wishes to make an acknowledgment to Associate Professor Mitsuru Sano in School of Informatics, Nagoya University for his kind cooperation and advice on the EXAFS study.

The author sincerely thanks Dr. Takashi Hibino and Mr. Takahiro Tsubouchi for their collaboration in Nagoya University. Grateful thanks are also due to Mr. Koh-ichi Muto, Mr. Takuya Toyama, Mr. Jun-ichi Nagahiro, Mr. Yasushi Hibino, Mr. Hideaki Ishiguro and Mr. Hitoshi Fukui for their collaboration in Tottori University. The author extends a grateful acknowledgment to Mr. Shin-ichi Komai for his kind helpfulness in Nagoya University. The author wishes to express his

gratefulness to Dr. Korandla Ramesh Reddy and Mr. Nobuaki Kodakari for their hearty cooperation in Tottori University.

An acknowledgment is made to Mr. Toshimi Sawano, Mr. Shunkichi Adachi, Mr. Hiroshi Yoshida, Dr. Michio Ueshima and Mr. Yoshinori Sano in Nippon Shokubai Company Limited for their deep understanding and cooperation to measure the NMR spectra. The author also extends a gratefulness to Dr. Shin-ichi Nakata in Chiyoda Corporation for his kind advice on the NMR experiments.

The author thanks all the members in the Laboratory of Professor Murakami and the Laboratory of Professor Niwa for their valuable cooperation. The author wishes to express an acknowledgment to his wife and parents for their supports and understandings without which this work would not have been possible.

Finally, the author wishes to express his special thanks to Professor Tadashi Hattori, Professor Yusuke Izumi, Professor Kosuke Shobatake, Associate Professor Kazuo Urabe and Assistant Professor Atsushi Satsuma for serving on his dissertation committee.

Tottori
November 1995

Naonobu Katada

Contents

Chapter 1. General Introduction

Combined Oxide Solid-Acid Catalyst

Acidic materials show various catalytic activities, and can be applied to various practical reactions. Such liquid acids as sulfuric acid, called as homogeneous acid catalysts, are used for a number of industrial processes. Many kinds of solids are also known to show the acidities and catalytic activities, and are called as heterogeneous acid catalysts or solid-acid catalysts[1]. Tanabe classified the solid-acids in 1981 as shown in Table 1 - 1[2], and various synthetic zeolites, related micro-

Table 1 - 1 : Various solid-acid catalysts listed by Tanabe[2].

1. Natural clay minerals: Kaolinite, bentonite, attapulgite, montmorillonite, clarit, fuller's earth, zeolites
2. Mounted acids: H_2SO_4, H_3PO_4, $CH_2(COOH)_2$ mounted on silica, quartz sand, alumina or diatomaceous earth
3. Cation exchange resins
4. Charcoal heat-treated at 300 °C
5. Metal oxides and sulfides: ZnO, CdO, Al_2O_3, CeO_2, ThO_2, TiO_2, ZrO_2, SnO_2, PbO, As_2O_3, Bi_2O_3, Sb_2O_5, V_2O_5, Cr_2O_3, MoO_3, WO_3, CdS, ZnS
6. Metal salts: $MgSO_4$, $CaSO_4$, $SrSO_4$, $BaSO_4$, $CuSO_4$, $ZnSO_4$, $CdSO_4$, $Al_2(SO_4)_3$, $FeSO_4$, $Fe_2(SO_4)_3$, $CoSO_4$, $NiSO_4$, $Cr_2(SO_4)_3$, $KHSO_4$, K_2SO_4, $(NH_4)_2SO_4$, $Zn(NO_3)_2$, $Ca(NO_3)_2$, $Bi(NO_3)_3$, $Fe(NO_3)_3$, $CaCO_3$, BPO_4, $AlPO_4$, $CrPO_4$, $FePO_4$, $Cu_3(PO_4)_2$, $Zn_3(PO_4)_2$, $Mg_3(PO_4)_2$, $Ti_3(PO_4)_4$, $Zr_3(PO_4)_4$, $Ni_3(PO_4)_2$, AgCl, CuCl, $CaCl_2$, $AlCl_3$, $TiCl_3$, $SnCl_2$, CaF_2, BaF_2, $AgClO_4$, $Mg_2(ClO_4)_2$
7. Mixed oxides: SiO_2-Al_2O_3, SiO_2-TiO_2, SiO_2-SnO_2, SiO_2-ZrO_2, SiO_2-BeO, SiO_2-MgO, SiO_2-CaO, SiO_2-SrO, SiO_2-ZnO, SiO_2-Ga_2O_3, SiO_2-Y_2O_3, SiO_2-La_2O_3, SiO_2-MoO_3, SiO_2-WO_3, SiO_2-V_2O_5, SiO_2-ThO_2, Al_2O_3-MgO, Al_2O_3-ZnO, Al_2O_3-CdO, Al_2O_3-B_2O_3, Al_2O_3-ThO_2, Al_2O_3-ZrO_2, Al_2O_3-V_2O_5, Al_2O_3-MoO_3, Al_2O_3-WO_3, Al_2O_3-Cr_2O_3, Al_2O_3-Mn_2O_3, Al_2O_3-Fe_2O_3, Al_2O_3-Co_3O_4, Al_2O_3-NiO, TiO_2-CuO, TiO_2-MgO, TiO_2-ZnO, TiO_2-CdO, TiO_2-ZrO_2, TiO_2-SnO_2, TiO_2-Bi_2O_3, TiO_2-Sb_2O_5, TiO_2-V_2O_5, TiO_2-Cr_2O_3, TiO_2-MoO_3, TiO_2-WO_3, TiO_2-Mn_2O_3, TiO_2-Fe_2O_3, TiO_2-Co_3O_4, TiO_2-NiO, ZrO_2-CdO, ZnO-MgO, ZnO-Fe_2O_3, MoO_3-CoO-Al_2O_3, MoO_3-NiO-Al_2O_3, TiO_2-SiO_2-MgO, MoO_3-Al_2O_3-MgO

porous materials and heteropolyacids were added as new categories of solid-acids during the last 15 years[3]. The properties of solids, particularly those of clay minerals, zeolites, metal oxides and mixed oxides, give some advantages to these solid-acid catalysts[2]. These solids are generally durable at high temperatures compare to liquids, which makes possible to use solid-acids at high temperatures, resulting in a high reaction rate. And other advantages of these solid-acids to protect the environment and to save the resources are as follows:

1) Solid-acid causes no corrosion of chemical plant;

2) Repeated use of solid-acid is possible, while the used liquid-acid is usually disposed as a salt after the reaction;

3) Separation of solid-acid from liquid or gaseous products is easy and economically beneficial, while the liquid-acid usually requires the neutralization with a strong base to separate from the reaction mixture, resulting in the disposal of waste salt;

4) No or less problems are caused when solid acid is disposed, while the disposal of liquid acid usually requires special treatment to make it safety.

Because of these advantages, the solid-acids are widely used for the industrial reactions in the present time. Such petrochemical reactions as the cracking, reforming, isomerization of paraffins and olefins, and alkylation and dealkylation of aromatics are important for the effective use of natural feed-stocks of hydrocarbons. These reactions have been carried out by using the solid-acids, mainly on Brønsted acidic catalysts such as silica-alumina. This catalyst has been used for more than 30 years, and the improvements are still being made[4]. On the other hand, the addition, substitution and elimination of functional groups, *e.g.* the hydration, dehydration and amination are useful reactions in organic syntheses. The applications of solid-acids to organic syntheses especially using zeolites are remarkably being developed as listed by Hölderich (Table 1 - 2)[5]. Moreover, the advantages to protect the environment shown above are being recognized to be more important, because the destruction of global environmental becomes the most serious problem of human society in the present time. Therefore, the applications of solid-acid catalysts will be anticipated to further fields of chemical industry[6]. From this view point, creation of novel solid-acid catalysts is still now being made, and is considered to become more important in the near future.

Among the mixed oxide catalysts, or among all of the solid catalysts, the natural or synthetic silica-alumina is one of the most popular ones and has been widely utilized for many years. Silica is also known to create acidities, especially useful Brønsted acidities in most cases, when it was combined with various kinds of oxides; 16 kinds of oxides were listed to create the acidity by the

Table 1 - 2 : Recent developments in reactions catalyzed by solid-acids listed by Hölderich[5].

Reaction	Catalyst	Reference
2,5-Dimethyl-*2,4*-hexadiene from isobutene and isobutyraldehyde	Nb_2O_5	7
Di- and monomethylamine from ammonia and methanol	Modified mordenite	8
Production of *m*-chlorotoluene, *m*-dichlorobenzene and *2,6*-dichlorotoluene	H-ZSM5	9
Pyridine from acetaldehyde, formaldhyde and ammonia	H-ZSM5	10
Methyl-*tert*-butylether (MTBE) from isobutene and methanol	Boron-pentasil zeolite	11
Skeletal rearrangement from tetrahydrodicyclopentadinene into adamantane	Pt / Y-zeolite	12
tert-Butylamine from ammonia and isobutene	Metalosilicates	13
Beckmann rearrangement of cyclohexanone oxime into ε-caprolactam	SAPO-11 and 41	14
Formation of enol ethers from acetals	Na-ZSM5	15
Conversion of acetal	Precipitated metal phosphates	16
Alkylation of benzene and acylation of *p*-xylene by benzylchloride	Heteropolyacid supported on silica	17
Fredel-Crafts reactions	Cesium salt of heteropolyacid	18
Beckmann rearrangement	Pt doped super acids	19

combination with silica in Table 1 - 1[2] (shown by under lines).

The silica-based combined oxide usually forms an amorphous phase, and therefore the structure is unclear. The acidic properties, *i.e.* the acid amount (number or surface concentration of acid sites), acid strength and identification between Brønsted (proton donor) and Lewis (electron acceptor) acidity, are significantly changed by the composition and preparation technique. The amorphous combined oxide usually has a wide distribution of acid strength, and / or both of Lewis and Brønsted acid sites. Since the acid sites are created by the combination of oxides, the acidity is presumably generated where the interface between the two components of the combined oxide catalyst appears

on the surface. Therefore, the complex acidic property of combined oxide catalysts are presumably due to the heterogeneous structure of interface. Although it must be important to understand the principle of generation of acidity to design a novel catalyst, even the exact structure of acid site on the amorphous mixed oxide is hardly analyzed.

Since Hansford proposed the mechanism of generation of acidity on silica-alumina in 1947[20], the structure of acid site and the mechanism of generation of acidity on silica-alumina were proposed by a number of researchers[2, 21 - 33]. Some of these are important, because common rules were proposed for the generation of acidities on combined oxide catalysts. Thomas explained that Brønsted acid site was the proton which was generated by the isomorphous substitution of metal cations into the matrix of another oxide[22]. Tanabe extended this explanation to apply to various kinds of mixed solid-acids, including those generated Lewis acidity[2].

According to Tanabe's hypothesis, the acidity generation is caused by an excess of a negative or positive charge in a model structure of binary oxide. The model structure is pictured according to the following two postulates: 1) coordination numbers of the cations of both the major and minor metal oxides are maintained by mixing; 2) the coordination numbers of all oxygen anions are determined by that of the major component. For example, the models of TiO_2-SiO_2 is shown in Figure 1 - 1. In the case of a), the four positive charges of a silicon atom are distributed to four bonds, *i.e.* one positive charge is distributed to each one bond. Two negative charges of an oxygen atom are distributed to three bonds, *i.e.* -2/3 of a valence unit is distributed to each bond. The difference in charge for one bond of Si-O is hence +1-2/3 = +1/3, and for all the four bonds the valence unit of +4/3 is excess. In this case, a Lewis base is supposed to bond with the

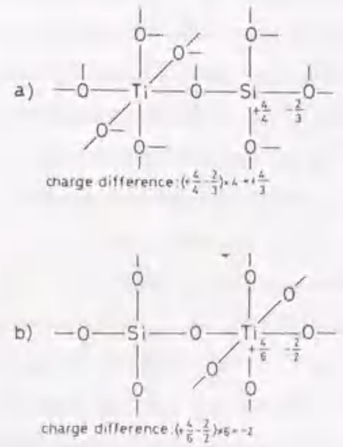

Figure 1 - 1 : Model structures of TiO_2-SiO_2 pictured according to the hypothesis by Tanabe[2]. a) shows the structure when TiO_2 is the major component, and b) shows that when SiO_2 is the major component.

site possessing this positive charge to neutralize it. Such a site is so-called the Lewis acid site. In the case of b), four positive charges are distributed to six bonds of a titanium atom. Two negative charges of an oxygen atom are distributed to two bonds, resulting in -1/3 of the charge difference for each Ti-O bond and the valence unit of -2 is excess for all the six bonds. These negative charges can be neutralized by a proton, which is predicted to possess a Brønsted acidity.

Later, the explanations were also made by quantnum chemical calculations[34-36] accompanying with the development of computer technology. However, it seems difficult to confirm these explanations directly because in practical the combined oxide catalysts usually have the heterogeneous structures.

In order to overcome such a difficulty, a crystal compound consisting of the two components with a homogeneous bulk structure is generally used as a model for a complicated binary material. As this type of model materials, good compounds can be obtained for the mixed solid-acid catalysts; proton-form zeolites and some of clay minerals, which consist of silica and alumina, are regarded as models of silica-alumina; metallosilicates are also regarded as models for other silica-based catalysts. The uniformity in the structure and acidic property on these compounds gave simple relationships between them. On the zeolites, a strong Brønsted acidity was observed. The number of acid site was proven to be same to the number of aluminum[37]. This indicates the stoichiometric generation of acidic proton by the isomorphous substitution of aluminum into the silica matrix as proposed for the amorphous silica-alumina by Thomas[22]. The acid strength had a narrow distribution, and the averaged strength was changed by the crystal phase of zeolite; the acid strength was determined only by the crystal structure, but not by the number of aluminum cations[38]. This indicates that the micro structure, *i.e.* arrangement of cations and anions, and bond length and angle, controls the acid strength. Moreover, the theoretical calculations and spectroscopic studies are making clear of the origin of acid sites with the uniform structures in very recent years[39].

On the other hand, the amorphous silica-alumina has a wide distribution of acid strength, which includes quite weak acid sites, and / or both of Lewis and Brønsted acid sites. According to the fact that the micro structure controls the acid strength, the variety in the acidic property on the amorphous mixed oxide is considered to be due to the heterogeneous structure. Various model compounds other than zeolite can be proposed, and these are promising to show novel catalytic properties.

As well as the crystal compounds like zeolites, a surface thin layer with a uniform structure of one component loaded on another component is often used as a model to understand the catalytic

or other function generated on a binary material. In the case of the mixed oxide solid-acid catalyst, the advantages to use such a model are as follows: 1) since all the loaded oxide locates on the surface, the surface concentration can be determined, and a simple model of structure can be speculated in the atomic-order scale; 2) thus speculated structure will directly become the model of interface, namely the active site; 3) because all the loaded component attaches to both of the surface and interface, both of such a surface characterization as test reaction and such a bulk characterization as NMR (nuclear magnetic resonance) will directly show the property of active site. For the model of silica-based combined oxide catalysts, a thin silica layer (Figure 1 - 2) is thus promising. The thickness has to be ultra thin, because the catalytic activity must be generated on the species with a nanometric size. Standing on these view points, the author anticipated to prepare a surface ultra thin layer of silica on alumina, titania and zirconia, with which silica is known to form the combined solid-acid.

The obtained compound will be a model for one type of acid site on the combined oxide with various types of acid sites. Of course, no model with a simple structure can independently clarify the mechanisms for generation of all the acid sites; one simple model may show an origin of one type of acid site. After similar attempts will be made, various models will lead understanding the general rule for generation of acidity in the future. Not only the origin of acidity but also the role of acid site for a complex reaction will be clarified by using such a model compound. The role of acidic solid as a catalyst support is also expected to be understood. The expected fine distribution of acid strength will possibly give an excellent catalytic activity, selectivity or catalyst life.

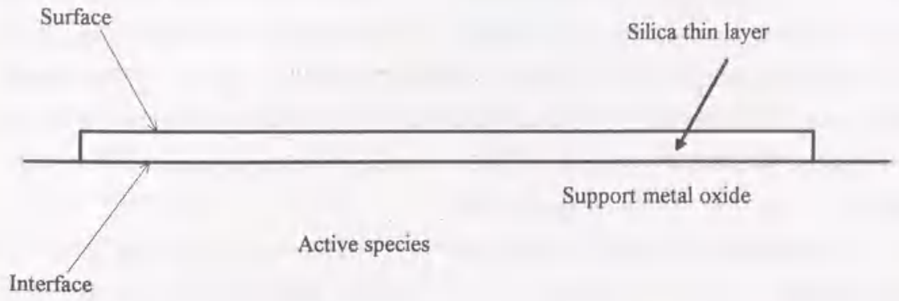

Figure 1 - 2 : Concept of surface thin layer of silica loaded on metal oxide.

Chemical Vapor Deposition

The complex structure of interface on the combined oxide catalyst is considered to be caused by the conventional liquid phase preparation method. For example, the impregnation method of aluminum on silica is as follows: 1) silica solid is put into an aqueous solution of aluminum salt as $Al(NO_3)_3$; 2) it is heated to dry up water; 3) the yielded solid is calcined to convert the precursor into the oxide. Thus, the formation of interface between aluminum and silicon, *i.e.* the formation of Si-O-Al bond, is not controlled but proceeds under various conditions, resulting in the heterogeneous structure. In addition, a bulky alumina particle, which can be formed, presumably shows an additional acidity in the case of silica-alumina to mislead the interpretation of acidic property.

In some particular cases, an oxide thin layer can be obtained even by the liquid phase impregnation method. Vanadium and molybdenum oxides readily form the monolayers on such basic oxides as alumina and titania[40]. This is supposed to be due to strong bondings, like neutralization, between the substrate and promoter caused by the difference in the electronegativity. However, the precursor of silica, *e.g.* sodium silicate, has a tendency to polymerize itself, resulting in the formation of heterogeneous thickness or particle of silica. A specific technique is therefore necessary to load a thin homogeneous layer of silica.

The deposition of gaseous precursor on solid is a useful procedure to prepare a thin surface layer. The gaseous deposition method is classified as physical vapor deposition (PVD) and chemical vapor deposition (CVD). The former is based upon the condensation of vapor or physical adsorption. The CVD is based upon the chemical reaction, and it is further classified as follows: 1) the method using a reaction among the gaseous reactants, *e.g.* $SiCl_4 + H_2 \rightarrow Si\ (\downarrow) + HCl$; 2) the method using a reaction between the deposit and substrate, *e.g.* $Si(OCH_3)(CH_3)_3$ + -OH (surface hydroxyl group) $\rightarrow$ -O-$Si(CH_3)_3$ (alkoxide anchored on the surface). The former is suitable for forming a multilayer, because the reaction must proceed on any kinds of substrate, namely, even on the deposited material itself. The latter is suitable for loading a thin layer, because the reaction must proceed only on the exposed surface of the substrate. Therefore, the present author adopts the CVD of silicon alkoxide which can react with the surface hydroxide.

The earliest study of CVD appeared in the late of the past century, in order to improve the carbon filament by coating with tungsten chloride[41]. Since the technique of CVD was remarkably developed in 1950's, it has been utilized for various fields of functionalized materials[42].

The gas-solid reaction was employed to prepare solid catalysts also[43, 44]. Banks *et al.* proposed a preparation method of molybdenum catalyst by gas-phase loading of molybdenum carbonyl on alumina in 1964[45]. This supported catalyst showed a high activity for the metathesis of olefin. Carbonyl complexes of metal elements, *i.e.* molybdenum[46 - 50], chromium[51 - 53], iron[54, 55], nickel[56, 57], cobalt[58] and ruthenium[59 - 61], have been used since the early period to improve the transition and noble metal catalysts for the oxidation, hydrogenation and photosynthesis. Chlorides of vanadium[62 - 64], molybdenum[65 - 69], tin[70] nickel[71], and titanium[72] also became to be used in the last decade. These methods were not called as CVD, because the clear gas-solid reaction was not aimed. A fine surface modification with a molybdenum allyl complex was proposed by Iwasawa *et al.* in 1978[73], and the use of organometal complexes of copper[74], vanadium[75], nickel[77 - 79], titanium[80], tin[81], chromium[82] and palladium[83] are being developed in this field of redox catalysis.

In the field of solid-acid catalysis, Barrer *et al.* proposed a gas phase deposition method of SiH_4 (silane) over zeolite to modify the shape-selectivity[84]. Niwa *et al.* carried out the deposition of $Si(OCH_3)_4$ (tetramethoxysiliane) on mordenite[85], and found an enhancement of shape-selectivity on it[86]. The uniformity in the structure and thickness of thin layer was strongly suggested by the fact that the surface layer showed a fine control effect for the pore-opening size of zeolite[87, 88]. Therefore, this new method became to be called as the CVD, and to be distinguished from the conventional liquid-phase impregnation method. This method was applied to modify the platinum loaded mordenite[89], ZSM5[90 - 93], zeolite A[94 - 96] and barium ion-exchanged mordenite[97]. These modified zeolites showed high shape-selectivities for the cracking[86, 87, 92] and hydrocracking[89] of paraffin, methanol conversion into hydrocarbons[90, 97], alkylation and disproportionation of benzene, toluene and xylenes[91], alkylation of naphthalenes[93] and separation of gases[94 - 96]. The mechanism of CVD was studied[98 - 100], and a continuos-flow CVD method was developed[101, 102] on the basis of the analyzed mechanism. In place of $Si(OCH_3)_4$, $Ge(OCH_3)_4$ (germanium tetramethoxide) was also used[103], and the EXAFS (extended X-ray absorption fine structure) analysis, which was available for germanium but not for silicon, was applied[104, 105]. Suppression of unexpected activity over the external surface by the CVD of $Si(OCH_3)_4$[106] and $Si(OCH_3)(C_3H_7)_3$ (monomethoxy-tripropylsilane)[107] was also studied. The CVD methods of silyl compound[108] and zirconia[109] over zeolites were also reported by other authors.

All of these CVD methods on zeolites aimed the modification of morphology by loading an inactive material on the external surface[110 - 114]. Controlling of the pore diameter of packing material for chromatography was also reported[115]; this also aimed the modification of morphology. On the contrary, Sato and Izumi *et al.* loaded boria[116, 117] and phosphorus[118] by the CVD method on silica

and alumina to create or modify the chemical property, *i.e.* the acidity, on the oxide surface. Thus prepared boria catalysts showed high activities for Beckmann rearrangement of cyclohexanone oxime[119, 120].

In most cases of the CVD methods above mentioned, the static or continuous-flow method is used. A typical continuous-flow CVD apparatus was used to load boria on alumina as shown in Figure 1 - 3[116]. With such an apparatus, a large amount of catalyst can be prepared by one operation. However, selection of conditions on the basis of the fluid mechanics must be needed to form a homogeneous structure[121]. In comparison with the flow method, the static method probably makes it easy to control the surface reaction. The homogeneous thickness of the silica layer deposited from $Si(OCH_3)_4$ on zeolite seems owing to a preferable balance between the reaction rate and mass transfer in the static system. In order to obtain a surface thin and homogeneous layer, the latter method seems to be more suitable. The apparatus used by Niwa *et al.* is shown in Figure 1 - 4[85 - 107]. After evacuation of substrate, vapor of alkoxide is introduced into the chamber in which the sample is hung by the spring. The temperature is controlled by a furnace. The weight of sample is measured by stretching of the spring converted into an electric signal, and the change of signal is continuously monitored by the computer. Although the purpose is different, the present author anticipated to introduce this method on alumina, titania and zirconia.

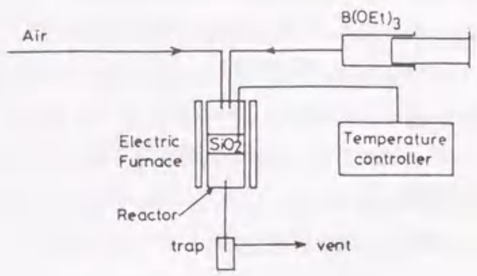

Figure 1 - 3 : Typical continuous-flow CVD apparatus used by Sato *et al.*[116]

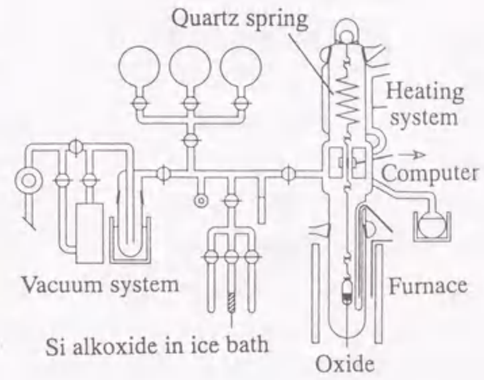

Figure 1 - 4 : Static CVD apparatus used by Niwa *et al.*[85 - 107]

Sintering of Oxide Catalyst

Alumina is one of the most durable materials with the high surface area at high temperature. For example, it keeps the surface area above 100 $m^2 g^{-1}$ at *ca.* 1300 K as shown in Figure 1 - 5[122]. However, it losses the surface area above 1400 K by the sintering. The mechanism of sintering is generally explained as follows; 1) two particles form a grain boundary (a in Figure 1 - 6); 2) the neck growth proceeds *via* the movements of oxygen and aluminum ions (b); 3) at last, the particle is reconstructed into a large particle (c)[123]. For alumina, the neck growth is suggested to be mainly caused by the surface and bulk diffusions of oxygen and aluminum ions[124]. The phase-transformation from metastable phases (γ, η and θ-Al_2O_3)

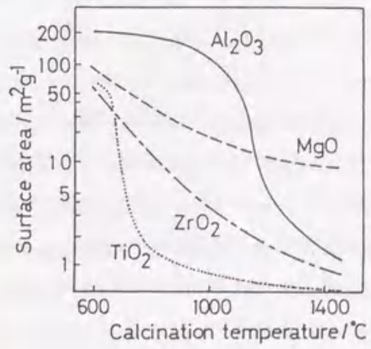

Figure 1 - 5 : Temperature dependence of surface area of metal oxide[122].

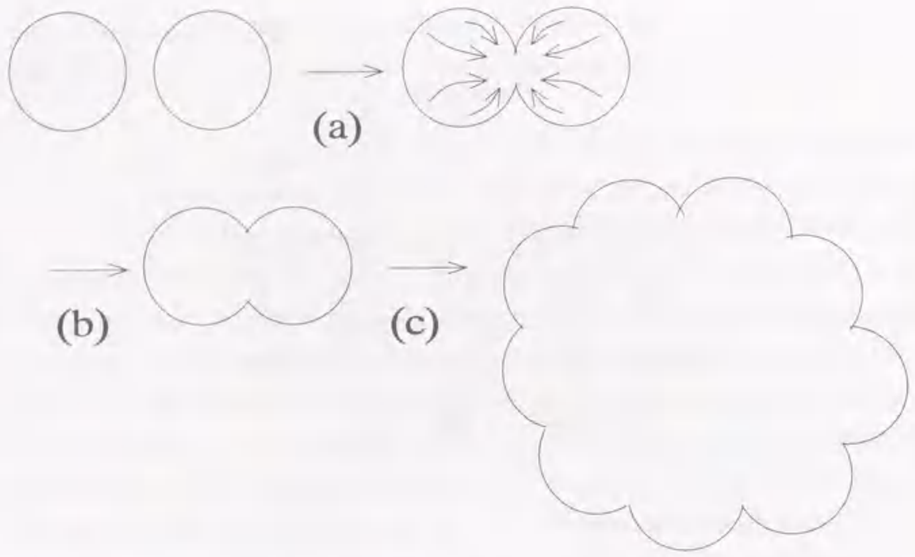

Figure 1 - 6 : Schematic mechanism of sintering of alumina at *ca.* 1573 K.

into α-Al_2O_3 accompanies with the sintering.

Attempts were made to enhance the thermal stability of alumina[122]. Alkaline metal[125], alkaline earth[126] and rare earth[127] were found to improve the stability. Especially, Machida *et al.* clarified that the hexaaluminate compound, which was formed *via* the solid reaction between alumina and the promoted alkaline or rare earth, was thermally stable and the origin of stabilization[128] as shown in Table 1 - 3. The hexaaluminate compounds possess the layered crystal structure, and the cations and anions hardly move onto the mirror plane, resulting in the difficulty of formation of grain boundary with another particle[129]. These improved materials are used as catalyst supports for the catalytic combustion, which can reduce the co-production of harmful nitrogen oxide accompanied with the combustion of fuel[130]. The stability can be enhanced also by the controlling of morphology of alumina particle without additives. A fume pyrolysis method of aluminum hydroxide was shown to give a fibrous alumina with 50 $m^2 g^{-1}$ of the surface area at 1473 K[131]. Sakata *et al.* prepared an alumina sample with a remarkably high surface area, *ca.* 100 $m^2 g^{-1}$ at 1773 K[132] by using a bilayer forming surfactant. This quite high stability was suggested to be owing to the layered structure constructed by the surfactant.

Silica is one of the known stabilizers for alumina[133]. In other words, the thermal stability is

Table 1 - 3 : Improvement of thermal stability of alumina by formation of hexaaluminate compound[122].

Additive	Effective amount	Surface area stabilization*	Product phase	Reference
BaO	*ca.* 8 atom%	4.3 (1723 K)	$BaAl_{12}O_{19}$	126
SrO	*ca.* 8 atom%	3.0 (1723 K)	$SrAl_{12}O_{19}$	126
CaO	*ca.* 8 atom%	3.6 (1723 K)	$CaAl_{12}O_{19}$	126
K_2O	*ca.* 8 atom%	5.0 (1723 K)	$KAl_{11}O_{17}$	122
La_2O_3	*ca.* 8 atom%	8.0 (1473 K)	$LaAl_{11}O_{18}$	135
Pr_2O_3	*ca.* 8 atom%	5.1 (1473 K)	$PrAl_{11}O_{18}$	135
Nd_2O_3	*ca.* 8 atom%	5.1 (1473 K)	$NdAl_{11}O_{18}$	135

*: Surface area of calcined sample / surface area of alumina under the same conditions.

one of the functions generated by combination of silica and alumina as well as the acidity. Yoldas reported that the phase transformation temperature increased from 1473 to 1503 K with the loading of 6 wt% of silicon[134]. It has been explained that the loaded silica formed a glassy structure, because no X-ray diffraction other than that of alumina was observed on alumina stabilized by silica[133]. No explanation has been done about the stabilization mechanism by the glassy silica. However, it is predicted that the glassy silica never stabilizes the surface indeed, because amorphous materials usually possess low stabilities. Thus, the origin of stabilization by silica has not been understood well. The surface thin layer of silica with a uniform and simple structure is promising to clarify the mechanism of control for sintering as well as the origin of acidity.

The solid-acid catalysts have been used below *ca.* 1000 K, because conventional chemical processes have been able to be operated in chemical plant under the conditions controlled to be mild. No solid-acid is predicted to be usable at high temperature about 1200 K, because of the loss of surface area by sintering and / or the destruction of active sites, *e.g.* hydrothermal dealumination of zeolite. However, some novel utilization will demand the operation at quite high temperature.

The catalytic removal of nitrogen oxide from exhaust gas is being studied, because the environmental pollution by acid rain becomes serious. Alumina and other solid-acids, *i.e.* zeolites, silica-alumina and sulfur-promoted metal oxides, are used as the catalyst supports[136 - 139], and in addition, the solid-acids themselves are used as the catalysts[140 - 142] for the removal of nitrogen oxide in the

presence of hydrocarbon and oxygen. Although the dependence of catalytic activity on the acidic property has not been clarified, some roles are presumed on the acid sites. If an active catalyst is found, the thermal instability of solid-acid will be a fatal problem, because the temperature of exhaust gas from automobile engine often exceeds 1000 K. It is therefore considered that a material which exhibits both high thermal stability and acidity, namely a heat-resisting acid catalyst, will have many potential applications.

In addition, the solid-acids are potential catalysts for organic syntheses as described in the previous section[5]. The deactivation is sometimes caused by the deposition of heavy molecules and / or in the presence of hetero elements such as nitrogen, sulfur and halogens. Since combustion at about 1400 K will completely remove these deposited materials to regenerate the catalyst, a number of applications in organic syntheses can be expected for heat-resisting acid catalysts.

No acidity has been reported on alumina thermally stabilized by alkaline and rare earths, and silica in the studies shown above. One of the reasons is, of course, these studies aimed only the improvement of catalyst support but did not anticipate the heat-resisting acid catalyst. In addition with this, it is presumed that the alkaline and rare earths never generate the acidity, because these possess strong basic properties. Silica is also supposed to show no acidity in these cases, because sodium silicate was used as the precursor in these studies. On the other hand, the thermal stability of conventional silica-alumina is quite low even in comparison with alumina. The high stability appears only on the silica loaded on alumina, but not on the silica-based binary oxide. It is concluded that no conventional material has both of the stability and acidity above *ca.* 1400 K. The silica ultra thin layer prepared by the CVD method is possibly considered to create a thermal stability and acidity simultaneously, because it contains no basic element and simultaneously possess the structure of silica loaded on alumina.

Objective and Scope

As described in the previous sections, the main purpose of the present thesis is to obtain a novel silica layer with a uniform thickness in the atomic-order on three oxides, *i.e.* alumina, titania and zirconia, and to find a simple acidic property on it. The expected simple correlation between the structure and acidic property will clarify the structure of acid site, origin of acidity and role of acid site for a complex reaction. On the basis of the background shown in the previous sections, the author clarifies the relationships among the structural, chemical and catalytic properties, and the correlation between these properties of obtained material and preparation conditions. To clarify the mechanism of thermal stabilization of alumina by silica is another important objective of this thesis, and therefore the thermal behavior is investigated. Creation of a heat-resisting acidity, *i.e.* an acidic property compatible with the thermal stability, is also aimed. The mechanism of CVD, determination of structure by spectroscopic and chemical characterizations, dependence of properties on the preparation conditions and procedure, application to an industrially important reaction and measurement of thermal behavior are dealt with in order to give a general understanding for the principle of creation of catalytic function by the combination of two oxides.

In Chapter 2, the author introduces the CVD method of $Si(OCH_3)_4$ on the three oxides under the conditions according to the studies on zeolites, by which the uniform layer was obtained[85 - 107]. In Section 2 - 1, the structure and acidity of the surface layer on alumina is investigated. In Section 2 - 2, titania and zirconia are used as the substrates, and the properties of the surface silica layers loaded on these oxides are compared. The estimation of thickness is, of course, most important to characterize the surface layer. However, the conventional surface analysis methods, *e.g.* XPS (X-ray photon spectroscopy), cannot distinguish between the surface and bulk in the atomic order. These methods are therefore impossible to determine the surface structure in the atomic-order thickness. The author applies a novel chemical titration, the BAT (benzaldehyde-ammonia titration) method, which was developed by Niwa *et al.*[143, 144] In this chapter, the spreading and thickness of the surface silica layer are discussed mainly on the basis of this BAT method. The acidic property is determined by several test reactions, and the relationship against the structure is displayed. Section 2 - 3 describes the application of the silica layers to an industrially important reaction, Beckmann rearrangement of cyclohexanone oxime. Not only the performances of these novel catalysts, but also the role of active site for this complex reaction is discussed from the correlation between the activity and structure. In Section 2 - 4, $Ge(OCH_3)_4$ is deposited on alumina in place of $Si(OCH_3)_4$, and the EXAFS is utilized to determine the structure.

Chapter 3 deals with the mechanism of CVD, structure of the deposited silica in the atomic order and the change of acidity by varying the structure, in order to clarify the micro structure and origin of acid site. In Section 3 - 1, the mechanism for deposition of $Si(OCH_3)_4$ is investigated by means of gravimetry, gaseous product analysis and IR spectroscopy. Dependence of structure on the CVD conditions is also discussed. In Section 3 - 2, various silicon alkoxides, *i.e.* $Si(OCH_3)_n(CH_3)_{4-n}$ ($n = 1 - 3$), are used in place of $Si(OCH_3)_4$ in order to change the micro structure. Section 3 - 3 mainly deals with the ^{29}Si NMR spectra, which directly determine the micro structure of the silica

Table 1 - 4 : Studies to load a thin silica layer on another metal oxide by the CVD method or liquid phase impregnation of silicon alkoxide.

Silicon source used	Substrate	Characterization	Application	Reference
$Si(OCH_3)_n(CH_3)_{4-n}$ (n = 1 - 4) *etc.*	MgO, Al_2O_3	CO adsorption, test reactions	NO removal	145, 146
$Si(OC_2H_5)_4$	MgO		Decomposition of triethylamine	147
$Si(OC_2H_5)_4$	ZrO_2, ZnO	AES, ISS		148 - 150
$Si(OC_2H_5)_4$	Al_2O_3	^{29}Si NMR, TPD	Various reactions	151 - 154
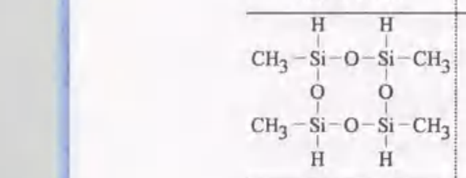	TiO_2	IR, XPS, Porosity measurement	Reduction of unexpected activity on pigment particle	155
$Si(OCH_3)_4$	Al_2O_3	^{29}Si NMR, TPD		156, 157
$Si(OCH_3)_4$	Al_2O_3	EPMA		121
$Si(OC_2H_5)_4$*	Al_2O_3	Surface area measurement, IR	Catalyst support	158
$Si(OC_2H_5)_4$*	Al_2O_3	IR	Support for molybdenum	159
$Si(OC_2H_5)_4$*	Al_2O_3	XRD, DTA	Catalyst support	160

* : Liquid phase impregnation or grafting method.

layer. Independently or referring to this work, several researchers reported the methods to load the thin layers of silica in gas phase as shown in Table 1 - 4. These are related with the present results in this chapter. Some of the liquid phase loading methods of silicon alkoxide, which are included in Table 1 - 4, are also discussed.

In Chapter 4, the sintering behavior, *i.e.* the changes in surface area and XRD (X-ray diffraction), of silica layer on alumina is demonstrated at 1373 - 1573 K. The BAT method is employed to solve which surface of silica or alumina is lost by sintering. The mechanism of stabilization is speculated on the basis of this method. The acidity is examined after the high temperature calcination in order to find a novel heat-resisting acid catalyst.

Chapter 5 summarizes the findings obtained by this study, and shows the future prospects.

References

1. K. Tanabe, *Solid Acids and Bases: their Catalytic Properties,* Kodansha and Academic Press, Tokyo, New York and London (1970).
2. K. Tanabe, in *Catalysis: Science and Technology, Vol. 2,* eds. J. R. Anderson and M. Boudart, Springer-Verlag, Berlin (1981) p. 231.
3. W. O. Haag, in *Zeolites and Related Microporous Materials,* eds. J. Weitkamp, H. G. Karge, H. Pfeifer and W. Hölderich, Elsevier, Amsterdam (1994) p. 1375.
4. J. A. Rabo, in *New Frontiers in Catalysis,* eds. L. Guczi, F. Solymosi and P. Tétényi, Elsevier, Amsterdam, (1993) p. 1.
5. W. F. Hölderich, in *New Frontiers in Catalysis,* eds. L. Guczi, F. Solymosi and P. Tétényi, Elsevier, Amsterdam, (1993) p. 127.
6. M. Iwamoto, in *Zeolites and Related Microporous Materials,* eds. J. Weitkamp, H. G. Karge, H. Pfeifer and W. Hölderich, Elsevier, Amsterdam (1994) p. 1395.
7. Y. Higashio and K. Takahashi, EP 0215567 (1990).
8. M. Misono and N. Nojiri, *Appl. Catal.,* **64,** 1 (1990).
9. S. Okazaki and H. Jouhouji, *Bull. Chem. Soc. Jpn.,* **59,** 1931 (1986).
10. D. Feitler, W. Scimming and H. Wetsbein, EP 0278729 (1987).
11. M. Taramasso, G. Manara, V. Fattore and B. Notari, US 4656016 (1987).
12. K. Honna, M. Sugimoto, N. Shimizu and K. Kurisaki, *Chem. Lett.,* **1986,** 315.
13. V. Taglieber, W. F. Hölderich, R. Kummer, W. D. Mross and E. Saladin, EP 0133938 (1983).
14. K. D. Olson, EP 0251168 (1988).
15. W. F. Hölderich, N. Goetz and L. Hupfer, DE 3720850 (1987).
16. F. Merger, W. F. Hölderich, J. Frank, T. Docker and M. Sauerwald, DE 3826303 (1988).
17. Y. Izumi, N. Natsume, H. Takamine, I. Tamaoki and K. Urabe, *Bull. Chem. Soc. Jpn.,* **62,** 2159 (1989).
18. M. Misono, *Catal. Rev.-Sci. Eng.,* **29,** 269 (1987).
19. K. Tanabe and T. Yamaguchi, *Stud. Surf. Sci. Catal.,* **44,** 99 (1989).
20. R. C. Hansford, *Ind. Eng. Chem.,* **39,** 849 (1947).
21. S. Yamaguchi and S. Tsutsumi, *Nippon Kagaku Zasshi,* **69,** 6 (1948).
22. C. L. Thomas, *Ind. Eng. Chem.,* **41,** 2564 (1949).
23. M. W. Tamele, *Discuss. Faraday Soc.,* **8,** 270 (1950).

24. J. D. Danforth, *J. Phys. Chem.*, **59,** 564 (1955).
25. C. J. Plank, *J. Colloid Sci.*, **2,** 413 (1947).
26. B. S. Greensfelder, H. H. Voge and G. M. Good, *Ind. Eng. Chem.*, **41,** 2573 (1949).
27. A. G. Oblad, S. G. Hindin and G. A. Mills, *J. Am. Chem. Soc.*, **75,** 4096 (1953).
28. R. G. Haldeman and P. H. Emmett, *J. Am. Chem. Soc.*, **78,** 2917 (1956).
29. J. K. Lee and S. W. Weller, *Anal. Chem.*, **30,** 1057 (1958).
30. L. Leonard, S. Suzuki, J. J. Fripiat and C. De Kimpe, *J. Phys. Chem.*, **68,** 2608 (1964).
31. W. K. Hall, F. E. Lutinski and H. R. Gerberich, *J. Catal.*, **3,** 512 (1964).
32. A. E. Hirschler, *J. Catal.*, **6,** 1 (1966).
33. T. Seiyama, in *Kinzoku Sankabutsu to Fukugo Sankabutsu (Metal Oxides and Complex Oxides)*, eds. K. Tanabe, T. Seiyama and K. Fueki, Kodansha, Tokyo (1978) p. 375.
34. W. Grabowski, M. Misono and Y. Yoneda, *J. Catal.*, **61,** 103 (1980).
35. H. Kawakami, S. Yoshida and T. Yonezawa, *J. Chem. Soc., Faraday Trans. 2,* **80,** 205 (1984).
36. G. M. Zhidomirov and V. B. Kazanski, *Adv. Catal.*, **34,** 131 (1984).
37. M. Niwa, M. Iwamoto and K. Segawa, *Bull. Chem. Soc. Jpn.*, **59,** 3735 (1986).
38. M. Niwa, N. Katada, M. Sawa and Y. Murakami, *J. Phys. Chem.*, **99,** 8812 (1995).
39. J. Sauer, in *Zeolites and Related Microporous Materials,* eds. J. Weitkamp, H. G. Karge, H. Pfeifer and W. Hölderich, Elsevier, Amsterdam (1994) p. 2039.
40. M. Niwa, Y. Matsuoka and Y. Murakami, *J. Phys. Chem.*, **91,** 4519 (1987).
41. A. de Lodyguine, US 575002 (1897).
42. H. O. Pierson, *Handbook of Chemical Vapor Deposition: Principles, Technology and Applications,* Noyes Publications, New Jersey (1992).
43. Y. Iwasawa, *Shokubai (Catalyst),* **37,** 292 (1995).
44. Y. Iwasawa, in *Handbook of Heterogeneous Catalysis,* eds. H. Knözinger and G. Ertl, VCH, Berlin, in press.
45. R. L. Banks and G. C. Bailey, *Ind. Eng. Chem. Prod. Res. Dev.*, **3,** 170 (1964).
46. E. S. Davie, D. A. Whan and C. Kemball, *Chem. Commun.*, **1969,** 1430.
47. R. F. Howe, D. E. Davidson and D. A. Whan, *J. Chem. Soc., Faraday Trans. 1,* **68,** 2266 (1972).
48. A. Brenner and R. L. Burwell, Jr., *J. Am. Chem. Soc.*, **97,** 2565 (1975).
49. Y. Okamoto, A. Maezawa, H. Kane, I. Mitsushima and T. Imanaka, *J. Chem. Soc., Faraday Trans. 1,* **84,** 851 (1988).
50. J. S. Yoo, J. A. Donohue, M. S. Kleefisch, P. S. Lin and S. D. Elfine, *Appl. Catal.*, **105,** 83 (1993).
51. R. L. Banks, US 3463827 (1969).
52. A. Brenner, D. A. Hucul and S. J. Hardwick, *Inorg. Chem.*, **18,** 1478 (1979).
53. Y. Okamoto, H. Onimatsu, M. Hori, Y. Inui and T. Imanaka, *Catal. Lett.*, **12,** 239 (1992).
54. J. B. Nagy, M. van Eenoo and E. G. Derouane, *J. Catal.*, **58,** 230 (1979).
55. Y. Iwasawa, *Adv. Catal.*, **35,** 187 (1987).
56. D. C. Bailey and S. H. Langer, *Chem. Rev.*, **81,** 109 (1981).
57. K. Omata, H. Mazaki, H. Yagita and K. Fujimoto, *Catal. Lett.*, **4,** 123 (1990).
58. Y. Iwasawa, M. Yamada, Y. Sato and H. Kuroda, *J. Mol. Catal.*, **23,** 95 (1984).
59. H. Miura, K. Oki, H. Ochiai and J. Kimura, *Shokubai (Catalyst),* **31,** 417 (1989).
60. U. Kiiski, T. Venalinen, T. A. Pakkanen and O. Krause, *J. Mol. Catal.*, **64,** 163 (1991).
61. L. Alvila, T. A. Pakkanen and O. Krause, *J. Mol. Catal.*, **84,** 145 (1993).
62. G. C. Bond and K. Bruckman, *Faraday Discuss., Chem. Soc.*, **72,** 235 (1981).
63. T. Hattori, M. Matsuda, K. Suzuki, A. Miyamoto and Y. Murakami, in *Proc. 9th Int. Congr. Catal.*, eds. M. J. Phillips and M. Ternan, the Chemical Institute of Canada, Ottawa (1988) p. 1640.
64. M. Anpo, M. Sunamoto and M. Che, *J. Phys. Chem.*, **93,** 1187 (1989).
65. M. Cornac, A. Jeannin and J. C. Lavalley, *Polyhedron,* **5,** 183 (1986).
66. M. Anpo, M. Kondo, Y. Kubokawa, C. Loius and M. Che, *J. Chem. Soc., Faraday Trans. 1,* **84,** 2771 (1988).
67. C. C. Williams, J. G. Ekerdt, J.-M. Jehng, F. D. Hardcastle, A. J. Turek and I. E. Wachs, *J. Phys. Chem.*, **95,** 8781 (1991).
68. M. de Boer, A. J. van Dillen, D. C. Koningsberger, J. W. Geus, M. A. Wuurman and I. E. Wachs, *Catal. Lett.*, **11,** 227 (1991).
69. A. N. Desikan, L. Huang and S. T. Oyama, *J. Phys. Chem.*, **97,** 5699 (1993).
70. T. Hattori, S. Itoh, T. Tagawa and Y. Murakami, in *Preparation of Catalysts IV,* eds. B. Delmon, P. Grange, P. A. Jacobs and G. Poncelet, Elsevier, Amsterdam (1987), p. 113.
71. Y. Harano and M. Yano, *Hyomen (Surface),* **26,** 551 (1988).
72. M. Anpo and K. Chiba, *J. Mol. Catal.*, **74,** 207 (1992).

73. Y. Iwasawa, Y. Nakano and S. Ogasawara, *J. Chem. Soc., Faraday Trans. 1,* **74,** 2968 (1978).
74. H. Miura, H. Taguchi, K. Sugiyama and Y. Matsuda, *Shokubai (Catalyst),* **30,** 372 (1988).
75. K. Inumaru, T. Okuhara and M. Misono, *Chem. Lett.,* **1990,** 1207.
76. T. Okuhara, K. Inumaru, M. Misono and N. Matsubayashi, in *Proc. 10th Int. Congr. Catal.,* Elsevier, Amsterdam (1993), p. 1767.
77. R. Sekine, M. Kawai, K. Asakura and Y. Iwasawa, *Proc. Mater. Res. Soc. Meeting,* **222,** 333 (1991).
78. J.-P. Jacobs, L. P. Lindfors, J. G. Reintjes, O. Jylha and H. H. Brongersma, *Catal. Lett.,* **25,** 315 (1994).
79. E.-L. Lakomaa, *Appl. Surf. Sci.,* **75,** 185 (1994).
80. K. Asakura and Y. Iwasawa, *J. Phys. Chem.,* **96,** 829 (1992).
81. K. Tomishige, K. Asakura and Y. Iwasawa, *J. Catal.,* **149,** 70 (1994).
82. S. Haukka, E.-L. Lakomaa and T. Suntola, *Appl. Surf. Sci.,* **75,** 220 (1994).
83. C. Dossi, R. Psato, R. Ugo, Z. C. Zhang and W. M. H. Sachtler, *J. Catal.,* **149,** 92 (1994).
84. R. M. Barrer, E. M. Vansant and G. Peeters, *J. Chem. Soc., Faraday Trans. 1,* **74,** 1871 (1978).
85. M. Niwa, H. Itoh, S. Kato, T. Hattori and Y. Murakami, *J. Chem. Soc., Chem. Commun.,* **1982,** 819.
86. M. Niwa, S. Morimoto, T. Hattori and Y. Murakami, *Chem. Lett.,* **1983,** 737.
87. M. Niwa, S. Morimoto, M. Kato, T. Hattori and Y. Murakami, in *Proc. 8th Int. Congr. Catal., Vol. 4,* ed. M. Boudrt, Verlag Chemie, Weinheim (1984) p. 701.
88. M. Niwa, S. Kato, T. Hattori and Y. Murakami, *J. Chem. Soc., Faraday Trans. 1,* **80,** 3135 (1984).
89. M. Niwa, Y. Kawashima and Y. Murakami, *J. Chem. Soc., Faraday Trans. 1,* **81,** 2757 (1985).
90. M. Niwa, M. Kato, T. Hattori and Y. Murakami, *J. Phys. Chem.,* **90,** 6233 (1986).
91. T. Hibino, M. Niwa and Y. Murakami, *J. Catal.,* **128,** 551 (1991).
92. M. Niwa, N. Senoh, T. Hibino, Y. Nakatsuka and Y. Murakami, in *Zeolites and Microporous Crystals,* eds. T. Hattori and T. Yashima, Kodansha, Tokyo (1994), p. 155.
93. M. Niwa, M. Endo and Y. Murakami, *Res. Chem. Intermed.,* **21,** 127 (1995).
94. M. Niwa, K. Yamazaki and Y. Murakami, *Chem. Lett.,* **1989,** 441.
95. M. Niwa, K. Yamazaki and Y. Murakami, *Ind. Eng. Chem. Res.,* **30,** 39 (1991).

96. M. Niwa, K. Yamazaki and Y. Murakami, *Ind. Eng. Chem. Res.,* **33,** 371 (1994).
97. M. Sawa, K. Kato, K. Hirota, M. Niwa and Y. Murakami, *Appl. Catal.,* **64,** 297 (1990).
98. M. Niwa, Y. Kawashima, T. Hibino and Y. Murakami, *J. Chem. Soc., Faraday Trans. 1,* **84,** 4327 (1988).
99. T. Hibino, M. Niwa, A. Hattori and Y. Murakami, *Appl. Catal.,* **44,** 95 (1988).
100. T. Hibino, M. Niwa, Y. Kawashima and Y. Murakami, in *Chemistry of Microporous Crystals,* eds. T. Inui, S. Namba and T. Tatsumi, Kodansha, Tokyo (1991) p. 151.
101. K. Yamazaki, M. Niwa and Y. Murakami, *Kagaku Kogaku Ronbunshu,* **16,** 564 (1990).
102. K. Tajima, M. Niwa and Y. Murakami, *Kagaku Kogaku Ronbunshu,* **19,** 258 (1993).
103. M. Niwa, C. V. Hidalgo, T. Hattori and Y. Murakami, in *New Developments in Zeolite Science and Technology,* eds. Y. Murakami, A. Iijima and J. W. Ward, Kodansha, Tokyo (1986), p. 297.
104. T. Hibino, M. Niwa, Y. Murakami and M. Sano, *J. Chem. Soc., Faraday Trans. 1,* **85,** 2327 (1989).
105. T. Hibino, M. Niwa, Y. Murakami, S. Komai and T. Hanaichi, *J. Phys. Chem.,* **93,** 7847 (1989).
106. T. Hibino, M. Niwa and Y. Murakami, *Zeolites,* **13,** 518 (1993).
107. J.-H. Kim, A. Ishida, M. Okajima and M. Niwa, *Shokubai (Catalyst),* **37,** 156 (1994).
108. H. Sato, K. Hirose, M. Kitamura and S. Nakamura, in *Zeolites: Facts, Figures, Future,* eds. P. A. Jacobs and R. A. van Santen, Elsevier, Amsterdam (1989) p. 1213.
109. K. Asakura, M. Aoki and Y. Iwasawa, *Catal. Lett.,* **1,** 395 (1988).
110. M. Niwa and Y. Murakami, *Hyomen (Surface),* **22,** 319 (1984).
111. M. Niwa and Y. Murakami, *Mater. Chem. Phys.,* **17,** 73 (1987).
112. M. Niwa and Y. Murakami, *Nippon Kagaku Kaishi,* **1989,** 410.
113. M. Niwa and Y. Murakami, *J. Phys. Chem. Solids,* **50,** 487 (1989).
114. M. Niwa and Y. Murakami, *Sekiyu Gakkaishi,* **35,** 128 (1992).
115. Y. Ohtsu, H. Fukui, T. Kanda, K. Nakamura, M. Nakano, O. Nakata and Y. Fujiyama, *Chromatographia,* **24,** 380 (1987).
116. S. Sato, H. Sakurai, K. Urabe and Y. Izumi, *Chem. Lett.,* **1985,** 277.
117. H. Sakurai, S. Sato, K. Urabe and Y. Izumi, *Chem. Lett.,* **1985,** 1783.
118. S. Sato, M. Hasegawa, T. Sodesawa and F. Nozaki, *Bull. Chem. Soc. Jpn.,* **64,** 516 (1991).

119. S. Sato, K. Urabe and Y. Izumi, *J. Catal.*, **102,** 99 (1986).
120. S. Sato, S. Hasebe, H. Sakurai, K. Urabe and Y. Izumi, *Appl. Catal.*, **29,** 107 (1987).
121. Y. Tatsusima, Y. Morioka and A. Ueno, in *Proc. Heisei 6 Nendo Shokubai Kenkyu Happyou-kai,* (1994) p. 554.
122. H. Arai and M. Machida, *Catal. Today,* **10,** 81 (1991).
123. E. Katoh, in *Muki Zairyo Kagaku I, 6th edition,* ed. I. Noda, Corona Publishing, Tokyo (1977) p. 158.
124. D. L. Johnson and L. Berrin, in *Sintering and Related Phenomena,* eds. G. C. Kuczynski, N. A. Hooton and C. F. Gibbon, Gordon and Research, New York (1967) p. 445.
125. R. M. Revy and D. J. Bauer, *J. Catal.*, **9,** 76 (1967).
126. M. Machida, K. Eguchi and A. Arai, *J. Catal.*, **103,** 385 (1987).
127. H. Schaper, E. B. M. Doesburg and L. L. van Reijan, *Appl. Catal.*, **7,** 211 (1983).
128. M. Machida, K. Eguchi and H. Arai, *Bull. Chem. Soc. Jpn.*, **61,** 3659 (1988).
129. M. Machida, K. Eguchi and H. Arai, *J. Catal.*, **123,** 477 (1990).
130. M. Machida, E. Eguchi and H. Arai, *J. Catal.*, **120,** 377 (1989).
131. T. Ishikawa, R. Ohashi, H. Nakabayashi, N. Kakuta, A. Ueno and A. Furuta, *J. Catal.*, **134,** 87 (1992).
132. N. Tsutsumi, K. Sakata and T. Kunitake, *Chem. Lett.*, **1992,** 1465.
133. I. Amato, D. Martorama and B. Sliengo, in *Sintering and Catalysis*, ed. G. C. Kuczynski, Plenum Press, New York (1975) p. 187.
134. B. E. Yoldas, *J. Mater. Sci.*, **11,** 465 (1976).
135. H. Yamashita, A. Kato, N. Watanabe and S, Matsuda, *Nippon Kagaku Kaishi,* **1986,** 1169.
136. W. Held, A. König, T. Richter and L. Puppe, *SAE Tech. Paper*, 900496 (1990).
137. S. Sato, Y. Yu-u, H. Yahiro, N. Mizuno and M. Iwamoto, *Appl. Catal.*, **70,** L1 (1990).
138. M. Misono and K. Kondo, *Chem. Lett.*, **1991,** 1001.
139. E. Kikuchi, K. Yogo, S. Tanaka and M. Abe, *Chem. Lett.*, **1991,** 1063.
140. H. Hamada, Y. Kintaichi, M. Sasaki and T. Ito, *Appl. Catal.*, **64,** L1 (1990).
141. Y. Kintaichi, H. Hamada, M. Tabata M. Sasaki and T. Ito, *Catal. Lett.*, **6,** 239 (1990).
142. Y. Kintaichi, H. Hamada, M. Tabata M. Sasaki and T. Ito, *Chem. Lett.*, **1991,** 2179.
143. M. Niwa, S. Inagaki and Y. Murakami, *J. Phys. Chem.*, **89,** 3869 (1985).
144. M. Niwa, K. Suzuki, M. Kishida and Y. Murakami, *Appl. Catal.*, **67,** 297 (1991).

145. Y. Imizu, A. Tada and I. Toyoshima, *Shokubai (Catalyst)*, **30,** 388 (1988).
146. N. Okazaki, T. Kohno, R. Inoue, Y. Imizu and A. Tada, *Chem. Lett.*, **1993,** 1195.
147. B.-Q. Xu, T. Yamaguchi and K. Tanabe, *Chem. Lett.*, **1989,** 149.
148. T. Jin, T. Okuhara and J. M. White, *J. Chem. Soc., Chem. Commun.*, **1987,** 1248.
149. T. Jin and J. M. White, *Surf. Interface Anal.*, **11,** 517 (1988).
150. S. K. Jo, T. Jin and J. M. White, *Appl. Surf. Sci.*, **40,** 155 (1989).
151. S. Sato, M. Toita, Y.-Q. Yu, T. Sodesawa and F. Nozaki, *Chem. Lett.*, **1987,** 1535.
152. S. Sato, M. Toita, T. Sodesawa and F. Nozaki, *Appl. Catal.*, **62,** 73 (1990).
153. S. Sato, M. Tokumitsu, T. Sodesawa and F. Nozaki, *Bull. Chem. Soc. Jpn.*, **64,** 1005 (1991).
154. S. Sato, T. Sodesawa, F. Nozaki and H. Shoji, *J. Mol. Catal.*, **66,** 343 (1991).
155. H. Fukui, T. Ogawa, M. Nakano, M. Yamaguchi and Y. Kanda, in *Controlled Interphases in Composite Materials,* ed. H. Ishida, Elsevier Science Publishing, New York (1990) p. 469.
156. T.-C. Sheng and I. D. Gay, *J. Catal.*, **145,** 10 (1994).
157. T.-C. Sheng, S. Lang, B. A. Morrow and I. D. Gay, *J. Catal.*, **148,** 341 (1994).
158. B. Beguin, E. Grabowski and M. Primet, *J. Catal.*, **127,** 595 (1991).
159. P. Sarrazin, S. Kasztelan, N. Zanier-Szyndlowski, J. P. Bonnelle and J. Grimblot, *J. Phys. Chem.*, **97,** 5947 (1993).
160. T. Horiuchi, T. Sugiyama and T. Mori, *J. Mater. Chem.*, **3,** 861 (1993).

Chapter 2. Structure and Brønsted Acidity of Silica Monolayer

2-1 Silica Monolayer on γ-Alumina

Synopsis

Chemical vapor deposition of tetramethoxysilane [$Si(OCH_3)_4$] was carried out on γ-alumina at 593 K. The structure, mainly the spreading of deposited silica and its relationship with the surface acidity, was studied by benzaldehyde-ammonia titration (BAT), infrared (IR) spectroscopy and several test reactions. Silica monolayer, which consisted of 1 : 1 bondings of Al-O-Si, was formed from the beginning of deposition until it covered the alumina surface almost completely. The silica monolayer showed Brønsted acidity. The surface hydroxyl species which attached on the interface like Al-O-Si-OH is suggested as the Brønsted acid site, because the maximum of activity for the test reaction was observed when the monolayer fully covered the surface. The acid strength of this species is estimated to be so weak because it was active only for facial reactions, *i.e.* double-bond isomerization of *1*-butene and dehydration of *tert*-butyl alcohol, but inactive for cumene cracking unlike the conventional silica-alumina catalyst. A fine distribution of acid strength due to the simple structure is suggested.

Introduction

As described in the previous chapter, the author applied the CVD (chemical vapor deposition) method to obtain an ultra thin layer of silica on metal oxide. This section deals with the CVD on alumina, the most popular oxide which forms the combined solid-acid catalyst with silica. The experiments were done under the same conditions as used for the modification of zeolite, *i.e.* at 593 K of the CVD temperature and 2.5 Torr of the vapor pressure of $Si(OCH_3)_4$ (1 Torr = 133.3 Pa), to prepare a homogeneous thin layer as observed in this case[1].

Determination of spreading of surface layer is the most important point in this section. The BAT (benzaldehyde-ammonia titration) method[2, 3] will be utilized for the quantitative analysis of the spreading. γ-Alumina itself has Lewis acidity, and this sometimes confuses the understanding of acidic property of silica-alumina catalyst. The infrared (IR) spectroscopy will distinguish between the Brønsted and Lewis acid sites. Several test reactions also will be applied to characterize the acid sites, *i.e.* to distinguish between the Brønsted and Lewis, and, strong and weak acid sites. Double-bond isomerization of olefin is known to be catalyzed by various acid and base catalysts even if the

strength is quite weak, and can distinguish between the Brønsted and Lewis acidity by the selectivity of product *trans*- and *cis*-olefins[4, 5]. Dehydration of *tert*-butyl alcohol is also a test reaction of the acid catalyst over a wide strength range[6]. Dehydration of ethanol is known to be specifically catalyzed by the acid-base dual sites or coordination unsaturated site on γ-alumina[7], and will be used to show the change of acid-base property of alumina surface in this section. Cracking of cumene requires the strong Brønsted acid site[8]. The comparison of activity for this reaction will clarify whether the strong Brønsted acid site of silica-alumina is generated on the simple interface between the silica layer and alumina or not. These characterizations will be related with each other in order to understand the origin of acid site on the interface between silica and alumina.

Experimental

Materials and Chemical Vapor Deposition

Alumina was prepared by the calcination of boehmite (one kind of aluminum hydroxide) at 973 K, and supplied by Catalysis Society of Japan as a reference catalyst, JRC-ALO4. The BET surface area was 161 $m^2 g^{-1}$, and the crystal phase was proven to be γ-Al_2O_3 by X-ray diffraction (XRD; as the data will be shown in Chapter 4). The supplied sample had been molded by extrusion, and it was crashed into 30 - 50 mesh granules in order to make the treatment easy. Since this material was very hydrophilic, uncertainties often appeared during the weight measurements due to unexpected change of the amount of adsorbed water. In order to avoid this, the alumina sample was exposed to a humid atmosphere with *ca.* 80 % of the relative humidity kept by the presence of an aqueous solution which was saturated with ammonium chloride, for several days before the experiment. Thus treated sample always contained *ca.* 11 wt% of water.

The static apparatus shown in Figure 1 - 4 was used for the CVD. The alumina sample was hung by a quartz spring in a vacuum line. The temperature of the quartz spring was kept constant at the boiling point of tetrachlorocarbon (CCl_4), *ca.* 350 K, by circulation of CCl_4 vapor in order to maintain the spring constant. The stretching of spring was converted into an electric signal by a magnetic displacement meter. The signal was analyzed by a personal computer: some experiments were done without the computer, but the principle was same. The calibration of weight was done by using glass beads with the known weights. A good linear relationship was always obtained between the weight and electric voltage. The weight of hung sample was thus monitored. The temperature of sample was measured with a thermocouple located near the sample, and the pressure in the vessel

was measured with a pirani gauge and a pressure-voltage transducer.

Tetramethoxysilane [$Si(OCH_3)_4$] was obtained from Tokyo Chemical Industry Co. Ltd. or Shin-Etsu Kagaku Co. Prior to the experiments, it was distilled *in vacuo* in order to remove the contaminated air and water, and dimethylether formed by self decomposition.

The alumina sample (0.5 - 1.5 g) was set in the apparatus and evacuated by rotary and diffusion pumps. After the pressure decreased down to *ca.* 10^{-3} Torr, the sample was heated up to 673 K. The weight always decreased with heating because the adsorbed water was removed, and the temperature was kept constant at 673 K until no further change of the weight was observed: it usually took 2 - 3 hours. The vapor of $Si(OCH_3)_4$ was admitted onto this pretreated sample at 593 K, and the increasing of weight was then observed. If only an empty basket was hung without the sample, no weight increase was detected: this confirms that the weight increase was due to the deposition of alkoxide on the sample. The vapor pressure was kept constant (*ca.* 2.5 Torr) by chilling the reservoir with an ice bath at 273 K. After 10 - 20 minutes, the weight increase was saturated, because of the vapor lock due to such gaseous products as dimethylether and methanol. The weight was readily increased by repetition of the evacuation and the introduction of vapor to remove the gaseous products. An example of weight increasing curve is shown in Figure 2 - 1 - 1. The difference of time interval of this cycle did not affect the properties of sample.

After the expected weight change was observed, the sample was evacuated at 593 K until the stable weight was observed, and the temperature was then raised up to 673 K. Oxygen (200 Torr) was introduced in order to combust the organic residue. The introduced oxygen was kept until the decrement of weight stopped (usually more than 4 hours), and the sample was again evacuated at 673 K. In some cases, water vapor was introduced to hydrolyze the methoxide in place of oxygen, but the change of treatment gas did not affect the properties of sample. The amount of deposited material was determined from the difference in the weight between this evacuated sample and alumina evacuated at 673 K on the basis of the assumption that the deposited material had a chemical composition of SiO_2. The samples with various loading were prepared as shown in Table 2 - 1 - 1.

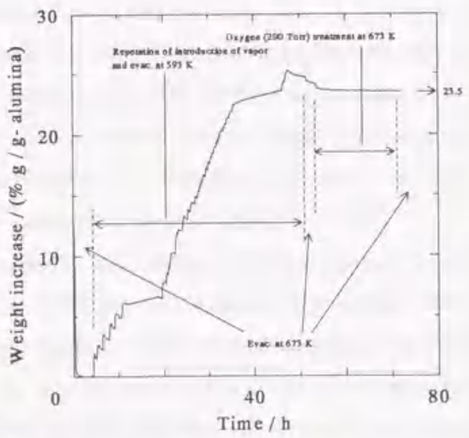

Figure 2 - 1 - 1 : Weight change during preparation of sample with 23.5 wt% of SiO_2 loading on alumina.

Table 2 - 1 - 1 : Samples prepared by CVD of $Si(OCH_3)_4$ on alumina at 593 K.

SiO_2 loading wt% (SiO_2 / Al_2O_3)	BET surface area m^2 g-cat^{-1}	Si concentration nm^{-2}
0 (ALO4)	161	0.0
1.94	153	1.2
4.84	160	3.0
6.96	156	4.2
9.88	165	5.5
10.2	145	6.4
10.2	153	6.1
10.3	166	5.6
14.9	145	9.0
19.6	141	11.7
19.6	144	11.4
23.2	156	12.1
23.5	154	12.4
27.5	147	14.7
28.4	146	15.1
29.7	141	16.3
37.0	135	20.1
37.7	140	19.6
42.3	130	22.8
44.9	129	24.1
49.6	111	29.8
52.4	123	28.1

Thus prepared sample was again calcined in flowing oxygen at 673 K to remove the organic material completely. The obtained sample was used for the characterization after the rehydration in the humid atmosphere with *ca.* 80 % of the relative humidity, like carried out for alumina support. All of the experimental results will be shown by the value based on the weight of thus hydrated sample.

As a comparison, a silica-alumina catalyst, Nikki Kagaku N631-L (Al_2O_3 content 13 wt%, surface area, 360 m^2 g^{-1}) and three silica gel samples (Godfrey L. Cabot Inc., Cab-O-Sil [173 m^2 g^{-1}], Fuji-Davidson Chemical Co. Ltd., Micro Bead 4-B [368 m^2 g^{-1}] and Nikki Kagaku Co. Ltd., N602-A [281 m^2 g^{-1}]) were used.

Characterization

The surface area was measured by BET one-point method[9] at 77 K with $p / p_0 = 0.3$ of nitrogen. About 40 mg of the sample was set in a Pyrex cell, and pretreated in flowing nitrogen at 673 K for 1 hour. A gaseous mixture of nitrogen and helium (3 : 7 in molar ratio) was then fed with 200 cm^3 min^{-1} of the flow rate. Nitrogen was adsorbed by chilling the cell at 77 K with liquid nitrogen.

The adsorbed nitrogen was desorbed by heating the cell with a water bath at the room temperature, and the desorption amount was determined by a TCD (thermal conductivity detector) directly connected after the cell.

In order to distinguish between the surfaces of alumina and silica, BAT method was utilized. This method was developed by Niwa *et al.* to measure the coverage by promoter on a binary oxide surface[2,3]. The sample (20 - 100 mg) was set in a 4 mm i.d. Pyrex tube, and 40 cm^3 min^{-1} of helium, which was purified by passing a liquid nitrogen trap to remove the moisture, was fed. After the pretreatment at 673 K for 1 hour, 1 mm^3 of liquid benzaldehyde ($9.8 \cdot 10^{-6}$ mol) was injected into the reactor tube at 523 K. The aldehyde was adsorbed on the sample to form benzoate anion, and the eluted aldehyde was detected with an FID (flame ionization detector) GC (gas chromatography) directly connected after the reaction tube. Until no adsorption was observed, the injections were repeated usually three to six times. Finally, 10 cm^3 of gaseous ammonia ($4.2 \cdot 10^{-4}$ mol) was injected to convert the adsorbed benzoate anion into benzonitrile, until no formation of the nitrile was observed. The amount of yielded benzonitrile shows the amount of benzoate anion adsorbed on the surface. The surface concentration of benzoate anion adsorbed on alumina is quite high (1.8 nm^{-2}; it almost corresponds to the complete coverage by a monolayer), but very little on silica; it is 0.009 and 0.003 nm^{-2} on Cab-O-Sil and Micro Bead 4-B, respectively, and these small concentrations correspond to the contamination of aluminum (11 and 8 ppm in Cab-O-Sil and Micro Bead 4-B, respectively); probably, no benzoate is adsorbed on a pure silica. The amount of the desorbed nitrile was therefore considered to show the exposed surface area of alumina. The coverage of surface by silica is given by the following equations:

S_a (m^2 g^{-1}) = BN (nm^{-2}) / BN on ALO4 (1.8 nm^{-2}) × S_t (m^2 g^{-1}), where S_a is the exposed surface area of alumina, BN is the concentration of desorbed benzonitrile and S_t is the BET surface area of the sample;

Cov. = 1 - S_a / S_t. where Cov. is the coverage on surface by silica.

IR (infrared) spectrum was recorded by a JASCO FTIR-3 spectrometer on a self-supporting disk (1 cm in diameter) molded from *ca.* 7 mg of the sample powder. The sample disk was set in an *in-situ* cell, and evacuated at the upper part of the cell with an electric furnace. The spectrum was recorded after the sample was cooled down at the lower part for more than 5 minutes. The hydroxyl region spectra were collected after the evacuation at 673 K for 1 hour. Ammonia was adsorbed at 373 K under 100 Torr of the pressure, and pyridine was adsorbed at 423 K under the vapor pressure at the room temperature on the sample evacuated at 673 K for 1 hour.

Several test reactions were carried out by the pulse method. The sample was set in a 4 mm i.d. Pyrex reactor, and pretreated at 673 K for 1 hour in flowing helium, which was purified by passing a liquid nitrogen trap. The catalyst amount was adjusted to keep conversion below 5 % in order to measure the reaction rate in the differential conditions, and the yielded product was analyzed by an FID-GC connected directly to outlet of the reaction tube. The reaction rate was calculated by the following equation;

Rate per surface area (mol m h^{-1}) = yield (mol) × flow rate of carrier (m^3 h^{-1}) / surface area of catalyst (m^2).

The double-bond isomerization of *1*-butene was carried out at 393 or 333 K. Three different conditions were adopted because of experimental problems: conditions (A), 0.1 cm^3 (= $4.2 \cdot 10^{-6}$ mol) of *1*-butene was injected from a syringe in 60 cm^3 min^{-1} of flowing helium under 1 atm (1 atm = $1.013 \cdot 10^5$ Pa) of the pressure in the reactor, and the produced *trans*- and *cis*-*2*-butene were analyzed with a capillary column silicone OV-101 operated at the room temperature; (B), the pulse size was 1 cm^3, the pressure was 4 atm, the flow rate of carrier was 40 cm^3 min^{-1}, and a VZ-7 column was used; (C), the same conditions as (B) but the pulse (1.3 cm^3) was injected from a sampling loop. For the cracking of cumene (isopropylbenzene), the reaction temperature was 623 K, and the pulse size of cumene was 4 mm^3 ($2.9 \cdot 10^{-5}$ mol). The flow rate of carrier gas was 60 cm^3 min^{-1}, and the product benzene was measured with a PEG 20M on celite column operated at 303 - 413 K. Dehydration of ethyl (ethanol), *sec*-propyl (*2*-propanol) and *tert*-butyl (*2*-methyl-*2*-propanol) alcohol was carried out at 523, 423 and 373 K, respectively, in 60 cm^3 min^{-1} of helium. The pulse size of alcohol was 10 mm^3 ($1.7 \cdot 10^{-4}$, $1.3 \cdot 10^{-4}$ and $1.1 \cdot 10^{-4}$ mol for ethyl, *sec*-propyl and *tert*-butyl alcohol, respectively), and the product ethylene (ethane), propylene (propene) and isobutene (*2*-methylpropene) were analyzed with a column of Porapak-Q operated at 353 K. Because the activity for the dehydration of *tert*-butyl alcohol was high, the experiments were not carried out under the differential conditions; the activity was compared over the same amount (5 mg) of catalyst. For some experiments, the pretreatment temperature was varied in order to show the influence of the degree of surface hydration.

Results

As shown in Figure 2 - 1 - 1, $Si(OCH_3)_4$ was readily deposited on alumina at 593 K. The deposition ceased quickly; however, it continued by repetition of the introduction of vapor and evacuation. The deposition was performed intermittently, and the sample weight increased gradually.

Thus, the samples with various amounts of silica were prepared as shown in Table 2 - 1 - 1. The surface concentration of silicon atom was defined from the loading and the BET surface area by the following equation;

Si concentration = number of deposited Si (atoms g-cat^{-1}) / surface area (nm^2 g^{-1} = 10^{-18} m^2 g^{-1}); number of Si = l_1 (SiO_2 loading, g-SiO_2 g-cat^{-1}) / 60.08 (formula weight of SiO_2) × 6.022 · 10^{23} (Avogadro number); $l_1 = l_2 / (l_2 + 1)$, where l_2 is the SiO_2 loading shown by the weight ratio of SiO_2 / Al_2O_3 like Table 2 - 1 - 1.

In the following description, the loading will be expressed by the Si concentration in order to imagine the surface structure in the atomic order.

The BET surface area divided by the weight of sample looked as if it decreased with increasing the concentration of Si, as shown in Figure 2 - 1 - 2 (○). However, this was simply caused by the increment of sample weight. The BET surface area divided by the weight of alumina (●) was almost unchanged by the loading of silica. It slightly increased in the range of Si concentration below 12 nm^{-2}, and kept constant by further deposition.

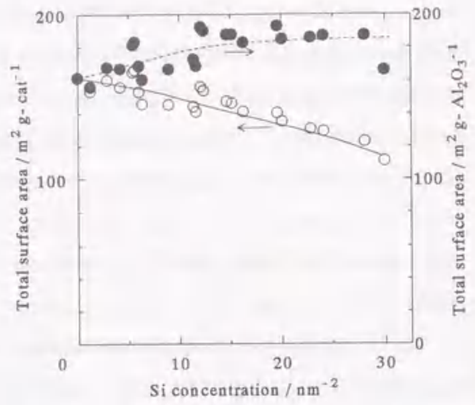

Figure 2 - 1 - 2 : Change of BET surface area divided by the weight of sample (○) and by the weight of alumina (●).

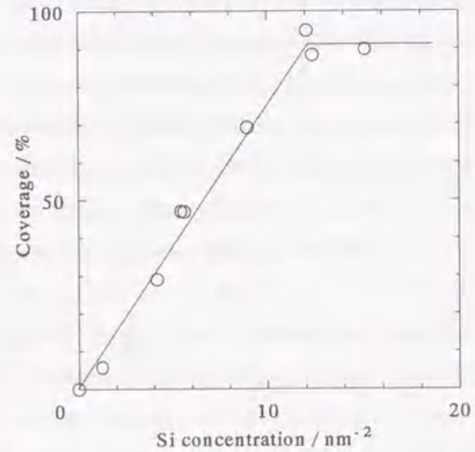

Figure 2 - 1 - 3 : Coverage on surface by silica measured by BAT method.

The coverage measured by the BAT method is shown in Figure 2 - 1 - 3. The coverage increased proportionally to the Si concentration, and arrived at 95 %. By extrapolating the linear relationship against the Si concentration, the coverage is estimated to reach 100 % at 13 Si nm^{-2}. Further deposition kept the constant coverage at 90 - 95 %.

Figure 2 - 1 - 4 shows the IR spectra of alumina and the deposited samples. Alumina exhibited four kinds of hydroxyl groups as described in the previous literature[10] (exactly, five kinds were described to appear, but one of them could not be seen clearly in these conditions). The deposition of silica changed the spectra. These four Al-OH groups disappeared gradually with the concentration of Si, and new hydroxyl species appeared at 3745 and 3610 cm^{-1} on the samples with > 15 Si nm^{-2} of the concentration. The former is clearly ascribable to the isolated silanol (Si-OH)[11].

The adsorption of ammonia complicatedly changed the hydroxyl region of spectrum. A large peak of ammonium cation (1455 cm^{-1}) adsorbed on Brønsted acid site was observed on the sample with silica, but not for the pure alumina (Figure 2 - 1 - 5). The ammonia molecule adsorbed on Lewis acid site (1620 cm^{-1}) was observed on alumina, and it was weakened by the deposition, because this peak became small on the silica-modified sample. The spectra of adsorbed pyridine (Figure 2 - 1 - 6) also showed the generation of Brønsted acidity on the coated sample, because the absorption of pyridinium cation (1545 cm^{-1}) was observed with the CVD of silica in place of the spe-

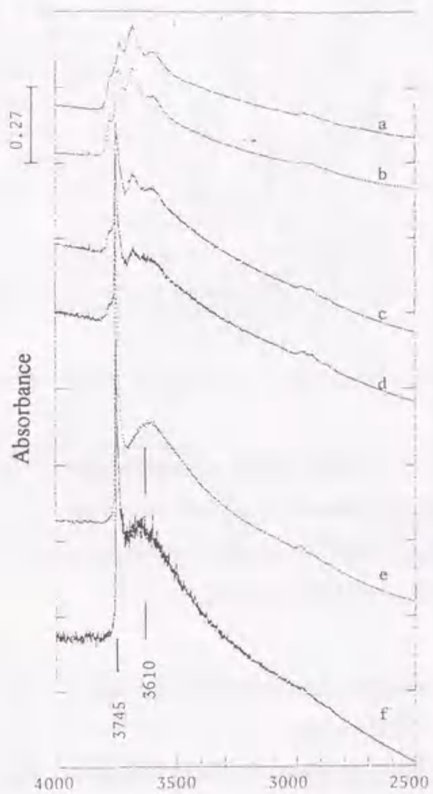

Figure 2 - 1 - 4 : Hydroxyl region IR spectra of alumina (a) and silica-modified alumina (b: 1.2 Si nm^{-2}, c: 4.2 Si nm^{-2}, d: 5.6 Si nm^{-2}, e: 15.1 Si nm^{-2} and f: 22.8 Si nm^{-2}) evacuated at 673 K.

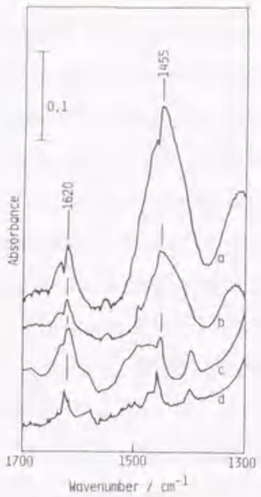

Figure 2 - 1 - 5 : IR spectra of ammonia adsorbed on alumina (c, d) and the sample with 15 Si nm^{-2} (a, b) after evacuation at 373 (a, c) and 473 K (b, d).

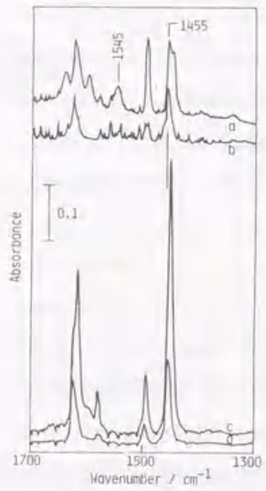

Figure 2 - 1 - 6 : IR spectra of pyridine adsorbed on alumina (c, d) and the sample with 15 Si nm^{-2} (a, b) after evacuation at 423 (a, c) and 573 K (b, d).

cies coordinated on the Lewis acid site (1455 cm^{-1}) of alumina.

For double-bond isomerization from *1*- to *2*-butene after the pretreatment at 673 K, very little activity was observed on alumina. The deposition of silica obviously created the activity, and the maximum activity was obtained on the sample with 12 nm^{-2} of the Si concentration over various experimental conditions. Further deposition again decreased the activity, as shown in Figure 2 - 1 - 7. The change of activity at > 20 Si nm^{-2} was complicated. The maximum activity was comparable to that on the conventional silica-alumina (Table 2 - 1 - 2). The

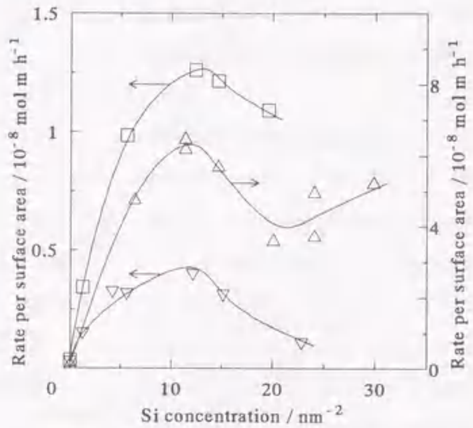

Figure 2 - 1 - 7 : Activity for double-bond isomerization of *1*-butene at 393 K under the conditions (A) [▽], (B) [□] and (C) [△] over silica-modified alumina pretreated at 673 K.

Table 2 - 1 - 2 : Comparison of activities on alumina, deposited silica layer, conventional silica-alumina and silica gel pretreated at 673 K.

Catalyst	Activity per surface area / 10^{-10} mol m h^{-1} for				
	cracking of cumene 623 K	isomerization of *1*-butene (*cis* / *trans*)† 393 K	dehydration of alcohols ethyl 523 K	*sec*-propyl 423 K	*tert*-butyl 373 K
Alumina (ALO4)	0.0	3.6 (3.3)	97	59	18
12 Si nm^{-2} / alumina	5.5	126 (1.9)	32	67	515
Silica-alumina (N631-L)	89	183 (1.3)	62	not measured	688
Silica gel	0.1*	0.1 (2.3)**	0.0**	not measured	1.1**

†: Conditions (B) (see text). *: N602-A. **: Micro Bead 4-B

Table 2 - 1 - 3 : Ratio of *cis* / *trans* measured by varying conversion at 333 K under conditions (A).

Catalyst	Conversion / %	cis / trans
Silica-modified alumina (15 Si nm^{-2})	9	1.08
	12	1.09
Silica-alumina (N631-L)	5	0.82

activity was clearly generated on the interface between silica and alumina, because both silica and alumina showed almost no activity.

Over the most active sample (12 Si nm^{-2}), *cis* / *trans* ratio was 1.9, while that on alumina was higher (3.6). The *cis* / *trans* ratio was also measured on the sample with 15 nm^{-2} of silicon at 333 K with varying the conversion in order to determine the initial selectivity, as shown in Table 2 - 1 - 3. The *cis* / *trans* ratio was almost 1 under these conditions, and this was similar to the case of conventional silica-alumina. In conclusion, the initial ratio of *cis* / *trans* was 1 - 2 on the silica-modified sample.

The dependence of activity on the pretreatment temperature is shown in Figure 2 - 1 - 8. After the pretreatment at 393 K, the activity was quite low in 0 - 12 Si nm^{-2} of the Si concentration range. The activity in this Si concentration range was shown to be enhanced by the dehydration of surface in the pretreatment. Above 15 Si nm^{-2}, similar activities were obtained after the pretreatment at 393 - 673 K. As a result, the dependence of activity on the Si concentration was changed by the pretreatment temperature. At 393 K of the pretreatment temperature, the activity was low below 12 Si nm^{-2}, and jumped at 15 Si nm^{-2}. At 523 K, it gradually increased with the Si concentration from 0

to 15 Si nm^{-2}. Above 673 K, it showed the maximum at 12 Si nm^{-2} as described previously.

As shown in Table 2 - 1 - 2, very small activity for the cracking of cumene appeared on the deposited silica pretreated at 673 K in comparison with the conventional silica-alumina. This small activity was generated by the deposition, and showed the maximum at 12 nm^{-2} of the concentration of Si, as shown in Figure 2 - 1 - 9. The pretreatment temperature (673 or 743 K) did not affect the activity.

A high activity was observed on alumina pretreated at 523 K for the dehydration of ethanol, as shown in Figure 2 - 1 - 10 (○ and ●). The activity slightly increased with the small amount of silica, and decreased from 1 to 15 Si nm^{-2}, in the case that the pretreatment was done at 573 K. On some samples, the pretreatment temperature was changed into 673 K, but this did not affect the activity. Therefore, it is concluded that the activity for the dehydration of ethanol decreased with the CVD of silica in this pretreatment temperature range, whereas the conventional silica-alumina possessed a high activity as shown in Table 2 - 1 - 2.

The activity for dehydration of *tert*-butyl alcohol was created by the deposition of silica, as shown in Figure 2 - 1 - 10 (△).

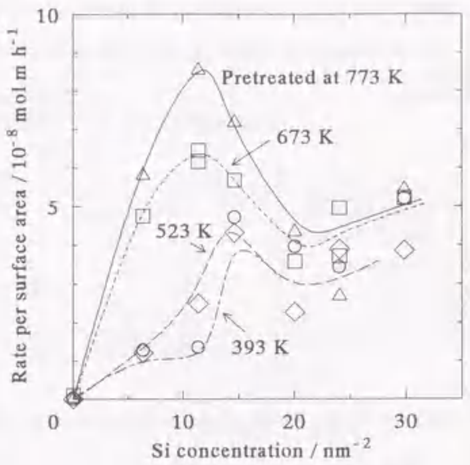

Figure 2 - 1 - 8 : Activity for isomerization of 1-butene at 393 K after pretreatment at 393 (○), 523 (◇), 673 (□) and 773 K (△). The conditions were (C) (see text).

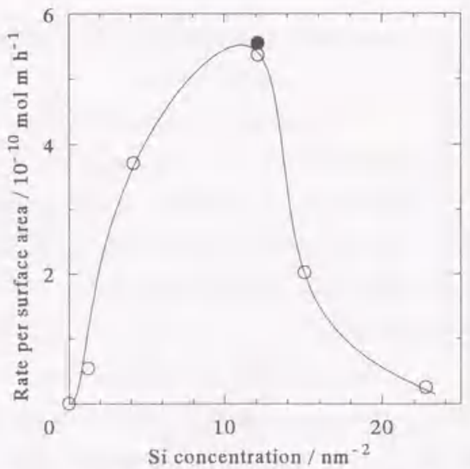

Figure 2 - 1 - 9 : Activity for cracking of cumene (623 K) over silica-modified alumina pretreated at 673 (○) and 743 K (●).

In contrast with the case of ethanol, the activity was monotonously enhanced by the Si concentration. The activity on the sample with 12 Si nm^{-2} was comparable to that on the conventional silica-alumina, and those on the samples with > 15 Si nm^{-2} were higher (Table 2 - 1 - 2).

Change of the activity for dehydration of *sec*-propyl alcohol was complicated (□). It once increased with the deposition of 1 nm^{-2} of Si, and then decreased at 1 to 4 Si nm^{-2}. In this region, the change seems similar to the change of activity for the dehydration of ethanol. The deposition of 5 to 15 nm^{-2} of Si slightly enhanced the activity, and further deposition kept the high activity. The change of activity seems similar to the case of *tert*-butyl alcohol in this Si concentration region.

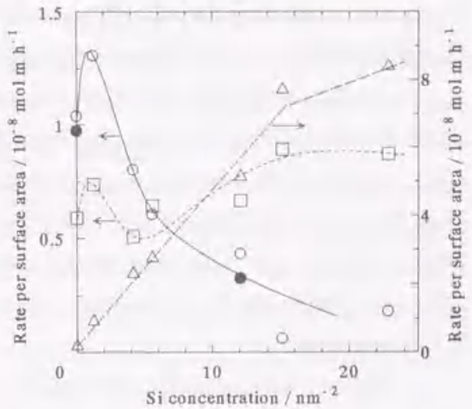

Figure 2 - 1 - 10 : Activity for dehydration of ethyl (523 K, ○ and ●), *sec*-propyl (423 K, □) and *tert*-butyl (373 K, △) alcohol over silica-modified alumina pretreated at 573 (●) and 673 K (○, □ and △).

Discussion

Formation of Silica Monolayer

The BET surface area divided by the weight of alumina was almost unchanged by the loading of silica. This shows no formation of neither silica particle which blocks the micro pore of alumina nor porous particle of silica which increases the surface area.

The linear increase of coverage by silica with increasing Si concentration indicates a common structure of silica in low to high surface concentrations. On extrapolating the linear relationship, about 13 Si nm^{-2} is required for fully covering the alumina surface. Since the surface concentration of aluminum cation is reported to be 14.5 to 9.3 nm^{-2} [12], depending on the exposed face, the silicon concentration required for the full coverage is close to that of cation on alumina. The formation of 1 : 1 bonding between silicon and aluminum (Al-O-Si) upon deposition of silicon alkoxide on alumina is thereby rationalized. In other words, the monolayer of silica was formed until the alumina

surface was almost fully covered. The coverage by the silica layer is supported by the IR measurement of surface hydroxides, because Si-OH appeared in place of Al-OH.

In place of the silica monolayer, it is possible to assume the surface aluminosilicate compound on which benzaldehyde is not adsorbed. Even in this case, the low adsorption amount of benzoate anion shows the compound mainly consists of SiO_2, and the thickness must be ultra thin because it completely covers the surface with only 13 nm^{-2} of Si atoms. Although the micro structure has been unknown, the surface layer can be regarded as the silica monolayer because of the highly siliceous composition and the mono-atomic order thickness. Further structural analysis will be made in the next chapter.

These observations suggest the deposition of $Si(OCH_3)_4$ on alumina is preferred compare to silica deposited. Otherwise, silicon alkoxide would accumulate on the deposited silica as well as on alumina to form the thick layer or particle of silica. The site-specific deposition may be due to the properties of support and deposit reagent or oxide. In this case, alumina is regarded to be a basic medium, whereas silica, an acidic oxide. These different properties seem to make it easy to form the interface layer. In the previous studies using the BAT method on spreading of vanadium[13] and molybdenum[14] oxides on supports, a similar conclusion was drawn; the more the difference in electronegativities of cations of support and promoter, the easier promoter spreads on support. These phenomena may be fundamentally based on the readiness of formation of chemical bonds between different elements. Of course, the silicon precursor has a trend to polymerize itself. The role of conditions and procedure are also supposed. The origin of formation of monolayer will be clarified in the next chapter.

Silica is doubly accumulated, as found from the Si concentration. However, there is no evidence of the formation of double-layer, because the coverage by secondly deposited silica cannot be measured. Characterization and test reactions thereon will help one to understand the structure shown below.

Generation of Brønsted Acid Site on Silica Monolayer

The IR investigation using the basic probe adsorbents indicates the diminishing of Lewis acid sites and the generation of Brønsted acidity on the deposited silica. The initial *cis* / *trans* ratio in the products of isomerization of *1*-butene is reported to show the type of active site[4]: the ratio *ca.* 1 (1 to 2) shows Brønsted acid, because the reaction on the Brønsted acid site must proceed *via* the butenyl cation [CH_3-CH^+-CH_2-CH_3] formed by the protonation of *1*-butene, and the same amount of

trans- and *cis-2*-butene should be formed from it; such high ratio as more than 5 shows the base or Lewis acid-base dual site, because *cis* isomer is easy to be formed from the intermediate strongly adsorbed on these sites locates on solid surface. The observed ratio was 1 to 2 on the silica monolayer. This shows that the reaction was catalyzed by the Brønsted acid site.

The activity for the isomerization of *1*-butene was significantly affected by the pretreatment temperature. The reaction after the pretreatment at > 673 K must show the surface acidity without the influence of adsorbed water molecule. Under these conditions, the active species is ascribable to the silica monolayer, because the activity was created by the formation of monolayer, and the maximum was observed at 12 Si nm^{-2} where the monolayer fully covered the surface. Therefore, the hydroxyl species on the silica monolayer, *i.e.* Al-O-Si-OH, is suggested to be the Brønsted acid site active for the isomerization.

The enhanced activity again decreased with further deposition of silica. This indicates the accumulation of further silica layer on the monolayer, and diminishing of Brønsted acid sites by topping one more layer. In other words, the species Al-O-Si-O-Si-OH had no acidity. However, the change of activity is complicated in > 15 Si nm^{-2} of the Si concentration region. This suggests that the simple layered structure was not constructed on the monolayer, probably due to the random deposition forming a heterogeneous structure.

The activity of monolayer for the isomerization of *1*-butene was comparable to that of the conventional silica-alumina. On the other hand, it showed a quite small activity for the cracking of cumene, which was known to proceed on such a strong Brønsted acid site as found on zeolites[8]. In comparison with the cracking of cumene, the double-bond isomerization of olefin is known to be catalyzed by various acidic materials even if the strength is quite weak[4]. These findings indicate weak strength of Brønsted acid sites on the silica monolayer.

The enhancement of activity is also found for the dehydration of *tert*-butyl alcohol, but the activity monotonously increased even with > 12 Si nm^{-2} of Si, unlike for the isomerization of butene. This should be related with the dependence of activity for the isomerization of butene on the pretreatment temperature. Under the humid conditions, *i.e.* after the pretreatment at 393 K, the samples with the Si concentrations below 12 nm^{-2} showed the low activities for the isomerization, and the activity increased with Si more than 15 nm^{-2}. These results suggest that the activity on monolayer is affected by water molecule adsorbed on the exposed surface of alumina in the case of low concentration of Si below 12 nm^{-2}, but less affected on the samples with >15 nm^{-2} of silicon because the exposed surface was rarely remained. Since it is difficult to analyze the structure and chemical behav-

ior of hydrated surface, further explanation is still impossible. However, it is presumed that the dependence of activity for the dehydration of *tert*-butyl alcohol on the Si concentration is confused by the water formed by the reaction itself. It is thus concluded that the weak Brønsted acid site on the silica monolayer catalyzed also the dehydration of *tert*-butyl alcohol.

The dehydration of ethanol is the different case from those mentioned above, because the activity is ascribable to the exposed alumina surface. It has been known that primary and secondary alcohols are dehydrated by a concerted mechanism on the acid-base dual sites or coordinately unsaturated site, formed upon dehydration of alumina surface[7]. The deposition of silica inhibited the reaction through this reaction path. Although the different reaction mechanism, *i.e.* the path through the protonation by the Brønsted acid site to form the CH_3-CH_2^+ cation, is possible, it seems that the strength of Brønsted acid site of silica monolayer is not enough to catalyze this reaction path. As a result, the activity was decreased by the CVD of silica. The conventional silica-alumina is considered to catalyze this reaction by the latter mechanism.

The change of activity for dehydration of *sec*-propyl alcohol is complex. This reaction is probably catalyzed by the dual sites or coordinately unsaturated site on the pure alumina like that for ethanol. The deposited silica layer inhibited this reaction path, but the monolayer seems to have the activity *via* the protonation of this alcohol to form propenyl cation [CH_3-CH^+-CH_3]. Moreover, the activities of samples with < 12 nm^{-2} of Si was weakened by the product water like as found for *tert*-butyl alcohol, and this mislead the understanding of activity. Therefore, the activity randomly changed with the Si concentration, but the silica monolayer, as well as alumina, seems to be active for this reaction.

This behavior of dehydration activity was caused by the difference in basicity of primary, secondary and tertiary alcohols. The basicity is ordered as *tert*-butyl > *sec*-propyl > ethylalcohol, because the substitution of methyl group in place of hydrogen enhances the basicity[15]. According to this, the stronger basic alcohol is catalyzed by the weaker acid site[6]. The activity for the dehydration of *tert*-butyl and *sec*-propyl alcohols and lack of activity for ethanol support that the strength of Brønsted acid site on the silica monolayer is weak. The change of activity by the CVD of silica was distinct for the type of alcohols: the activity decreased for ethanol, almost same for *sec*-propyl alcohol and increased for *tert*-butyl alcohol. This strongly supports the diminishing of Lewis acid site and acid-base dual sites on alumina and the formation of relatively weak Brønsted acid site on the silica monolayer.

Sato *et al.* investigated the acidic property of alumina modified with silica by the CVD

method similar to this study; the conditions for CVD was so different[16]. On the basis of the fact that the maximum activity was obtained with different SiO_2 loadings for different reactions as shown in Figure 2 - 1 - 11, they proposed that the modification effect for acidity of alumina by silica is continuously varied by loading. This phenomenon can be explained by the influence of adsorbed water. Anyway, this catalyst is reported to be active for the cumene cracking, and so that, strong Brønsted acid sites are presumed. Imizu *et al.* also reported the generation of acidity on silica-modified alumina[17]. The acidic properties of these types of silica layers is related with the structures and will be discussed in the next chapter.

Very recently, Sheng *et al.* reported the acidic property of silica layer prepared by a similar method to the present study; the CVD of $Si(OCH_3)_4$ was carried out on a γ-alumina sample at 593 K in a continuos-flow system[18]. They clearly showed the generation of Brønsted acid site on the monolayer by means of the combination of temperature programmed desorption (TPD) and nuclear magnetic resonance (NMR) of alkyl phosphine. As shown in Figure 2 - 1 - 12, the amount of Brønsted acidity reached maxima when the Si concentration arrived at 8 nm^{-2}, which was near to the Si concentration on the monolayer

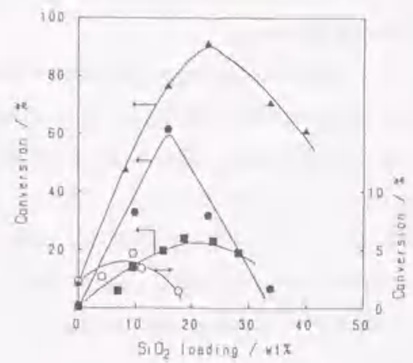

Figure 2 - 1 - 11 : Dependence of activity for cracking of cumene (●) and *n*-heptane (○), dehydration of *2*-butanol (▲) and isomerization of *m*-xylene (■) on amount of deposited silica reported by Sato *et al.*[16]

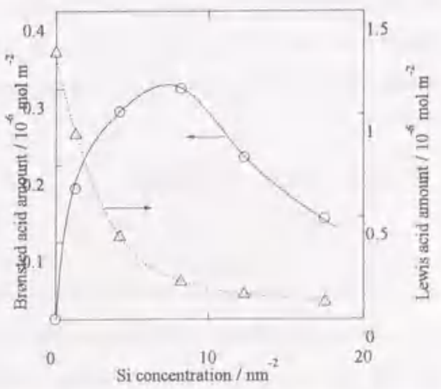

Figure 2 - 1 - 12 : Brønsted (○) and Lewis (△) acid amount on silica-modified alumina determined by Sheng *et al.*[18]

shown by the present study. This strongly supports the formation of Brønsted acidic hydroxyl species on the monolayer.

In zeolites the strong acid sites are generated by isomorphous substitution aluminum cations in the tetra-coordinated cation site of silica matrix. The high activities for the cumene cracking and dehydration of ethanol on the conventional silica-alumina clearly shows the presence of strong acid sites on it. The conventional mixed-oxide catalyst has a wide distribution of acid strength probably due to the acid sites of both substituted aluminum and the Al-O-Si-OH species, and possibly, interfaces with other structures. In contrast, the silica monolayer prepared by the CVD method is shown to have a narrow distribution of acid strength, and this suggests only one type of weak Brønsted acid sites on it.

Lack of strong acidity is in agreement with the conclusion by Kawakami *et al.* on the basis of the quantum chemical calculations[19]. They proposed a distorted structure consisting of tetra-coordinated silicon and aluminum for the strong Brønsted acid sites, whereas silanol attached to tri-coordinated aluminum with a long distance between Al and H (Al-O-Si-OH) has no or weak acidity. Moreover, the present author exactly determined the acid strength and its distribution on zeolites with the TPD method of ammonia and found that the acid strength was determined by the crystal phase of zeolite but not by the composition (Si / Al ratio)[20, 21]. In agreement, the present results show a principle that the acid strength is controlled by the micro structure of acid site. The narrow distribution of acid strength on the silica monolayer is presumably given by the simplicity in structure, and therefore, this novel material can be regarded as a simple model of one type of acid sites on the mixed-oxide solid acid catalyst. There are many kinds of aluminosilicates such as zeolites to be models for the strong acid site, but this material is the first one to be the model of weak Brønsted acid site.

Conclusion

1. Chemical vapor deposition of $Si(OCH_3)_4$ on γ-alumina at 593 K formed a silica monolayer fully covering the surface, which consisted of 1 : 1 bondings of Al-O-Si.
2. The silica monolayer does not possess the strong Brønsted acid site like that on zeolite, but has weak Brønsted acidity to catalyze the double-bond isomerization of olefin and the dehydration of *tert*-butyl alcohol. The hydroxyl species on the monolayer, *i.e.* Al-O-Si-OH, is suggested to be the weak Brønsted acid site. A fine distribution of the acid strength due to the simple structure is expected.

References

1. M. Niwa, Y. Kawashima, T. Hibino and Y. Murakami, *J. Chem. Soc., Faraday Trans. 1,* **84,** 4327 (1988).
2. M. Niwa, S. Inagaki and Y. Murakami, *J. Phys. Chem.,* **89,** 3869 (1985).
3. M. Niwa, K. Suzuki, M. Kishida and Y. Murakami, *Appl. Catal.,* **67,** 297 (1991).
4. J. W. Hightower and W. K. Hall, *Chem. Eng. Proc. Symp. Ser.,* **63,** 122 (1967).
5. T. Okuhara and M. Misono, *Shokubai (Catalyst),* **25,** 279 (1983).
6. Y. Murakami, C. Nishizawa and H. Uchida, *Shokubai (Catalyst),* **13,** 108 (1971).
7. H. Pines and J. Manse, *Adv. Catal.,* **16,** 49 (1966).
8. A. Corma and B. W. Wojciechowski, *Catal. Rev. -Sci. Eng.,* **24,** 1 (1988).
9. S. Burner, P. H. Emmett and E. Teller, *J. Am. Chem. Soc.,* **40,** 1361 (1918).
10. J. B. Peri, *J. Phys. Chem.,* **69,** 211 (1965).
11. J. B. Peri and A. L. Henley, Jr., *J. Phys. Chem.,* **72,** 2926 (1968).
12. H. Knözinger and P. Ratnasamy, *Catal. Rev.- Sci. Eng.,* **17,** 31 (1978).
13. M. Niwa, Y. Matsuoka and Y. Murakami, *J. Phys. Chem.,* **91,** 4519 (1987).
14. H. Yamada, M. Niwa and Y. Murakami, *J. Phys. Chem.,* **94,** 1477 (1990).
15. E. L. Mackor, A. Hofstra and J. H. Van der Waals, *Trans. Faraday Soc.,* **54,** 186 (1958).
16. S. Sato, M. Toita, T. Sodesawa and F. Nozaki, *Appl. Catal.,* **62,** 73 (1990).
17. Y. Imizu, A. Tada and I. Toyoshima, *Shokubai (Catalyst),* **30,** 388 (1988).
18. T. -C. Sheng and I. D. Gay, *J. Catal.,* **145,** 10 (1994).
19. H. Kawakami, S. Yoshida and T. Yonezawa, *J. Chem. Soc., Faraday Trans. 2,* **80,** 205 (1984).
20. M. Niwa, N. Katada, M. Sawa and Y. Murakami, *J. Phys. Chem.,* **99,** 8812 (1995).
21. H. Igi, N. Katada, J.-H. Kim and M. Niwa, in *Proc. Heisei 7 Nendo Shokubai Kenkyu Happy-oukai,* (1995) p. 185.

2-2 Silica Monolayers on Titania and Zirconia

Synopsis

Chemical vapor deposition of tetramethoxysilane [$Si(OCH_3)_4$] was carried out at 593 K on titania and zirconia, which form solid-acids with silica. The deposited silica formed monolayers on titania and zirconia, and showed the Brønsted acidity similar to that on alumina. These two silica deposited oxides showed catalytic activity for only facial reactions, *i.e.* double-bond isomerization of *1*-butene and dehydration of *tert*-butyl alcohol, but showed no activity for cumene cracking and dehydration of ethanol. Surface concentration of silicon atoms on a monolayer about equal to the cation concentration of support surface, and this suggests the affinity of deposited silica towards support oxide. The activities for isomerization of *1*-butene on the silica monolayers loaded on alumina, titania and zirconia were *ca.* 100, 10 and 1, respectively, whereas these catalysts showed similar activity for dehydration of the *tert*-butyl alcohol. These findings suggest that the acid strength of the formed species as a M-O-Si-OH (M = Al, Ti or Zr) is dependent upon the support, and the sequence of acid strength as follows: M = Al > Ti > Zr > Si.

Introduction

According to Tanabe, titania and zirconia form quite strong acid catalysts with silica, like on alumina[1]. The origin of acid site was explained by the combination of coodination number and valence of cations, as shown in Figure 1 - 1. This section will deal with the CVD of silica on these oxides. Since aluminum, titanium and zirconium cation has 6, 6 and 8 of the coordination number and +3, +4 and +4 of the valence, respectively, the origin of acidity will be clarified from the comparison acidic properties of the surface thin layers formed on these metal oxides. The strong acidity on the binary oxide consisted of silica and these metal oxides is explained to be owing to the large electronegativities of cations. Since the electronegativity is estimated as $Zr^{4+} > Ti^{4+} > Al^{3+}$ [1], the order of acid strength on silica monolayers loaded on these supports is also interested. Other properties, for example, the crystal structure, are different for these oxides. Simple acidic character based on the predicted simple structure will make clear which property of support metal oxide controls the acidic property of the silica layer loaded on it.

The characterization methods used in this section are same as those for the silica monolayer on alumina in the previous section: BAT method, IR spectroscopy and several test reactions will be

applied. Particularly, the BAT method will be useful for the silica layer loaded on these supports as well as on alumina, because these oxides have basic properties and adsorb benzaldehyde in high surface concentrations[2].

Experimental

Materials and Chemical Vapor Deposition

Titania was supplied from Nippon Aerosil Co. Ltd., P-25; the surface area was 44 $m^2\ g^{-1}$, and the crystal phase was proven to be anatase with small concentration of rutile. Zirconia was prepared from a $ZrOCl_2$ solution. An aqueous ammonia solution was added to the $ZrOCl_2$ solution in order to hydrolyze to get zirconium hydroxide, which was then dried and calcined in air at 773 K. This was proven to be baddeleyite, and the surface area was 66.4 $m^2\ g^{-1}$. These oxides were used after the exposure to *ca.* 80 % of the relative humidity as alumina.

Because titania was reduced by the high temperature evacuation, the treatment in 200 Torr of oxygen at 673 K for 1 hour was done before the CVD. After this step, the CVD was carried out in the same way as used for alumina. For zirconia, this oxidation step was skipped. After the evacuation of support at 673 K, the vapor of $Si(OCH_3)_4$ (2.5 Torr) was repeatedly introduced. Finally, the sample was oxidized, and the loading was determined from the weight gain. The obtained samples were listed in Table 2 - 2 - 1.

Characterization

The BET surface area and BAT measurements were carried out as described in the previous section. The pretreatment for the BAT measurement were done in flowing oxygen, because the oxidation state of support metal cation affects the concentration of benzoate adsorption on titania and zirconia. Benzoate was ad-

Table 2 - 2 - 1 : Samples prepared by CVD of $Si(OCH_3)_4$ on titania and zirconia at 593 K.

SiO_2 loading wt% (SiO_2 / support)	BET surface area $m^2\ g\text{-}cat^{-1}$	Si concentration nm^{-2}
On titania		
0 (P-25)	44.0	0.0
0.65	45.8	1.4
1.49	45.3	3.3
4.56	46.8	9.3
5.82	46.2	11.9
8.81	46.3	17.5
On zirconia		
0 (ZrO_2)	66.4	0.0
2.47	64.0	3.8
4.38	64.5	6.5
5.52	65.4	8.0
8.77	60.9	13.2

sorbed with 1.6 and 2.2 nm^{-2} on titania and zirconia, respectively, and the coverage was calculated based on these values.

Test reactions to indicate the acidic profile were performed by the pulse technique after the pretreatment at 673 K. Double-bond isomerization of *1*-butene was carried out under two conditions. In order to measure the dependence of activity on Si concentration, conditions shown in the previous section as (A) were used; the pulse (0.1 $cm^3 = 4.2 \cdot 10^{-6}$ mol) was injected from a syringe into 60 $cm^3\ min^{-1}$ flow of carrier gas under the atmospheric pressure. The reaction temperature was 473 and 503 K on titania and zirconia, respectively, and a capillary column (silicone OV 101) was used at room temperature. For comparison of activities among various support oxides, the conditions (B) were adopted; the pulse (1.0 $cm^3 = 4.2 \cdot 10^{-5}$ mol) was introduced into 40 $cm^3\ min^{-1}$ flow of carrier gas under 4 atm of the pressure. The reaction temperature was 393 K, and a VZ-7 column was used. Cracking of cumene was carried out at 623 K on the catalyst pretreated at 673 K, according to the previous section. Dehydration of ethyl and *tert*-butyl alcohols was performed on the catalyst pretreated at 673 K. The reaction temperature for ethanol on titania and zirconia was 573 and 543 K, respectively, and that for *tert*-butyl alcohol was 373 K on both supports. Porapak Q was used at 373 K for product analysis. All of these reactions were carried out under the differential conditions (conversion < 5 %), which were maintained by adjusting either the amount of catalyst or reactant concentration.

Infrared (IR) spectra were recorded by a JASCO FTIR-3 spectrometer on a self-supporting disk as used for alumina. Spectra of adsorbed pyridine and ammonia were taken after adsorption at 423 and 373 K, respectively, on the sample evacuated at 673 K.

Results

Stepwise increase of weight was observed on both titania and zirconia, like on alumina. Figure 2 - 2 - 1 shows the BET surface areas. The total surface area of

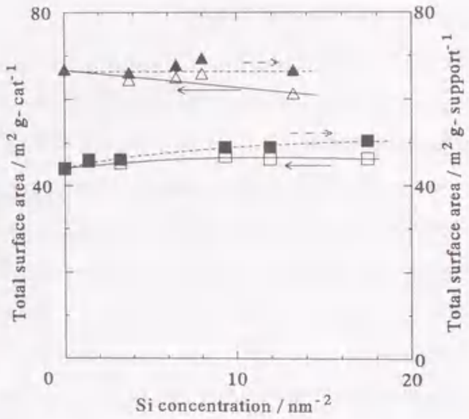

Figure 2 - 2 - 1 : Change of BET surface area divided by the weight of sample (□, △) and by the weight of support (■, ▲) of titania (□, ■) and zirconia (△, ▲).

titania and zirconia was independent of Si concentration, which suggests unblocking of micro-pores of supports by the deposition of silica.

Then, the extent of the support surface covered by silica was measured using the BAT method. The coverage increased monotonously or linearly with the Si concentration on titania and zirconia, and attained more than 90 % as shown in Figure 2 - 2 - 2. Further deposition of silicon did not change the high coverage. The mini-

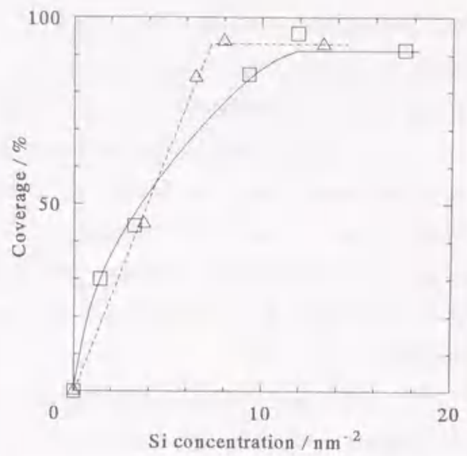

Figure 2 - 2 - 2 : Coverage on titania (□) and zirconia (△) surface by silica measured by BAT method.

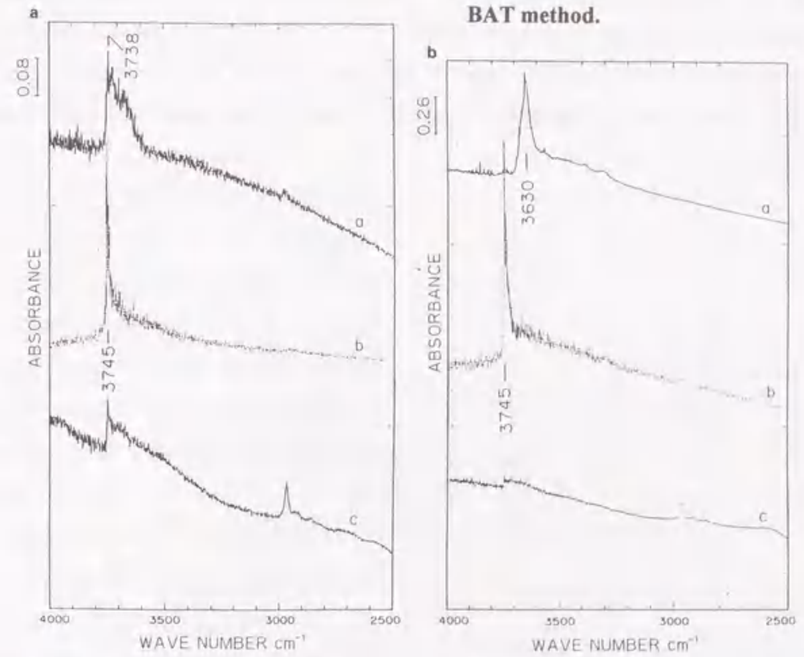

Figure 2 - 2 - 3 : Hydroxyl region IR spectra of support oxide (a), full-coverage monolayer sample (b) and secondary deposited sample (c) on titania (a) and zirconia (b) evacuated at 673 K.

mum concentration of silicon to cover the support completely was found to be 12 and 8 Si nm^{-2} for titania and zirconia, respectively, by extrapolating the linear portion. The catalyst with this concentration of silicon will be termed as the full-coverage monolayer sample in the following description.

Stretching vibration of hydroxyl groups measured by IR spectroscopy showed a clear change by the deposition, as shown in Figure 2 - 2 - 3. Hydroxyl groups observed at 3738 and 3630 cm^{-1} on titania and zirconia, respectively, disappeared and the 3745 cm^{-1}-band ascribable to isolated silanol appeared on the full-coverage monolayer sample. In addition, broad absorptions were overlapped at about 3600 cm^{-1}. Further deposition of silica, *i.e.* after monolayer capacity, intensities of silanols decreased.

Acidity was then characterized by the IR spectroscopy using base molecules, *i.e.* ammonia and pyridine. Adsorption of ammonia revealed a band at 1620 cm^{-1} ascribable to ammonia coordinated on Lewis acid site or hydrogen bonded on the supports, while the ammonium ion band at 1450 cm^{-1} in place of the 1620 cm^{-1} band on the full-coverage monolayer samples. This phenomenon is common on both the supports (Figure 2 - 2 - 4). However, the intensity of ammonium cation band was weak, and almost disappeared upon evacuation at 473 K. Adsorption of pyridine, on the other hand, showed hydrogen-bonded pyridine bands at 1615 and 1455 cm^{-1} both on supports and full-coverage monolayer samples, in Figure 2 - 2 - 5. The intensities were weak on the full-coverage

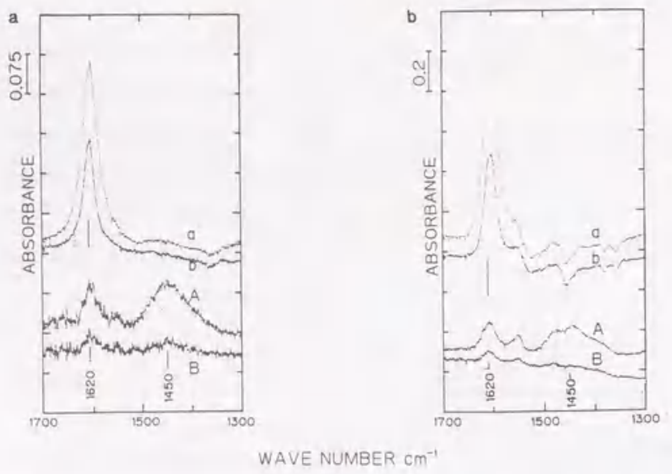

Figure 2 - 2 - 4 : IR spectra of ammonia adsorbed on support (a, b) and full-coverage monolayer sample (A, B) after evacuation at 373 (a, A) and 473 K (b, B): titania (a) and zirconia (b).

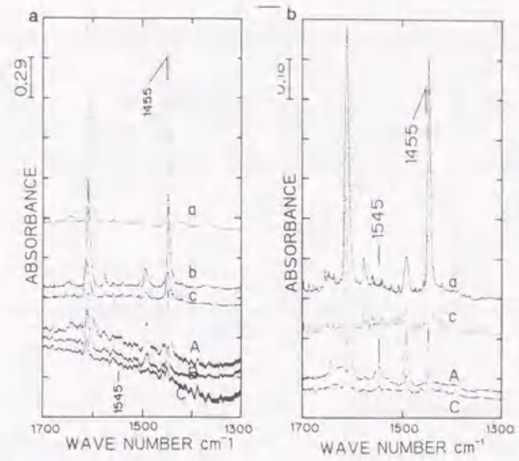

Figure 2 - 2 - 5 : IR spectra of pyridine adsorbed on support (a, b, c) and full-coverage monolayer sample (A, B, C) after evacuation at 423 (a, A), 473 (b, B) and 573 K (c, C): titania (a) and zirconia (b).

monolayer samples, and a small absorption at 1545 cm^{-1} for pyridinium cation was overlapped at 423 K evacuation. The IR spectra of adsorbed bases, thereby, showed the formation of weak Brønsted acid sites on the full-coverage monolayer samples.

The activity for double-bond isomerization of *1*-butene was enhanced by the deposition of silica both on titania and zirconia, as shown in Figure 2 - 2 - 6. The maximum activity was obtained at 12 and 8 Si nm^{-2} on titania and zirconia, respectively, where the coverage arrived at almost 100 %. Further deposition decreased the activity, and almost 20 and 16 nm^{-2} of the Si concentrations seem to be required to inactivate the

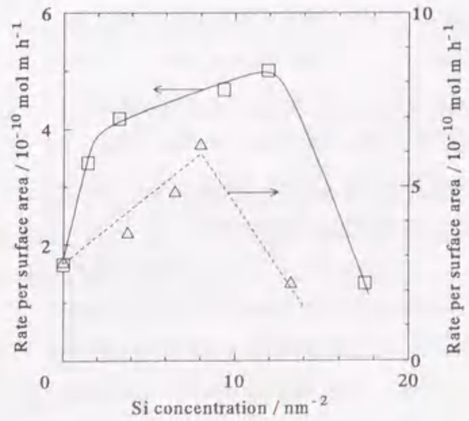

Figure 2 - 2 - 6 : Activity for double-bond isomerization from *1*- to *2*-butene on silica-modified titania (473 K, □) and zirconia (503 K, △).

Table 2 - 2 - 2 : Comparison of activity among silica layers on various supports.

Catalyst	Si concentration nm^{-2}	Activity per surface area / 10^{-10} mol m h^{-1} for isomerization of *1*-butene at 393 K (*cis* / *trans*)	dehydration of *tert*-butyl alcohol at 373 K	cracking of cumene at 623 K
SiO_2 / Al_2O_3	12	126 (1.9)	515	5.5
SiO_2 / TiO_2	12	9.9 (1.2)	933	0.3
SiO_2 / ZrO_2	8	1.5 (1.3)	336	0.2
SiO_2	-	0.1 (2.3)*	1.1**	0.1**
Silica-alumina***	-	183 (1.3)	688	89

*: N602-A. **: Micro Bead 4-B. ***: N631-L.

surface on titania and zirconia, respectively.

The activities on the silica layers loaded on three support oxides were compared under the same conditions, as shown in Table 2 - 2 - 1. The activity on alumina, titania and zirconia was *ca.* 100, 10 and 1, respectively. The smallest activity on the full-coverage sample loaded on zirconia was about 10 times higher than that of silica gel. The *cis*- / *trans*-2-butene ratio was also measured under this quite low conversion (SiO_2 / TiO_2 and ZrO_2, less than 1 %). It was almost 1 on both full-coverage samples loaded on titania and zirconia.

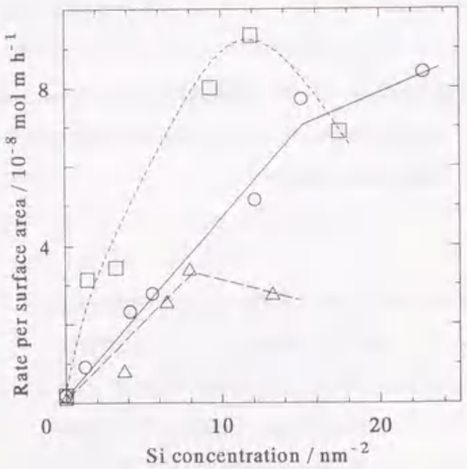

Figure 2 - 2 - 7 : Activity for dehydration of *tert*-butyl alcohol on silica-modified alumina (○), titania (□) and zirconia (△) at 373 K.

Figure 2 - 2 - 7 shows the enhancement of dehydration of *tert*-butyl alcohol by the deposition of silica on titania and zirconia. The activity showed the maximum at 12 and 8 Si nm^{-2} on titania and zirconia, respectively, and this behavior was different from the case of alumina support where a monotonous increase of activity was observed. Table 2 - 2 - 2 shows the activities on the full-coverage monolayer samples on titania and zirconia, which were higher than (titania) or comparable to (zirconia) that of silica-modified alumina and conventional silica-alumina catalyst. This was different from the case for the isomerization of butene. These

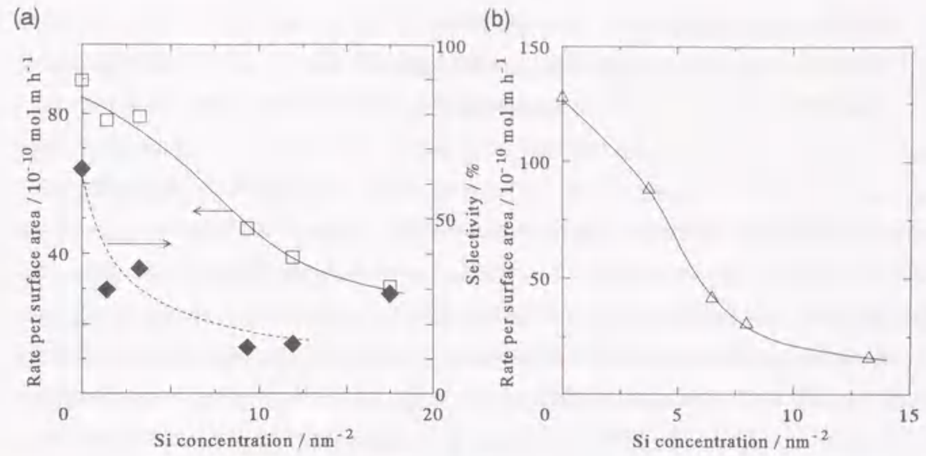

Figure 2 - 2 - 8 : Change of activity for conversion of ethanol by CVD of silica on titania at 573 K (a) and zirconia at 543 K (b). On titania, the total rate of conversion of ethanol into ethylene and butadiene (□) and selectivity for butadiene (◆) are plotted. On zirconia, the rate for ethylene (△) was shown: no butadiene was formed.

activity are shown to be generated by the combination of oxides, because the silica gel had only negligible activity.

This table also shows quite small activities for the cracking of cumene in comparison with that of conventional silica-alumina catalyst.

Finally, catalytic activity for the dehydration of ethanol was shown to decrease with increase of the Si concentration, but it was not inhibited completely (Figure 2 - 2 - 8). Butadiene was formed as a by-product on titania, but the formation of butadiene was also suppressed by the deposition of silica.

Discussion

Formation of Silica Monolayer

Titania anatase has a crystal morphology of tetragonal with dimensions and number of atoms: a = b = 0.379 nm; c = 0.951 nm; Z = 4[3]. Two metal atoms can be exposed in close to the (001) face, and the cation site concentration is estimated less than 14 nm^{-2}. This may be less than 11

nm^{-2} on (010) and (101) faces, and the maximum cation site concentration is thus estimated to be *ca.* 11 to 14 nm^{-2} on titania. On the other hand, zirconia baddeleyite has a monoclinic crystal morphology of 0.532, 0.521, and 0.515 nm in lengths with 4 atoms included[4]. The cation site concentration, based on the same calculation, is less than 7.5 nm^{-2} in every face of the crystal. The maximum cation site concentrations thus estimated on titania and zirconia are 11 - 14 and 7.5 nm^{-2}, respectively, agree well with the lowest concentration of Si to cover the surface of them. It is thereby suggested that the silica monolayers, which consisted of 1 : 1 bondings of M-O-Si (M = Ti or Zr), were formed on titania and zirconia as well as on alumina. The micro structure of monolayer, *i.e.* the arrangements of cations and anions along the surface, is supposed to be similar to that of the support metal oxide surface, because the Si concentration always equal with the concentration of cation on the support oxide surface. In other words, the silica monolayer grows like an epitaxy, as generally found by the CVD at high temperature[5].

A preferential deposition of silicon alkoxide on the support surface rather than on the deposited silica is concluded under the present experimental conditions. Otherwise, fairly big particle of silica would be formed with the exposed surface of support remained. Alumina, titania and zirconia possess the basicity not observed on silica, and it is hence expected that silica spreads easily on them, because in the previous investigation using the BAT method about the spreading of vanadium[6] and molybdenum[7] oxides on various supports, a simple conclusion was obtained; the greater the difference in the electronegativity of cations of support and supported oxide, the easier the spreading of metal oxide on the support. Based upon the aspect, the silica overlayer is expected to spread easily on various basic metal oxides. The formation of thin layer of silica or dispersed silicon species was reported on other basic oxides. Imizu *et al.* reported the CVD of silica on magnesia and generation of acidity as well as on alumina[8]. White and co-workers showed the formation of silica monolayer on zinc oxide by AES (auge electron-) and ISS (ion scattering-spectroscopy) analyses[9]. The present author reported that silica layer with molecular sieving function could be prepared by the CVD of $Si(OCH_3)_4$ using organic template molecule on tin oxide[10]. The formation of thin overlayer strongly suggests stable bondings of M-O-Si between the basic substrate surface and silica.

Linear increase of coverage against the Si concentration on zirconia shows the formation of silica layer with a common structure from the beginning to the fully covering. On titania, however, a subtle difference in structure of silica is suspected, because the relationship between the coverage and Si concentration was not linear. This may be caused by either the heterogeneous distribution of cations on titania (as calculated above) or scrambling of titanium and silicon cations. White and co-workers reported that a homogeneous ultra thin layer was formed when silicon alkoxide was deposited in the ultra-high vacuum apparatus on zirconia[11] and zinc[9] oxides, but such a scrambling occurred on titania. The present study deals with the deposition in vacuum apparatus (< 10^{-3} Torr) below 673 K, and the deposition conditions are not so severe to deteriorate the titania surface.

Generation of Brønsted acidity

Generation of Brønsted acid sites on the full-coverage monolayer sample was confirmed by study of IR measurements as well as test reactions. The IR spectra of base molecules adsorbed on the full-coverage monolayer sample clearly showed the protonated cation of these molecules. The *cis* / *trans* ratio in the isomerization of *1*-butene (*ca.* 1) also shows the Brønsted acidity on the silica-modified samples. In contrast, Lewis acid sites on originally existed on supports, which were shown by IR spectra, disappeared with covering by the monolayer. The activity for dehydration of ethanol was lost presumably because of the diminishing of Lewis acid sites. The decrement of selectivity for butadiene from ethanol was also consistent with the fact that the titania surface with an original activity for dimerization was lost and the surface was covered by the simply Brønsted acidic monolayer.

Weakness of the acid sites is estimated from IR experiments, because the intensity of ammonium cation band was weak, and almost disappeared upon evacuation at 473 K. Because only facile reactions, olefin double-bond isomerization and dehydration of *tert*-alcohol were catalyzed, test reactions also revealed the strength of acidity to be weak, as observed on alumina. The maximum activities for these two reactions were obtained when the monolayer fully covered the surface. The acidity of silica monolayer was shown to diminish at 16 and 20 Si nm^{-2} on titania and zirconia, respectively. This indicates that deposition of one more layer can inactivate the acid site. Thus the generation of Brønsted acid site on silica monolayer was evidenced on these oxides. The acidic species is suggested to be M-O-Si-OH (M = Ti or Zr) also on these monolayers.

The activity for isomerization of butene was *ca.* 100 : 10 : 1 on the monolayers loaded on alumina, titania and zirconia. Since pure silica is regarded as a surface silica layer on silica, the activity of surface silica layer is determined by the support as $Al_2O_3 > TiO_2 > ZrO_2 > SiO_2$. On the other hand, the activity for dehydration of *tert*-butyl alcohol was comparable on the three monolayers. The secondary carbenium cation $CH_3\text{-}CH^+\text{-}CH_2\text{-}CH_3$ is supposed for the intermediate of isomerization of *1*-butene, while the tertiary carbenium cation $(CH_3\text{-})_3C^+$ for the dehydration of *tert*-butyl alcohol. Since the latter is easy to be formed by the weak acid site, quite weak acid can catalyze the dehydration. The catalytic behavior for these two reactions therefore suggests a not so large difference in the acid amount among the silica monolayers, and the order of acid strength of M-O-Si-OH species as M = Al > Ti > Zr > Si. A fine distribution of acid strength, which is suggested by the

simple structure, is considered to give the clear difference in the activity for the isomerization.

Tanabe proposed that the acid site is generated by the difference in coordination number and charge between two kinds of metal cations[1]. However, the coordination number of Al, Ti, Zr and Si in the pure oxide is 6, 6, 8 and 4, and the valence is +3, +4, +4 and +4, respectively. However, the acid strength was independent of these parameters. The acid strength of mixed-oxide is explained to be determined by the averaged electronegativity of cations of two components. The calculation of electronegativity of metal cation has been proposed[12], and dependence of acid strength on thus calculated parameter was shown[1]. However, the order of electronegativity of cation is $Ti^{4+} > Zr^{4+} > Al^{3+}$ [1]. All of these parameters are not correlated with the order of acid strength on the silica monolayer. The other explanation is required to understand the principle of generation of acid site on silica monolayer, and it will be discussed in the next chapter based on the micro structure of silica layer.

Conclusion

1. Like on alumina, chemical vapor deposition of $Si(OCH_3)_4$ at 593 K formed silica monolayers on titania and zirconia. The Si concentration on the monolayer agreed with the concentration of cation on the support oxide. Structural affinity, *i.e.* similar arrangements of cations and anions, is suggested between the loaded monolayer and support oxide.
2. The monolayer possessed weak Brønsted acidity, and a fine distribution of strength owing to the simple structure is suggested. The strength of proposed species M-O-Si-OH is estimated as M = Al > Ti > Zr > Si from test reactions.

References

1. K. Tanabe, in *Catalysis: Science and technology, Vol. 2,* eds. J. R. Anderson and M. Boudart, Springer-Verlag, Berlin (1981) p. 231.
2. M. Niwa, K. Suzuki, M. Kishida and Y. Murakami, *Appl. Catal.,* **67,** 297 (1991).
3. *Powder Diffraction File,* ed. International Centre for Diffraction Data, Pennsylvania (1988) vol. 21, p. 1272.
4. *Powder Diffraction File,* ed. International Centre for Diffraction Data, Pennsylvania (1988) vol. 36, p. 420.
5. H. O. Pierson, *Handbook of Chemical Vapor Deposition: Principles, Technology and Applications,* Noyes Publications, New Jersey (1992).
6. M. Niwa, Y. Matsuoka and Y. Murakami, *J. Phys. Chem.,* **98,** 7647 (1994).
7. H. Yamada, M. Niwa and Y. Murakami, *J. Phys. Chem.,* **94,** 1477 (1990).
8. Y. Imizu, A. Tada, K. Tanaka and I. Toyoshima, *Shokubai (Catalyst),* **29,** 98 (1987).
9. S. K. Jo, T. Jin and J. M. White, *Appl. Surf. Sci.,* **40,** 155 (1989).
10. N. Kodakari, N. Katada and M. Niwa, *J. Chem. Soc., Chem. Commun.,* **1995,** 623.
11. T. Jin and J. M. White, *Surf. Interface Anal.,* **11,** 517 (1988).
12. K. Tanaka and A. Ozaki, *J. Catal.,* **8,** 2 (1967).

2-3 Application to Beckmann Rearrangement of Cyclohexanone Oxime into ε-Caprolactam

Synopsis

Silica monolayers prepared on γ-alumina, zirconia and titania were used for an industrially important reaction, Beckmann rearrangement of cyclohexanone oxime. Formation of ε-caprolactam was enhanced by deposition of silica, whereas side reactions and deactivation were decreased. On alumina, yield of ε-caprolactam showed a maximum at *ca.* 15 Si nm^{-2}, where the monolayer covered the surface almost completely. The deposition of silica enhanced the formation of ε-caprolactam on zirconia and titania as well. Silica gel was inactive compared to the monolayers. These findings show that the rearrangement requires acidity, and the weak Brønsted acid sites on the monolayers are therefore considered to be active. In spite of the difference in the acid strength of M-O-Si-OH, where M = Al, Ti and Zr, similar activities for the Beckmann rearrangement were observed over these monolayers. Therefore, the rearrangement is considered to be insensitive to the strength of Brønsted acid sites. The simple structure and acidic property of silica monolayer thus clarified the role of acid site for this complex reaction.

Introduction

ε-Caprolactam is an industrially valuable compound because it is the starting material for 6-nylon. An important route to produce ε-caprolactam is the Beckmann rearrangement of cyclohexanone oxime (Figure 2 - 3 - 1) catalyzed by sulfuric acid in the liquid phase. This method, however, has draw backs such as corrosion of the equipment and co-production of waste salt. In order to overcome these problems, the vapor-phase Beckmann rearrangement has been investigated over various solid-acid catalysts, such as metal phosphates[1, 2], tungsten oxide[3], silica-alumina[4, 5], supported boria[6 - 8], clay[9] and zeolites[10 - 12]. However, the reaction mechanism is complex because cyclohexanone oxime

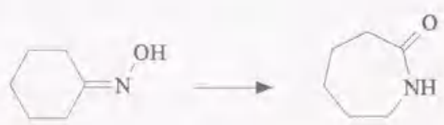

Figure 2 - 3 - 1 : Reaction formula of Beckmann rearrangement of cyclohexanone oxime.

is highly reactive so that a number of intermediate species and by-products can be considered, and this makes difficult to understand what type of acid site is active. Recently, Aucejo *et al.* proposed that the rearrangement is catalyzed by Brønsted acid sites with a strength pKa < 1.5 over Y type zeolite[13]. Takahashi *et al.* reported that the acid strength of ZSM-5 was weakened by modification with boria, and simultaneously the activity was enhanced[14]. Sato *et al.* found that the rearrangement proceeded over weak acid sites located in a region near the external surface of HY zeolite, rather than over the strong acid sites in the micro pores[15]. Thangaraj *et al.*[16] and Reddy *et al.*[17] revealed that titanium silicate and silicalite exhibited a high activity and selectivity in comparison with the zeolites. Based on those studies, it was suggested that weak Brønsted acid sites catalyze the Beckmann rearrangement. However, the relationship between acidic properties and activity has not been clarified, because these investigations were carried out over catalysts with a wide range of acid strength. Moreover, Sato *et al.* reported that silicalite catalyzed the Beckmann rearrangement[18]. It is thus unclear whether the rearrangement requires Brønsted acidity or proceeds even on a neutral catalyst.

The previous sections described that the silica monolayers were prepared by the CVD of $Si(OCH_3)_4$ on alumina, titania and zirconia; weak Brønsted acidity was observed on the species M-O-Si-OH, and the acid strength was determined by the support as M = Al > Ti > Zr. Usual mixed oxides, *e.g.* silica-alumina, often have a wide distribution of acid strength, and / or both of Lewis and Brønsted acid sites. In contrast with such catalysts, the silica monolayer possessed only weak Brønsted acid sites, which catalyzed only facile reactions such as double-bond isomerization of olefin. Hydroxyl species on the monolayer like M-O-Si-OH are supposed to possess weak acidity with a sharp distribution of strength based on the simple structure.

In the present section, the silica monolayer was applied as a model solid-acid catalyst to Beckmann rearrangement of cyclohexanone oxime. The monolayer is expected to make clear the catalytic activity of weak Brønsted acid sites, and moreover, to help understanding the relationship between acidic property of catalyst and catalytic activity for this complex reaction.

Experimental

Silica was deposited on γ-alumina, titania and zirconia as described in the previous sections; the deposition temperature of $Si(OCH_3)_4$ was 593 K. Beckmann rearrangement of cyclohexanone oxime was carried out in a flow reactor made of Pyrex glass under atmospheric pressure. Prior to the reaction, the catalyst was dried at 673 K in helium for 1 hour. A mixture of cyclohexanone ox-

ime, toluene and helium (1 : 26 : 30 molar ratio) was passed into the reactor at 623 K and W (weight of catalyst) / F (flow rate of mixed gas) = 1.6 or 0.14 g-cat h mol^{-1}. The products were trapped in acetone at 195 K, and analyzed with a column of diethyleneglycol succinate (DEGS) with H_3PO_4 at 533 - 683 K. ε-Caprolactam, cyclohexanone and some other by-products were detected by a flame ionization detector (FID). Activity of a silica gel (Nikki Kagaku N-602A, 281 $m^2 g^{-1}$) was measured as a comparison.

Results

Figure 2 - 3 - 2 shows the change of catalytic activity on alumina by deposition of silica at W / F = 1.56 g h mol^{-1}. The cyclohexanone oxime conversion was near 100 % over the unmodified alumina, but the ε-caprolactam yield was only 23 %. Simultaneously, 17 % yield of cyclohexanone and other by-products were detected. The yield of ε-caprolactam increased with the deposition and showed a maximum at *ca.* 15 Si nm^{-2}. The yield decreased again with excess silica. On the other hand, the yield of cyclohexanone decreased with the deposition. The cyclohexanone oxime conversion was almost 100 % at the silicon concentration below 13 nm^{-2}, and decreased with further deposition.

The conversion of cyclohexanone oxime decreased with time-on-stream over these catalysts. The deactivation behavior was analyzed using the equation $X = X_0 e^{-bt}$, where b is the deactivation factor, X is the conversion, X_0 is the initial conversion and t is time-on-stream. As shown in Figure 2 - 3 - 3, the deactivation factor decreased with the deposition of silicon below 5 nm^{-2}, and changed little with further deposition.

Figure 2 - 3 - 4 shows the change in catalytic activity of titania by the deposition of silica. Whereas no ε-caprolactam was obtained over the unmodified titania, it was observed over the samples with silica. The yield of ε-caprolactam increased with the deposition over the experimental range of silicon concentration. The conversion was constant, and the cyclohexanone yield decreased with the deposition. On zirconia, the activity for ε-caprolactam was also created by silica, and seems to be saturated at 8 - 13 Si nm^{-2}, whereas the conversion and formation of cyclohexanone were reduced (Figure 2 - 3 - 5).

In order to compare the activity of monolayers on various supports, the rate per surface area

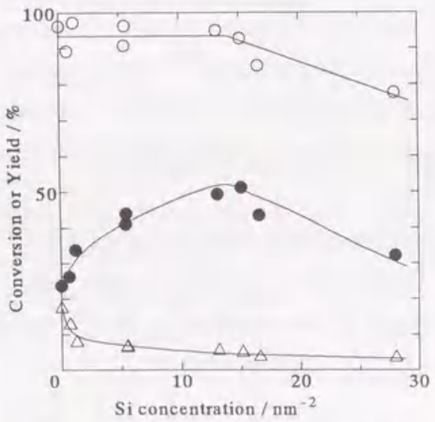

Figure 2 - 3 - 2 : Conversion of cyclohexanone oxime (○), and yield of ε-caprolactam (●) and cyclohexanone (△) on silica-modified alumina at W / F = 1.6 g-cat h mol^{-1} after 1 hour on stream.

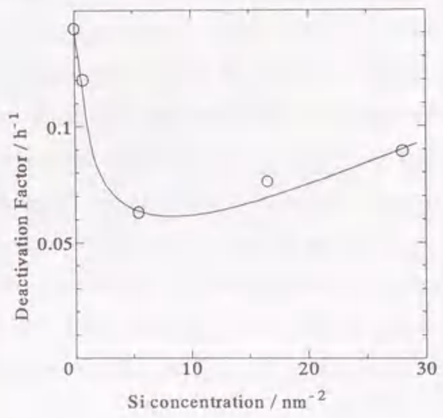

Figure 2 - 3 - 3 : Deactivation factor on silica-modified alumina under the conditions shown in Figure 2 - 3 - 2.

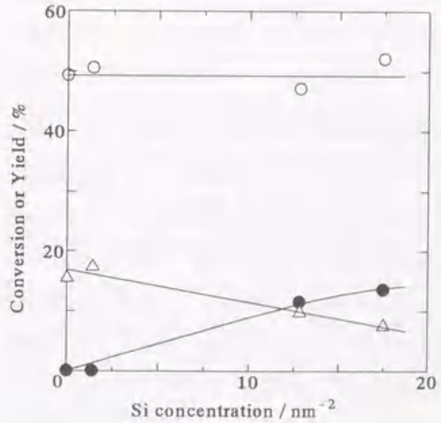

Figure 2 - 3 - 4 : Conversion of cyclohexanone oxime (○), and yield of ε-caprolactam (●) and cyclohexanone (△) on silica-modified titania at W / F = 1.6 g-cat h mol^{-1} after 1 hour on stream.

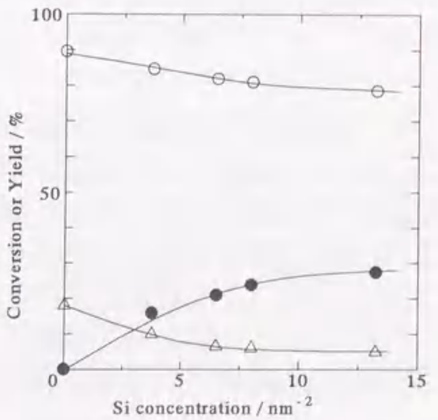

Figure 2 - 3 - 5 : Conversion of cyclohexanone oxime (○), and yield of ε-caprolactam (●) and cyclohexanone (△) on silica-modified zirconia at W / F = 1.6 g-cat h mol^{-1} after 1 hour on stream.

Table 2 - 3 - 1 : Comparison of activities for Beckmann rearrangement and isomerization of butene over silica monolayers loaded on various supports.

Support	Si concentration nm^{-2}	Rate per surface area for Formation of ε-caprolactam†	Isomerization from *1*- to *2*-butene‡
Alumina	12.4	22.8	126
Titania	11.9	6.4	9.9
Zirconia	8.0	27.3	1.5
Silica*	-	1.4	0.1

†: 10^{-5} mol h^{-1} m^{-2} at W / F = 0.14 g-cat h mol^{-1}. ‡: 10^{-10} mol m h^{-1} (yield / [mol] × flow rate of carrier [m^3 h^{-1}] / surface area [m^2]) under the conditions shown as (B) in section 2 - 1 at 393 K. *: Nikki Kagaku N-602A.

for the rearrangement was measured for conversions below 40 % (W / F = 0.14 g h mol^{-1}). As shown in Table 2 - 3 - 1, the monolayers on alumina and zirconia possessed a similar activity, which was *ca.* four times higher than that on titania. This behavior was different form the case of isomerization of *1*-butene, because the monolayer on alumina, titania and zirconia showed *ca.* 100 : 10 : 1 of the activities as described in Section 2 - 2. The activity over silica gel was low for both reactions, compared to those over the monolayers.

Discussion

On alumina, the deposition of silica enhanced the formation of ε-caprolactam. In contrast with this, the formation of cyclohexanone and the deactivation were weakened. As described in Section 2 - 1, the silica monolayer covered almost completely the surface of alumina at 13 Si nm^{-2}, and the doublelayer of silica set upon the monolayer during further deposition. The maximum ε-caprolactam yield was observed at *ca.* 15 Si nm^{-2}, where the silica monolayer covered the surface almost completely. This indicates that the active sites were formed on the monolayer. The conversion of cyclohexanone oxime decreased with further deposition of more than 13 nm^{-2} of silicon.

On zirconia and titania, the deposition of silica induced activity for ε-caprolactam. Therefore, the active sites for the rearrangement are suggested to be formed on the monolayers on these oxides also. The silica monolayer covers the surface of zirconia and titania at 8 and 12 Si nm^{-2}, respectively, as shown in Section 2 - 2. However, the yield of ε-caprolactam continued to increase with further deposition on the monolayer. It can be assumed that a small fraction of the support surface was uncovered and induced the side reactions even on the samples with 8 and 12 nm^{-2} of Si on

zirconia and titania, respectively; further deposition diminished the exposed surface, and improved the yield of ε-caprolactam.

Silica gel, which possessed almost no acidity, was inactive compared to the monolayers. This shows that the rearrangement requires acidity. The previous sections showed that Brønsted acid sites were generated on the monolayers; the acid strength was weak compared to the conventional silica-alumina. According to this, the Beckmann rearrangement is considered to proceed on the weak Brønsted acid sites of the monolayers. On the other hand, active sites on the support oxides, *e.g.* Lewis acid sites, were diminished by the deposition. Such sites may cause side reactions, because the pure oxide catalyzed only side reactions (zirconia and titania) or a less selective reaction (alumina).

All of the silica monolayers have species M-O-Si-OH (M = surface cation of oxide). Therefore, M-O-Si-OH is supposed to exhibit an acidity. A fine distribution of the acid strength due to the homogeneous structure is supposed. The activity for the double-bond isomerization of *1*-butene over the monolayer loaded on alumina, titania and zirconia was *ca.* 100 : 10 : 1. As shown in Section 2 - 2, this shows that the acidic property, particularly the acid strength of M-O-Si-OH is affected significantly by the support oxide, and a large difference in acid strength is suggested. However, the monolayers on alumina and zirconia possessed similar activities for the Beckmann rearrangement of cyclohexanone oxime, which was *ca.* four times higher than that of the monolayer on titania. The difference in activity for the rearrangement between the monolayers was small compared to that for the isomerization of butene. Therefore, the Beckmann rearrangement is concluded to require the Brønsted acid sites, but to be insensitive to acid strength.

In this section, the silica monolayer was applied as a model solid-acid catalyst to the industrially important but complicated reaction. It showed the high, but not satisfactory activity for the practical use. Higher activity, selectivity and long catalyst life have been obtained on such catalysts as boria loaded on alumina[6]. The present results, however, clearly pointed out the efficiency of weak Brønsted acidity and the insensitivity of reaction to the acid strength by using catalysts with simple structures.

Conclusion

1. The catalytic activity for Beckmann rearrangement of cyclohexanone oxime into ε-caprolactam was enhanced by the CVD of silica on γ-alumina, titania and zirconia.

2. The active site was shown to be the weak Brønsted acid site on silica monolayer, while Lewis acid site and other active sites originally existed on support oxide caused side-reactions and deactivation.
3. The activity for Beckmann rearrangement is suggested to be insensitive to the strength of Brønsted acid sites, because similar activities were obtained on M-O-Si-OH species.

References

1. D. England, U. S. Patent, 2634269 (1953).
2. A. Costa, P. M. Deya, J. V. Sinisterra and J. M. Marinas, *Can. J. Chem.*, **58,** 1266 (1980).
3. T. Yashima, S. Horie, S. Saito and N. Hara, *Nippon Kagaku Kaishi,* **1977,** 77.
4. Y. Murakami, Y. Saeki and K. Ito, *Nippon Kagaku Kaishi,* **1978,** 21.
5. E. Gutierrez, A. J. Aznar and E. Ruiz-Hitzky, *Stud. Surf. Sci. Catal.*, **59,** 539 (1991).
6. S. Sato, S. Hasebe, H. Sakurai, K. Urabe and Y. Izumi, *Appl. Catal.*, **29,** 107 (1987).
7. S. Sato, K. Urabe and Y. Izumi, *J. Catal.*, **102,** 99 (1986).
8. T. Curtin, J. B. McMonagle and B. K. Hodnett, *Catal. Lett.*, **17,** 145 (1993).
9. H. M. Meshram, *Synth. Commun.*, **20,** 3253 (1990).
10. P. S. Landis and P. B. Venuto, *J. Catal.*, **6,** 245 (1966).
11. M. C. Burguet, A. Aucejo and A. Corma, *Can. J. Chem. Eng.*, **65,** 944 (1987).
12. H. Sato, N. Ishii, K. Hirose and S. Nakamura, *Stud. Surf. Sci. Catal.*, **28,** (1986).
13. A. Aucejo, M. C. Burguet, A. Corma, and V. Fornes, *Appl. Catal.*, **22,** 187 (1986).
14. T. Takahashi, K. Ueno and T. Kai, *Can. J. Chem. Eng.*, **65,** 944 (1991).
15. S. Sato, K. Takematsu, T. Sodesawa and F. Nozaki, *Bull. Chem. Soc. Jpn.*, **65,** 1486 (1992).
16. A. Thangaraj, S. Sivasanker and P. Ratnasamy, *J. Catal.*, **137,** 252 (1991).
17. J. S. Reddy, R. Ravishankar, S. Sivasanker and P. Ratnasamy, *Catal. Lett.*, **17,** 139 (1993).
18. H. Sato, K. Hirose, M. Kitamura and S. Nakamura, *Stud. Surf. Sci. Catal.*, **49,** 1213 (1989).

2-4 Germanium Oxide Monolayer

Synopsis

Germanium tetramethoxide [$Ge(OCH_3)_4$] was deposited on γ-alumina in place of $Si(OCH_3)_4$. The BAT measurements showed the formation of germanium oxide monolayer as found for the CVD of silica. Extended X-ray absorption fine structure (EXAFS) supported the monolayer structure of deposited oxide. The monolayer showed the Brønsted acidity, like the silica monolayer.

Introduction

As shown in the previous sections, ultra thin layers of silica were prepared by the CVD of $Si(OCH_3)_4$ (tetramethoxysilane) on γ-alumina, titania and zirconia. It was observed that the monolayer, consisting of the 1 : 1 bonds of M-O-Si (M = was Al, Ti or Zr), covered the surface almost completely, and the monolayers generated weak Brønsted acid sites. The ability of thin oxide layer as a model of acid catalyst was also shown by Beckmann rearrangement. It is suggested that such layered oxide is generally promising as a model of mixed-oxide catalyst. However, few spectroscopic analyses are available for SiO_2, and, therefore, the monolayer structure has not been confirmed directly.

Germanium is included as the same group of the periodic table as silicon, and germanium alkoxide has the four coordinated structure as silicon alkoxide. It is therefore expected that the layer of germanium oxide with an atomic-order thickness will be prepared by the CVD of germanium alkoxide, and the EXAFS (extended X-ray absorption fine structure) analysis, which is available for GeO_2, is expected to give valuable information about the structure of oxide monolayer and the origin of acidity. The CVD of germanium alkoxide has already been made on zeolite in order to study the structure of thin silica layer, which controlled the opening size of micro pores[1, 2]. This section will show that the mono-atomic layer of germanium oxide was prepared on γ-alumina, and the novel material showed the Brønsted acidity like silica monolayer.

Experimental

γ-Alumina JRC-ALO4 (161 $m^2 g^{-1}$) was used as the support. Germanium tetramethoxide

[99.999 % $Ge(OCH_3)_4$] was obtained from Rare Metallic Co. Ltd., and purified further by vacuum distillation. The alumina sample was put in a basket hung by a micro balance, and evacuated at 673 K until no change of the weight was observed. The alkoxide vapor was then admitted on the sample at 473 K. Cycle of the introduction of vapor and the evacuation was repeated. The vapor pressure of alkoxide was kept constant by chilling the reservoir with an ice bath, and the evacuation was done at a pressure of *ca.* 10^{-3} Torr (1 Torr = 133.3 Pa). In order to remove the organic residue, the sample was calcined at 673 K under the presence of 200 Torr of oxygen. The loading of germanium oxide was determined from the weight gain. The treatment after this step was different from the case of the CVD of silica: the germanium oxide layer loaded on zeolite was unstable in humid conditions to transform into bulky oxide[2]; in order to avoid this, the samples were kept in a desiccator with dried molecular sieve.

The BET surface area was measured by the nitrogen adsorption at 77 K. The coverage by GeO_2 on the alumina surface was measured by the BAT (benzaldehyde-ammonia titration) method as utilized for the silica layer. Benzaldehyde was adsorbed in flowing helium at 523 K on the sample pretreated at 673 K until the adsorption was saturated. Ammonia was then introduced at 673 K, and the yielded benzonitrile was quantified.

The Ge-K edge EXAFS was measured on a thin disk molded from the sample powder at the Beam Line 10B of the Photon Factory in the National Laboratory for High Energy Physics (KEK-PF)[3]. The synchrotron radiation from the electron storage ring (25 GeV, average current 100 mA) was monochromatized with a channel-cut Si (311) monochromator. The incident- and transmitted-beam intensity was measured by an ionization chamber filled with a gaseous mixture (15 % argon and 85 % nitrogen) and with 100 % argon, respectively. The k^3 weighted EXAFS was extracted by the method according to Tanaka *et al.*[4], and Fourier transformed. As a reference, α-quartz type germanium oxide (Wako Pure Chemical Industries Ltd., 99.9999 %) was used.

In order to test the acidic property, the double-bond isomerization of *1*-butene was carried out by the pulse method under the conditions shown as (C) in Section 2 - 1 (conversion < 10 %). After the pretreatment of catalyst at 673 K, 1.3 cm^3 of *1*-butene was injected at 393 K. The products were analyzed by a column of VZ-7. The activity was calculated from the amount of yielded *2*-butene (mol) × flow rate of carrier gas (m^3 hr^{-1}) / surface area of catalyst (m^2). Infrared (IR) spectrum was recorded by a JASCO FT/IR-5300 spectrometer in an *in-situ* cell on the disk (1 cm in diameter) molded from 7 mg of the sample powder.

Results and Discussion

An example of the change of weight during the CVD operation is shown in Figure 2 - 4 - 1. The weight gain was observed with the introduction of germanium alkoxide vapor on alumina. This shows that the deposition readily proceeded. Since the deposited material was considered to contain the organic residue, the sample was calcined at 673 K under the presence of 200 Torr of oxygen in order to obtain the germanium oxide without the organic residue. The weight almost unchanged at 673 K after the quick decrement by the contact with oxygen. This shows that the stable oxide was obtained by the decomposition of the anchored alkoxide. It was assumed that the calcined material had the composition of GeO_2, and the loading was determined on the basis of the gravimetry.

In order to make clear of the change of surface area by the CVD, Figure 2 - 4 - 2 shows the BET surface area divided by the weight of alumina support (not by the weight of sample). The surface area was kept constant in the range of Ge concentration below 13 nm^{-2}, and a small decrement was observed above 13 nm^{-2}. This indicates that the deposited germanium oxide did not block the pores at the loading < 13 nm^{-2}, but a small fraction of the deposited material blocked the pores at > 13 nm^{-2}.

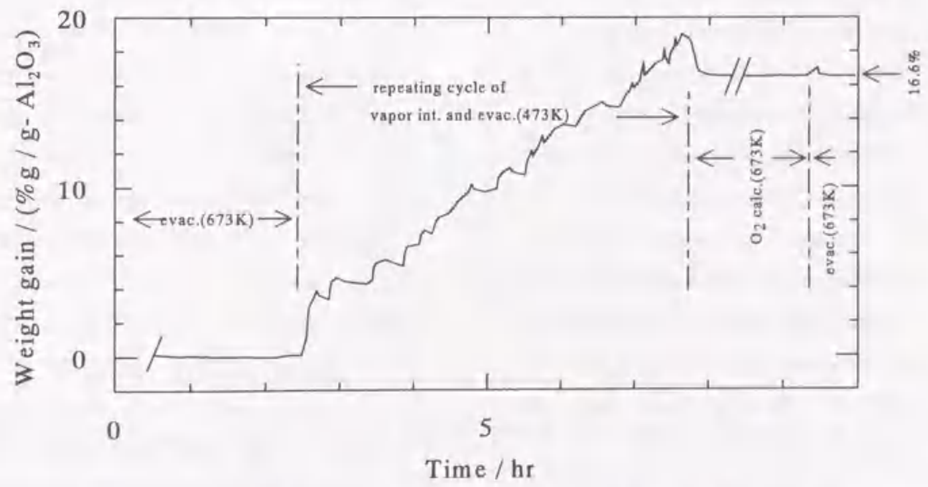

Figure 2 - 4 - 1 : Weight change during the preparation of GeO_2 (16.6 wt%) / Al_2O_3.

As described in the previous sections, benzaldehyde is adsorbed on alumina with the high surface concentration (1.8 molecules per 1 nm^2 of surface), and readily converted into benzonitrile by the contact with ammonia. Since the saturation of surface with benzaldehyde is estimated from this concentration, it is suggested that benzaldehyde was adsorbed on both of the external surface of particle and the inner surface of meso-pores. On the contrary, almost no adsorption of benzaldehyde was observed on germanium oxide[5] like on silica. Therefore, the coverage of alumina surface by silicon or germanium oxide was determined by the equation shown in Section 2 - 1. As shown in Figure 2 - 4 - 3, the coverage by GeO_2 increased linearly with increasing the germanium concentration. The linear relationship between them agreed well with that observed for the coverage by SiO_2. From this relationship, the deposited layer was estimated to cover 1 nm^2 of the alumina surface with 13 atoms of germanium or silicon. Because the concentration of aluminum cations on the surface of alumina was 9 - 15 nm^{-2} [6], the ultra thin layers of germanium and silicon oxides consisting of 1 : 1 of Al-O-T (T = Ge or Si) bonds, namely the monolayers, were suggested.

The coverage was saturated at *ca.* 85 % above 10 nm^{-2} of the germanium concentration. This shows that both the surfaces of outside and inside of alumina particle were covered almost completely by the mono-atomic layer. The constant BET surface area at the Ge concentration below 13 nm^{-2}, shows that the monolayer did not block the pores.

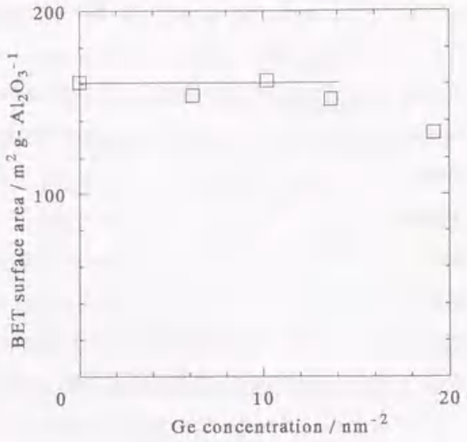

Figure 2 - 4 - 2 : BET surface area of GeO_2 / Al_2O_3.

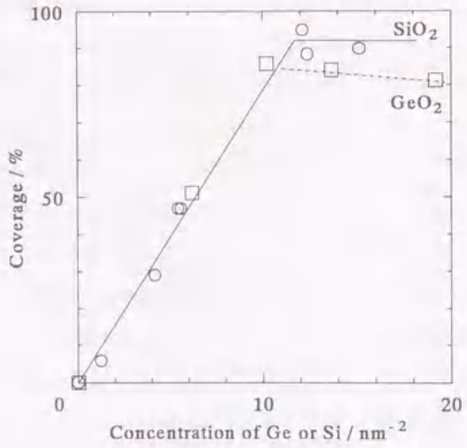

Figure 2 - 4 - 3 : Coverage by GeO_2 (□) and SiO_2 (○) on alumina surface measured by BAT method.

The EXAFS shows the obvious difference in absorption spectrum between the deposited GeO_2 layer and the α-quartz type GeO_2 (Figure 2 - 4 - 4). The α-quartz type GeO_2 shows both of the Ge-O and Ge-O-Ge bonds in Fourier transform (Figure 2 - 4 - 5), whereas the GeO_2 layer reveals only the Ge-O bond. Highly ordered structure is required to show a peak in EXAFS spectrum. Lack of the Ge-O-Ge peak therefore shows no formation or disordering of Ge-O-Ge bond. In the former case, the deposited Ge is dispersed on the alumina surface. In the latter case, the structure of deposited layer is significantly affected by the support. Anyway, the lack of Ge-O-Ge peak shows that the deposited GeO_2 formed the ultra thin layer, but not the bulk oxide.

Probably both of silicon and germanium oxide layers have structural similarities with the alumina surface, resulting in the formation of ultra thin layer. However, the BAT experiments show that the saturated coverage by GeO_2 on alumina, *ca.* 85 % is less than *ca.* 90 - 95 % of coverage on SiO_2 /

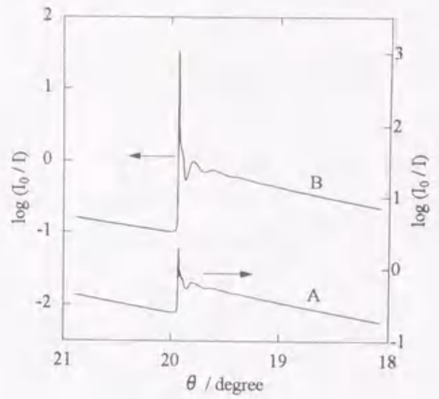

Figure 2 - 4 - 4 : X-ray absorption spectra on mixture of α-quartz type GeO_2 and alumina (A, 5 : 95 in weight), and sample prepared by CVD method with 13 nm^{-2} of Ge on alumina (B).

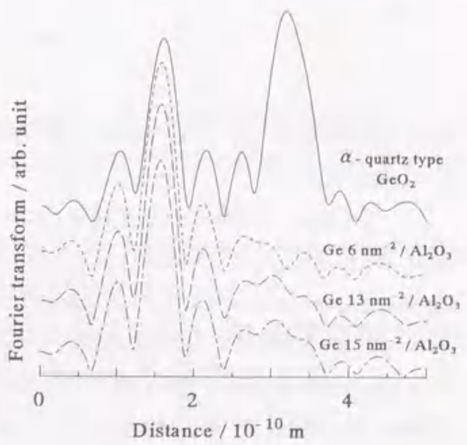

Figure 2 - 4 - 5 : Fourier transform of EXAFS. The distance was shown with the Ge-Ge distance of α-quartz type GeO_2 ($3.2 \cdot 10^{-10}$ m) as a reference.

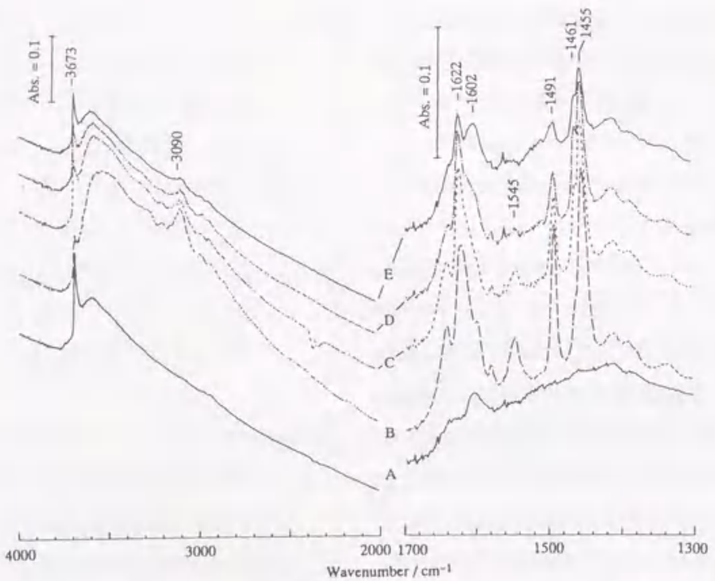

Figure 2 - 4 - 6 : IR spectra of GeO_2 / Al_2O_3 (13 Ge nm^{-2}) after evacuation at 673 K (A), after adsorption of pyridine at 373 K followed by evacuation at 373 (B), 473 (C), 573 (D) and 673 K (E).

Al_2O_3 (Figure 2 - 4 - 3). This seems to be due to the relatively low structural fitness of GeO_2 to Al_2O_3 than SiO_2.

On GeO_2 / Al_2O_3, a sharp peak at 3673 cm^{-1}, which is ascribable to isolated Ge-OH[7, 8], and a broad one at about 3600 cm^{-1} were observed in the hydroxyl region of IR spectrum (Figure 2 - 4 - 6, A); the species like Al-O-Ge-OH is suggested. No absorptions by Al-OH (3585, 3677, 3730 and 3763 cm^{-1}) confirm that the surface was covered by GeO_2 almost completely. No absorptions due to the methoxy group (2800 - 3000 cm^{-1}) were also observed; this confirms no organic residue. Alumina has only Lewis but not Brønsted acidity, whereas the spectrum of pyridine over the germanium oxide layer shows both species adsorbed on the Lewis and Brønsted acid sites at 1461 and 1545 cm^{-1}, respectively (Figure 2 - 4 - 6, B - E).

The activity for the isomerization from *1*- to *2*-butene was generated on both oxide layers of silicon and germanium (Figure 2 - 4 - 7). The activity showed the maximum at 10 - 14 nm^{-2} of the

concentration of germanium or silicon atoms, where the monolayers covered 80 - 95 % of the surface. These observations indicate that the Brønsted acid sites active for the isomerization were formed on the monolayers of silicon and germanium oxides and passivated by topping one-more layer. Therefore, the assumed species Al-O-T-OH (T = Si or Ge) is speculated to possess the Brønsted acidity.

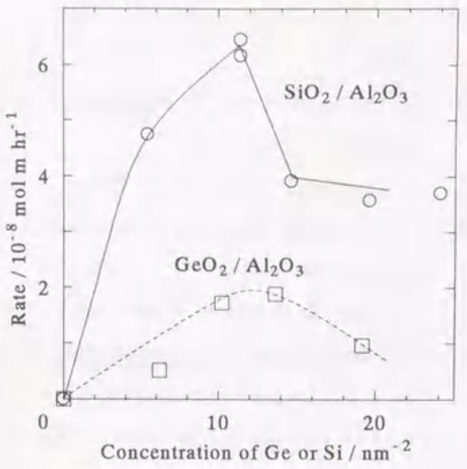

Figure 2 - 4 - 7 : Activity for double-bond isomerization of *1*-butene at 393 K over GeO_2 / Al_2O_3 (□) and SiO_2 / Al_2O_3 (○) pretreated at 673 K.

Conclusion

1. Chemical vapor deposition of $Ge(OCH_3)_4$ on γ-alumina at 473 K formed the germanium oxide monolayer fully covering the surface as well as the case of CVD of $Si(OCH_3)_4$. The ultra thin layer structure was confirmed by EXAFS.
2. The maximum coverage by GeO_2 was lower than that by SiO_2 on alumina, probably because of less structural affinity of GeO_2 to Al_2O_3 compared to that of SiO_2.
3. The germanium oxide monolayer showed Brønsted acidity, and therefore the assumed species Al-O-T-OH (T = Si or Ge) is considered to have the Brønsted acidity.

References

1. T. Hibino, M. Niwa, Y. Murakami and M. Sano, *J. Chem. Soc., Faraday Trans. 1,* **85,** 2327

(1989).
2. T. Hibino, M. Niwa, Y. Murakami, S. Komai and T. Hanaichi, *J. Phys. Chem.*, **93,** 7847 (1989).
3. H. Oyanagi, T. Matsushita, M. Ito and H. Kuroda, *KEK Report,* **1983,** No. 83 - 10.
4. T. Tanaka, H. Yamashita, R. Tsuchitani, T. Funabiki and S. Yoshida, *J. Chem. Soc., Faraday Trans. 1,* **84,** 2987 (1988).
5. M. Niwa, K. Suzuki, M. Kishida and Y. Murakami, *Appl. Catal.*, **67,** 297 (1991).
6. H. Knözinger and P. Ratnasamy, *Catal. Rev.-Sci. Eng.*, **17,** 31 (1978).
7. M. J. D. Low and P. Ramamurthy, *Chem. Commun.*, **1966,** 733.
8. M. J. D. Low and K. Matsushita, *J. Phys. Chem.*, **73,** 908 (1969).

Chapter 3. Origin of Brønsted Acid Site on Silica Monolayer

3-1 Mechanism of Growth of Silica Monolayer

Synopsis

The mechanism of chemical vapor deposition of tetramethoxysilane on γ-alumina was studied. A silica monolayer covered the surface almost completely upon the deposition at 593 K in a static system. Even at low temperatures (< 473 K), tetramethoxysilane was deposited quickly, but the deposition was readily saturated at low concentration of Si, and the silica layer thus covered only a part of the surface. The amount of methoxy groups on the surface was determined from gravimetry and product analysis by the pulse method; the ratio of CH_3O- / Si was high at low temperatures. The ratio decreased with increasing temperature, and simultaneously, silanol groups appeared. On these findings, the following mechanism is proposed; gaseous tetramethoxysilane is deposited on alumina quickly until the silicon alkoxide and a fraction of methanol cover the surface; at high temperatures, contaminated water hydrolyzes the silicon alkoxide into silanol, which is reacted with another tetramethoxysilane; the successive deposition thus proceeds, and at last, the monolayer with a network of siloxanes (Si-O-Si) covered the surface almost completely. The model of surface drawn by computer graphics based on the proposal is consistent with the experiments. Catalytic activity for isomerization of butene was observed over the monolayer deposited at 493 and 593 K, while the samples deposited at low temperatures (≤ 423 K) showed almost no activity. It is suggested that Al-O-Si-OH in the network of Si-O-Si possesses the Brønsted acidity, whereas dispersed silica species has no acidity. At 673 K, the random deposition formed a heterogeneous structure of silica including thick layers and / or particles, which showed low activity.

Introduction

As shown in Chapter 1, acidity on combined oxide solid-acid catalyst is presumed to be generated by interaction between the two components, because the combination is necessary for acidity. For such mixed solid-acids as silica-alumina, several models of the acid sites have been proposed and explanations about generation of the acidity have been made; the most important one was made by Tanabe[1]. Recently, quantum-chemical calculations have been made[2 - 4]. The origin of acidity is however difficult to be understood by such simple models, because the practical catalyst usually possesses complicated structure.

In order to overcome the difficulty, an ultra thin layer loaded on another oxide is promising.

Chapter 2 showed that the silica monolayer was formed over γ-alumina, titania and zirconia, and found to possess Brønsted acid sites. The acid strength of the monolayer on alumina was estimated to be weak compared with that on the conventional silica-alumina, because the monolayer was active for only facile reactions such as double-bond isomerization of olefin. Species M-O-Si-OH (M was surface cation of support oxide) was suggested to be the acid site, and the lack of strong acidity suggested a fine distribution of acid strength due to the homogeneous structure. However, the micro structure of monolayer has not been determined, and therefore the origin of acidity has been unclear. In order to determine the micro structure of active sites, it is important to clarify the mechanism of preparation of catalyst. Elementary steps of the CVD are expected to be simple as shown by Niwa and Hibino *et al.* on zeolite[5 - 7], in comparison with liquid-phase preparation of mixed oxides. In the present section, the mechanism of formation of monolayer will be investigated by varying conditions for deposition. Moreover, various species of silica are suggested to be formed on γ-alumina, and the acidic property is studied in order to determine the micro-structure of acid site, as the first step of this chapter which will solve the origin of acidity.

This chapter describes the comparison of present results with those of other studies used similar methods of the preparation[8 - 16], characterization[17, 18] and application[19, 20] of silica layers vapor-deposited over metal oxides, which were published independently or referring to the present study.

Experimental

Chemical Vapor Deposition in Static System

Alumina was supplied from Catalysis Society of Japan, as a reference catalyst JRC-ALO4. The crystal phase was γ-Al_2O_3, and the surface area was 161 $m^2 g^{-1}$.

Deposition behavior of $Si(OCH_3)_4$ was analyzed by the weight monitoring during the CVD operation using a micro balance as shown in Figure 1 - 4. In the experiments described in Section 2 - 1, the deposition rate was controlled by material transportation, and the stepwise increment of sample weight was therefore observed with cycle of introduction of alkoxide vapor and evacuation. In this section, a small sample size (0.1 g) was selected to avoid this, and the deposition was hence controlled only by the deposition temperature as shown below. Under these conditions, total rate of deposition seems to be controlled by the kinetics of surface reaction. The deposition temperature was varied from 373 - 673 K, and other conditions were same as shown in Section 2 - 1: evacuation

was carried out at 673 K until no change of the weight was observed, and the cycles of introduction of vapor and evacuation were repeated in order to allow the alkoxide vapor to be contacted with the sample. The vapor pressure was kept at *ca.* 2.5 Torr by chilling the reservoir with an ice bath, and the degree of evacuation was *ca.* 10^{-3} Torr. Finally, the sample was calcined with 200 Torr of oxygen at 673 K. The complete calcination in flowing oxygen shown in Section 2 - 1 was skipped in this section. Surface concentrations of Si and organic materials were estimated from gravimetry and BET surface area.

Deposition in Pulse System

The deposition behavior was also determined from another view point. Alumina (0.02 g) was set in a 4 mm i.d. Pyrex-glass reactor. The carrier gas, 50 cm^3 min^{-1} flow of helium, was passed through a liquid nitrogen trap in order to remove the moisture, and fed into the sample. After pretreatment at 673 K for 1 hour, 1 mm^3 ($6.4 \cdot 10^{-6}$ mol) of tetramethoxysilane was repeatedly injected. Products were analyzed by a column of Benton-34 which was directly connected with the reactor. The amount of deposited Si was estimated from the difference in amounts of injected and eluded tetramethoxysilane. In order to show the influence of degree of drying, the pretreatment temperature was varied in some experiments.

Infrared Spectroscopy

Alumina was molded into a thin disk, and set in an *in-situ* cell which was connected to a vacuum line. The vapor of tetramethoxysilane was admitted onto the sample at 423 K after the evacuation at 673 K. The vapor pressure was *ca.* 2.5 Torr, and the degree of evacuation was *ca.* 10^{-3} Torr. Spectrum was measured using a JASCO-FTIR/5300 spectrometer at the lower part of the cell with windows of CaF_2, after the sample was treated in the upper part with a furnace.

Measurement of Coverage using Benzaldehyde-Ammonia Titration Method

Benzaldehyde is adsorbed on alumina (the saturated concentration, 1.8 nm^{-2}), but only little (< 0.01 nm^{-2}) on silica. On the basis of this finding, the coverage of alumina surface by silica was estimated by using benzaldehyde-ammonia titration (BAT) method. Sample was set in a Pyrex tube (i.d. 4 mm). The carrier gas was helium purified by a liquid nitrogen trap. After calcination at 673 K for 1 hour, 1 mm^3 ($9.8 \cdot 10^{-6}$ mol) of benzaldehyde was repeatedly injected into the sample. The eluted benzaldehyde and products were analyzed by a silicone grease column kept at 513 K, and the injections of benzaldehyde were repeated until the adsorption was saturated. Finally, 10 cm^3

($4.2 \cdot 10^{-4}$ mol) of gaseous ammonia was injected at 673 K, and the desorbed benzonitrile was quantified. The injections of ammonia were repeated until no products were observed. The coverage by silica on alumina was calculated according to Section 2 - 1.

Test Reaction of Acidic Property

Isomerization of butene was chosen to test the acidic property of various species of silica under the conditions shown as (B) in Section 2 - 1. The catalyst was treated in a Pyrex reactor (i.d. 4 mm) at 673 K for 1 hour in flowing helium which was purified with a liquid nitrogen trap. Then, 1 cm^3 ($4.2 \cdot 10^{-5}$ mol) of gaseous *1*-butene was injected into the sample at 393 K. The flow rate of helium was 40 cm^3 min^{-1}, and the total pressure was 4 atm. Conversion was adjusted less than 5 % in order to measure the activity under the differential conditions. Products were analyzed by using a column of VZ-7 at room temperature.

Results

Deposition in Static System

Figure 3 - 1 - 1 shows the weight increase by deposition of tetramethoxysilane at various temperatures. The weight increased quickly up to *ca.* 7 wt% in all the cases. At temperatures between 373 and 423 K, the deposition was readily saturated at 8 wt%, where surface concentration of Si was calculated to be *ca.* 3 Si nm^{-2}. At 473 K, 12 wt% of SiO_2 was deposited, and more than 20 wt%, *i.e.* approximately 13 Si nm^{-2} of the surface concentration was obtained at high temperatures above 493 K.

The deposition was suggested to form Si alkoxide anchored on the surface, *i.e.* Al-O-Si$(OCH_3)_n$. Methanol, which was observed by the pulse method, is suggested to be adsorbed to form a surface alkoxide,

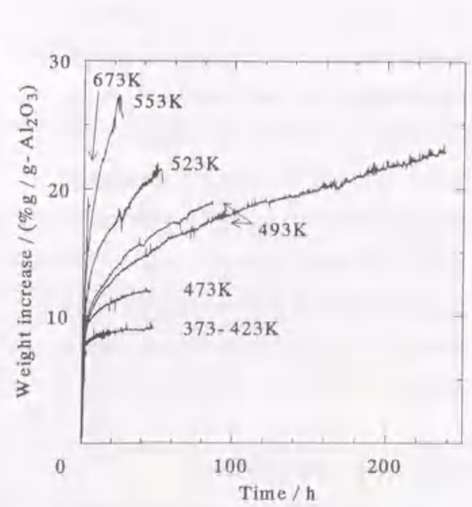

Figure 3 - 1 - 1 : Weight increase by deposition of tetramethoxysilane at various temperatures over 0.1 g of alumina evacuated at 673 K in the static system.

Table 3 - 1 - 1 : Estimated composition of deposited materials based on gravimetry in the static system.

Deposition temperature / K	Deposition time / h	Amount of SiO_2* / (% g / g-Al_2O_3)	Amount of organic material** / (% g / g-Al_2O_3)	Concentration of Si / nm^{-2}	CH_3O-/Si ratio
423	4	3.8	3.2	2.3	2.2
	45	5.1	4.0	3.2	2.1
473	1	4.5	2.3	2.9	1.3
	45	8.1	3.8	5.2	1.2
493	4	7.4	2.6	4.5	0.9
	230	17.3	5.6	7.7	0.8

*: Weight increase by deposition followed by calcination. **: Weight decrease by calcination.

Al-O-CH_3. In order to determine the composition of alkoxide, the amounts of SiO_2 and organic materials were estimated from the gravimetry based on the following assumptions; the deposition formed the species Al-O-Si$(OCH_3)_n$ and Al-O-CH_3; the calcination formed SiO_2; the physical adsorption of products and coke deposition were ignored. As shown in Table 3 - 1 - 1. Figure 3 - 1 - 2 shows the plot of CH_3O- / Si ratio against the deposition temperature. The ratio of CH_3O- / Si was *ca.* 2 at 373 - 423 K; obviously it decreased with increasing the temperature and arrived to almost zero at 593 K.

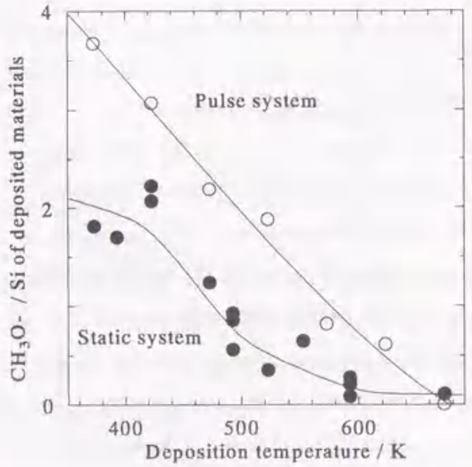

Figure 3 - 1 - 2 : Composition of deposited materials after deposition at various temperatures. The pretreatment of alumina was carried out at 673 K, and the composition was estimated from gravimetry in the static system (●) and from product analysis in the pulse system (○).

Deposition in Pulse System

The concentration of deposited Si was calculated based on the amount of deposited tetramethoxysilane and the surface area of alumina, and plotted against the number of pulse in Figure 3 - 1 - 3. At the first pulse, 1.2 nm^{-2} of tetramethoxysilane was deposited over the broad range of temperature, because almost all the injected tetramethoxysilane (1.21 nm^{-2}) was deposited. At 373 K, the concentration of Si was saturated at 1.7 Si nm^{-2}. However, the deposition was hardly saturated at temperatures above 423 K. In the temperature range from 423 to 473 K, the deposition continued until large amounts of Si were deposited. At higher temperatures, the deposition was not saturated during the experimental runs. At 673 K, almost all the injected tetramethoxysilane was deposited.

Methanol and dimethylether were observed in the products. As shown in

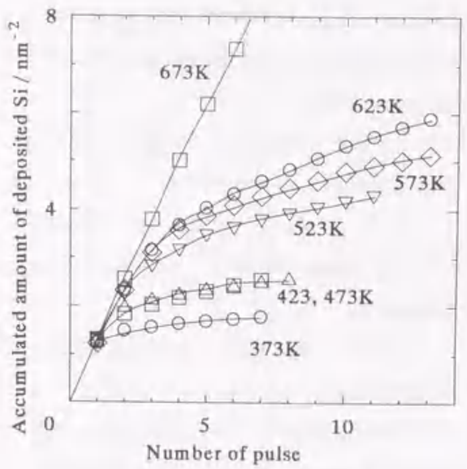

Figure 3 - 1 - 3 : Concentration of Si deposited by pulses of tetramethoxysilane at various temperatures over alumina pretreated at 673 K. Pulse size was 1.21 molecules of tetramethoxysilane per 1 nm^2 of alumina surface.

Table 3 - 1 - 2 : Products and estimation of composition of deposited materials in the pulse system.

Temperature of pretreatment / K	Temperature of deposition / K	Amount of deposited $Si(OCH_3)_4$ / (molecules / nm^2 of Al_2O_3 surface)	Amount of yielded CH_3OH	Amount of yielded CH_3OCH_3	Product distribution of CH_3OH (a)	Product distribution of CH_3OCH_3 (b)	CH_3O- / Si ratio (4 - a - b)
673	373*	1.8	0.53	0.03	0.30	0.032	3.7
	423*	2.5	2.1	0.12	0.84	0.093	3.0
	473*	2.6	3.8	0.42	1.5	0.33	2.2
	523**	4.2	5.0	2.0	1.2	0.93	1.9
	573**	4.8	6.6	4.3	1.4	1.8	0.8
	623**	5.3	1.3	10	0.21	3.2	0.6
	673**	11.1	2.6	22	0.23	4.0	0
573	473*	2.2	2.9	0.16	1.4	0.14	2.5
773	473*	2.6	3.3	0.86	1.3	0.67	2.1

*: Based on the total amounts of deposited and produced compounds until the deposition was saturated. **: Based on the total amounts of deposited and produced compounds by the first 10 pulses. The deposition was not saturated.

Table 3 - 1 - 2, the ratio of methoxy groups to deposited Si was calculated from the following equation;

a = number of formed CH_3OH molecules / (4 × number of deposited Si),

b = (2 × number of formed CH_3OCH_3 molecules) / (4 × number of deposited Si),

Ratio of CH_3O- / Si of the deposited materials = 4 - a - b.

As shown in Figure 3 - 1 - 4, the CH_3O- / Si ratio was almost constant against the number of pulse. Figure 3 - 1 - 2 shows that the ratio was about 4 at 373 K, and decreased with increasing the temperature. The decrease of the ratio by increasing the deposition temperature was observed also in the static system, but the value of CH_3O- / Si in the pulse system was higher than that obtained in the static system.

Figure 3 - 1 - 5 shows the influence of pretreatment temperature on the deposition amount. The amount of deposited tetramethoxysilane with the number of pulse was independent of the pretreatment temperature from 573 to 773 K.

IR Spectroscopy

As shown in Figure 3 - 1 - 6, absorptions of hydroxides (3585, 3677, 3730 and 3763 cm^{-1}) were observed on alumina evacuated at 673 K. The deposition of tetramethoxysilane at 423 K changed the

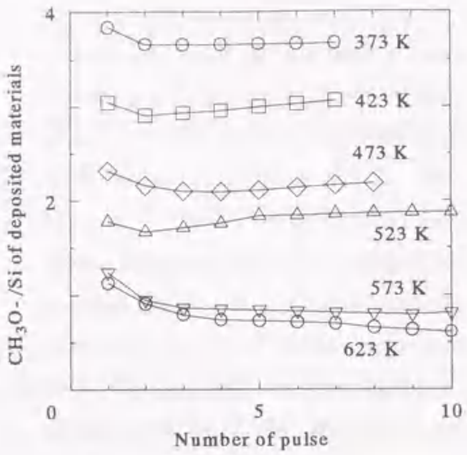

Figure 3 - 1 - 4 : Plot of composition on the surface against the number of pulse determined from the total amounts of deposited and produced molecules in the pulse system. The pretreatment of alumina was carried out at 673 K.

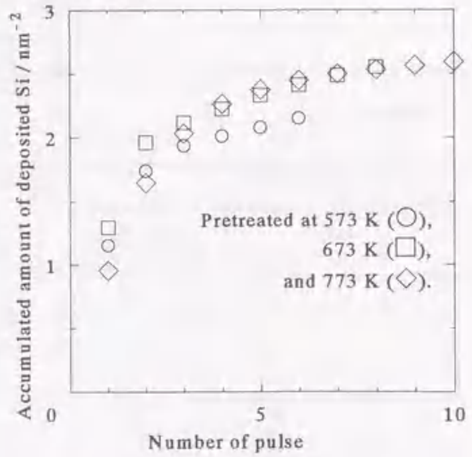

Figure 3 - 1 - 5 : Concentration of Si deposited over alumina pretreated at various temperatures. The deposition was carried out at 473 K in the pulse system.

absorptions and increased the noise level, probably due to the large absorption by the deposited organic materials. Simultaneously, two absorptions of C-H stretching (2951 and 2847 cm^{-1}) were observed. With increasing the temperature, the intensity of C-H stretching decreased, and simultaneously, isolated silanol (3745 cm^{-1}) appeared.

Coverage of Surface by Silica

Figure 3 - 1 - 7 shows the coverage measured by the BAT method over the catalysts with various concentrations of Si, which were obtained by varying the time of deposition as shown in Section 2 - 1. The deposition at 593 K increased the coverage linearly against the concentration of Si, and it arrived at almost 100 % with the concentration of 13 Si nm^{-2}. The deposition at temperatures lower than 593 K showed the coverage higher than that on the linear relationship obtained at 593 K. However, the silica layer deposited at temperatures below 473 K covered only a part of the surface (coverage < 70 %), because the deposition was saturated at the low concentration of Si. The sample deposited at 673 K showed the coverage lower than that estimated based on the relationship obtained upon the deposition at 593 K.

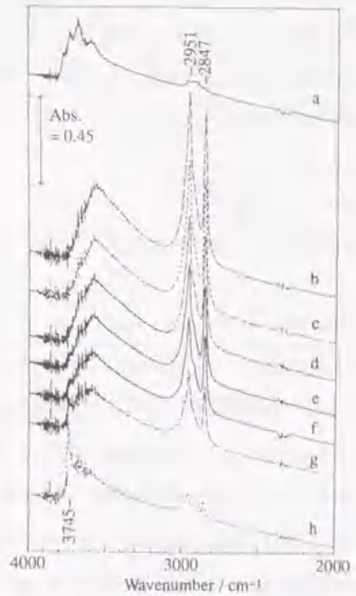

Figure 3 - 1 - 6 : IR spectra of alumina after the evacuation at 673 K (a), and after the deposition of tetramethoxysilane at 423 K (b), followed by the evacuation at 473 (c), 493 (d), 523 (e), 553 (f), 593 (g) and 673 K (h).

Test Reaction

Figure 3 - 1 - 8 shows the change of activity for isomerization of *1*-butene by increasing the Si concentration. The activity appeared with the deposition at 493 and 593 K. The activity over the samples deposited at 593 K showed the maximum at 13 Si nm^{-2}. Over the silica layers deposited at 473 K, only a small activity was observed. Almost no activity was observed by the deposition at 373 - 423 K. The deposition at 673 K made the activity lower than that estimated from the

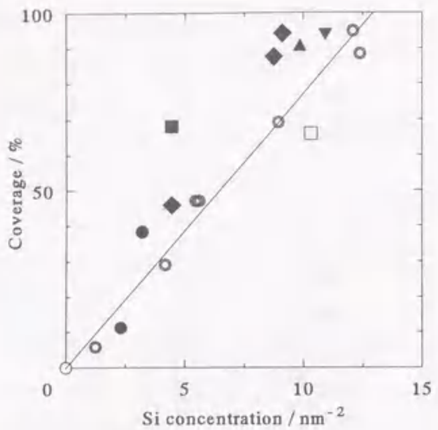

Figure 3 - 1 - 7 : Coverage by silica deposited at 423 (●), 473 (■), 493 (◆), 523 (▲), 553 (▼), 593 (◎) and 673 K (□) and calcined at 673 K in O_2 in the static system.

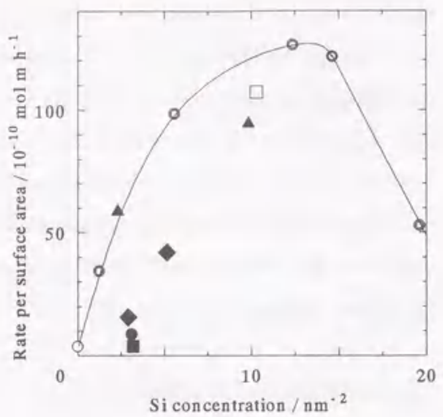

Figure 3 - 1 - 8 : Activity for isomerization of *1*-butene at 393 K under the conditions (B) over alumina (○) and silica deposited at 423 (●), 473 (■), 493 (◆), 523 (▲), 593 (◎) and 673 K (□) on alumina pretreated at 673 K.

relationship between the activity and Si concentration obtained by the deposition at 593 K.

Discussion

Mechanism of Saturation of Deposition

When the alkoxide was deposited at 593 K, the coverage by silica increased almost linearly against the concentration of Si. The coverage arrived at almost 100 % with the deposition of 13 nm^{-2} of silicon. Since the surface concentration of Al^{3+} on γ-alumina is 9 - 14.5 nm^{-2} [21], the silica layer covers the surface almost completely at the concentration of Si close to that of Al^{3+}. As described in the previous chapter, this shows that the silica monolayer, which consisted of 1 : 1 bond of Al-O-Si, covered the surface almost completely at 13 Si nm^{-2}.

Even at the low temperatures, tetramethoxysilane was deposited quickly in the early stage of deposition. However, the deposition at temperatures below 473 K was readily saturated at low concentration of Si (< 5 Si nm^{-2}), and the silica layer hence covered only a part of surface (coverage

< 70 %). Since the coverage was measured after the calcination, it is possible that the surface was saturated with the organic materials and exposed again by the calcination. The deposition of tetramethoxysilane may form the Si alkoxide species Al-O-Si$(OCH_3)_m$. Also methanol, which was observed in the products by the pulse method, is probably adsorbed on alumina to form the methoxide at such low temperatures. The ratio of CH_3O- / Si was high at the low temperatures, and it decreased with increasing the temperature. Based on these findings, it is suggested that the methoxides, *i.e.* the anchored Si methoxide and the adsorbed methanol covered the surface completely at the low temperatures, and the deposition was thus saturated.

Therefore, the following mechanism (Scheme 3 - 1 - 1) is proposed; gaseous tetramethoxysilane was quickly reacted with the alumina surface to form the Si alkoxide and methanol and / or dimethylether; the Si alkoxides and a fraction of methanol covered the surface completely (a); the Si

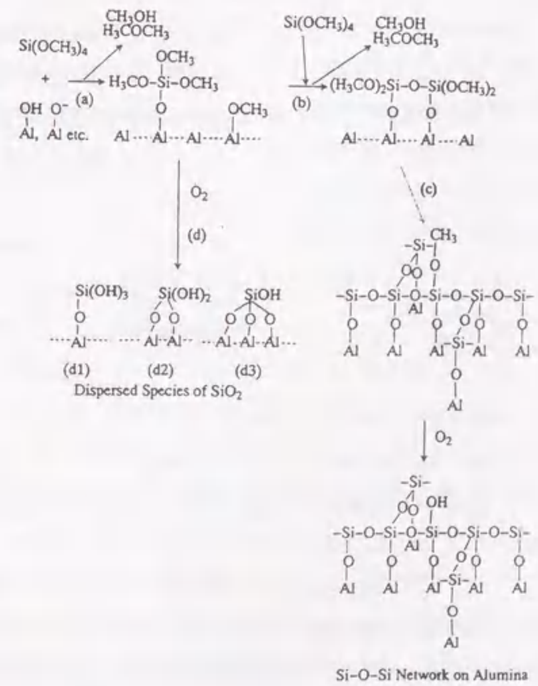

Scheme 3 - 1 - 1 : Mechanism of formation of monolayer.

alkoxides and the adsorbed methanol were so stable to inhibit the successive deposition at the low temperatures; increasing the temperature enhanced the eliminate of methoxides and the successive deposition, which formed the siloxane (Si-O-Si) bond (b); at last, the silica monolayer with a network of Si-O-Si covered the surface almost completely (c).

The deposition by the pulse method was also saturated at the low temperatures. The ratio of CH_3O- / Si was determined from the products; it was high at the low temperatures, and it decreased with increasing the temperature. Therefore, the same mechanism as in the static system is proposed.

Confirmation by Computer Graphics

According to Scheme 3 - 1 - 1, the surface was quickly saturated with the alkoxides of Si and methanol. In order to confirm this, computer graphics were used as follows; various Si alkoxides were assumed on the basis of covalent and Van der Waals radii of elements[22], and the relationship of Si concentration against the ratio of CH_3O- / Si was estimated on the surfaces saturated with the alkoxides. Figure 3 - 1 - 9 shows examples of the assumed species; (a) shows a surface trimethoxide isolated from other Si with the ratio of CH_3O- / Si = 3; (b) shows a dimer of silica with four methoxy groups with the ratio of CH_3O- / Si = 2; (c) and (d) show the oligomers with the ratio of CH_3O- / Si = 1 and 0.67, respectively. On a simple plane, these species were packed as shown in

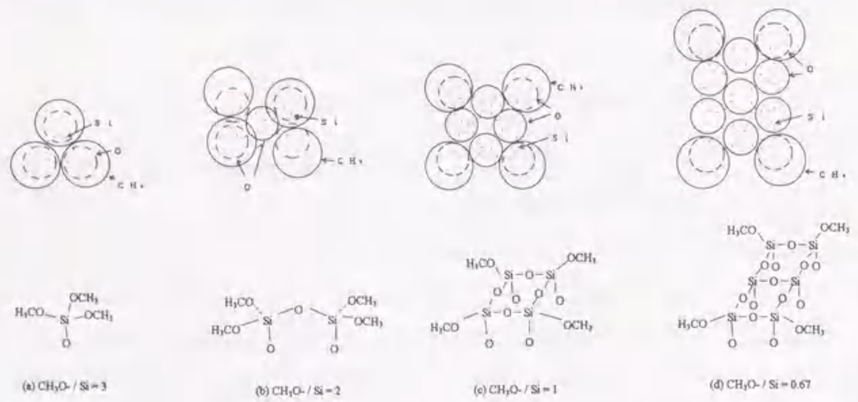

Figure 3 - 1 - 9 : Assumed Si alkoxides with various CH_3O- / Si ratio. It is assumed that the van der Waals radius of CH_3 and O is 0.20 and 0.140 nm, respectively, and the covalent radius of C, O and Si is 0.077, 0.066 and 0.117 nm, respectively[22].

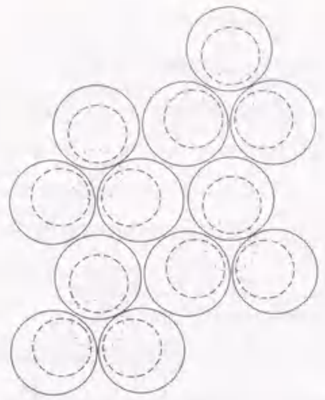

Figure 3 - 1 - 10 : Simple plane saturated with the Si alkoxide at CH_3O- / Si = 3 shown in Figure 3 - 1 - 9 (a).

Figure 3 - 1 - 10, and a relationship of the Si concentration against the CH_3O- / Si ratio was obtained (Figure 3 - 1 - 11 +); the concentration of Si decreased with the increase of ratio of CH_3O- / Si. In a similar way, the alkoxides were assumed to be bonded to oxygen anions on the surfaces of γ-Al_2O_3[23, 24] (Figure 3 - 1 - 12), and the concentration of Si was calculated (Figure 3 - 1 - 11 ×). The relationship between the CH_3O- / Si ratio and the Si concentration was similar to that obtained on the simple plane. Not only the Si alkoxide, methanol was also assumed to cover the surface. Figure 3 - 1 - 13 shows an example of the simple plane saturated with the Si alkoxides and methanol; the ratio of CH_3O- / Si is 2. As shown in Figure 3 - 1 - 11 (□), such assumptions gave a similar relationship to that obtained by assuming only the Si alkoxides.

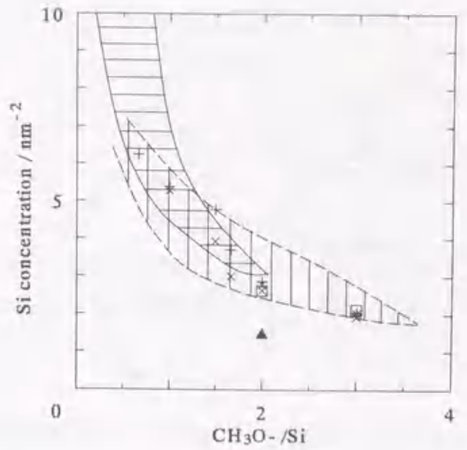

Figure 3 - 1 - 11 : Concentration of Si on surface saturated with alkoxides calculated from computer graphics. The alkoxides shown in Figure 3 - 1 - 9 (+ and ×), Figure 3 - 1 - 13 (□) and Figure 3 - 1 - 14 (▲) were packed on a simple plane (+, □ and ▲) and the proposed alumina surfaces[23, 24] (×). Experimental data measured by the static (≡) and pulse (|||||||) methods were overlapped.

Experimental data obtained in the static system were overlapped on Figure 3 - 1 - 11 as a region shown by ≡; the Si concentration and the CH_3O- / Si ratio were determined from the gravimetry in a region of more than 10 hours of the deposition time. Broadness of the shaded relationship

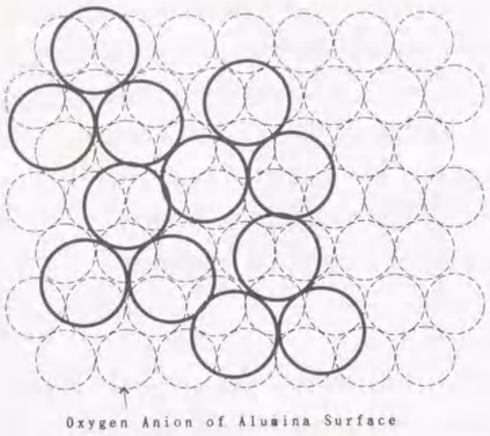

Figure 3 - 1 - 12 : Surface model of γ-alumina[24] saturated with the alkoxide shown in Figure 3 - 1 - 9 (a).

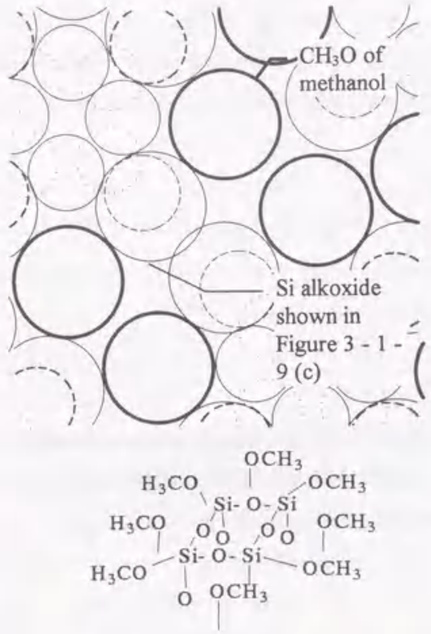

Figure 3 - 1 - 13 : Simple plane saturated with the anchored Si alkoxide and methanol; CH_3O- / Si = 2.

shows some uncertainties. From the pulse method, the Si concentration and the ratio of CH_3O- / Si were calculated at the temperatures below 623 K and the number of pulse above 5 (Figure 3 - 1 - 11 ||||||). The experimental data approximately agreed with the relationship obtained from the computer graphics. The proposed mechanism was thus confirmed.

At 2 of the CH_3O- / Si ratio, the alkoxide species with a bridged structure shown in Figure 3 - 1 - 14 was assumed. As shown in Figure 3 - 1 - 11 (▲), the relationship of Si concentration and CH_3O- / Si ratio was estimated on the surface saturated with this alkoxide; it disagreed with the experimental data. Therefore, it is suggested that the Si alkoxide did not have such a bridged form.

Mechanism of Formation of Siloxane

The C-H stretching of methoxy groups was observed by the IR measurements. The intensity of the methoxy groups was decreased by the evacuation at high temperatures after the deposition, and simultaneously, isolated silanol was observed. This indicates that the Si alkoxide was reacted with water to form the silanol at high temperatures, as shown in Scheme 3 - 1 - 2 (a). The silanol is

supposed to be active for the reaction with gaseous tetramethoxysilane into Si-O-Si. Therefore, tetramethoxysilane is suggested to be deposited on the site of alumina located at the edge of silica layer to grow it as shown in Scheme 3 - 1 - 2 (b).

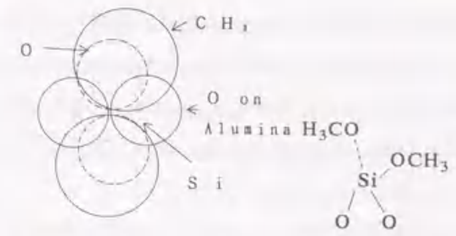

Figure 3 - 1 - 14 : Assumed alkoxide with a bridged structure at 2 of the ratio of CH_3O- / Si.

Because the pretreatment temperature did not affect the amount of deposited Si in the pulse system, the hydrolysis of Si alkoxide is presumed to be independent of the water content of alumina. Quite low concentration of water vapor contaminated into the system is therefore supposed to hydrolyze the alkoxides. It is concluded that the Si alkoxide anchored on alumina was highly reactive and decomposed by the low concentration of contaminated water at the high temperatures. The difference between values of CH_3O- / Si in the static and pulse systems can be explained by the difference in the concentration of water vapor.

Direct reaction of the anchored Si alkoxide and gaseous tetramethoxysilane to form Si-O-Si and dimethylether at high temperature is supposed. However, no evidence of this reaction was shown.

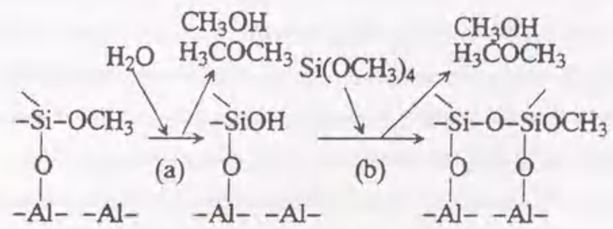

Scheme 3 - 1 - 2 : Formation of Si-O-Si from alkoxide.

Origin of Brønsted Acidity of Al-O-Si-OH

According to the proposed mechanism, it is suggested that dispersed Si alkoxides are formed by the deposition at low temperature, while concentrated species is formed at high temperature. The dispersed alkoxides is suggested to form the well dispersed silica species during the calcination. For example, trihydroxide (Scheme 3 - 1 - 1 - d1) can be formed from the alkoxide with the ratio of CH_3O- / Si of 3. Because this species is supposed to be easily converted into bridged (d2 and d3) species by dehydration, these species are also possible to be formed. Anyway, these dispersed silicon species are probably formed from the dispersed alkoxide. On the other hand, the deposition at high temperature is suggested to develop the silica monolayer with the network of Si-O-Si as shown in Scheme 3 - 1 - 1 (c). The coverage by silica deposited at the temperatures below 523 K was higher than that on the linear relationship against the Si concentration obtained over the monolayer formed at 593 K. This supports that the species prepared at low temperatures were dispersed, because the well dispersed species is suggested to cover the surface more effective than the concentrated species.

In support with this, the coverage was lower over the sample prepared at 673 K. This indicates that a structure including thick layers and / or particles of silica was formed by the random deposition because of too high temperature.

The activity for isomerization of *1*-butene was generated by the deposition at 493 and 593 K, and showed the maximum at 13 Si nm^{-2}, where the monolayer covered the surface almost completely. This indicates that the silica monolayer with the network of Si-O-Si had Brønsted acidity. On the other hand, the deposition at the low temperatures (373 - 423 K) generated almost no activity. Therefore, it is suggested that the Brønsted acidity was generated on Al-O-Si-OH in the layer with the network of Si-O-Si, whereas the isolated species of silica had no acidity.

The deposition at 673 K made the activity lower than that obtained at 593 K. It is presumed that the random deposition decreased the activity. This agrees with that the thick layer of silica is suggested to be inactive, because the activity on the silica layer deposited at 593 K was decreased by silica more than 13 Si nm^{-2}. Silica gel was also inactive, thus it is concluded that the deposited silica including the thick layers and / or the particles was inactive.

The low temperature deposition must be related with the study carried out in the liquid phase. Sarrazin *et al.* studied the deposition site of $Si(OC_2H_5)_4$ on alumina in ethanol solvent by means of the IR spectroscopy in order to improve the support of molybdenum catalyst[25]. The alkoxide was deposited on the basic Al-OH group to form a silica species which was strongly interacted with alumina. Further addition of the alkoxide formed particles of silica which was not interacted with the alumina

surface. Probably, the deposition can proceed only on the specific reactive hydroxides, and can hardly occur all over the surface to completely cover it at the low temperature in both gas and liquid phases. No acidity was observed on the SiO_2 / Al_2O_3 prepared from $Si(OC_2H_5)_4$ in the liquid phase, whereas the basicity diminished with the loading[25]. These facts support the lack of acidity on the dispersed Si species.

As shown by the influence of contaminated water vapor, not only the temperature but also co-presence of reactive gas can affect the structure of deposited silica. The effect of presence of oxygen was shown by Sato *et al.*[9 - 12] The CVD of $Si(OC_2H_5)_4$ was studied at the medium range of temperature (513 - 573 K) in flowing air to enhance the deposition rate. ^{29}Si NMR spectrum showed $Si(OSi)_4$ (-110 ppm) species at *ca.* 20 wt % of the loading, which corresponded to only 8 nm^{-2} of the concentration of silicon. This suggests that the multiple layer was formed in air, probably due to the fast and non-selective deposition enhanced by oxygen. ^{31}P NMR (nuclear magnetic resonance) of adsorbed trimethylphosphine and test reactions showed that strong Brønsted acidity, like on the conventional silica-alumina catalyst. Migration of aluminum cation into the silica multiple layer under the presence of oxygen, which probably causes unexpected high temperature, is suggested for this case. This behavior is specific for catalyst prepared under the presence of oxygen, and the simple monolayer with simple weak Brønsted acidity is obtained from the CVD in the present vacuum system.

Sheng *et al.* agreed with this, because weak Brønsted acid sites were confirmed by ^{31}P NMR and TPD of alkyl phosphine on the monolayer which was prepared from $Si(OCH_3)_4$ at 593 K in flowing nitrogen[17]. However, the same authors proposed a random deposition of $Si(OCH_3)_4$ forming a heterogeneous thickness even in nitrogen[18]. The present results suggest a difference of deposition behavior is caused by the difference in water vapor concentration between the static and flow systems. It should be noted that the structure of surface silica species is controlled by balance of reactions between the gaseous and anchored alkoxides, and the substrate. The important factors are the deposition temperature and atmosphere as described in this section. In addition, Tatsushima *et al.* recently observed an enrichment of silicon on the external surface of alumina particle for the case of CVD of $Si(OCH_3)_4$ in flowing inert gas[26]. This pointed out the dependence of deposition behavior on fluid mechanical factors, *e.g.* flow rate and sample size. Therefore, the static method used in the present study probably has an advantage to load a thin and homogeneous layer, in comparison with the flow system. Details will be discussed with ^{29}Si NMR in Section 3 - 3.

The acidic property was sensitive to the structure, and the silica monolayer with Al-O-Si-OH structure had Brønsted acidity. The acidity was shown to require the network of Si-O-Si. It is

suggested that such a network developed on another oxide is strained due to the difference in structures between the two oxides. The acidity of Al-O-Si-OH is therefore speculated to be owing to the strained structure. The isolated species also will be prepared by the CVD of $Si(OCH_3)_n(CH_3)_{4-n}$ (n = 1 - 3) in the next section, and this will directly confirm this speculation.

Conclusion

1. The mechanism of chemical vapor deposition of tetramethoxysilane on γ-alumina was proposed. Gaseous tetramethoxysilane is deposited on alumina quickly until the silicon alkoxide and a fraction of methanol cover the surface; only at high temperature (493 - 593 K), contaminated water hydrolyzes the silicon alkoxide into silanol, which is reacted with another tetramethoxysilane; the successive deposition thus proceeds, and at last, the monolayer with a network of siloxanes (Si-O-Si) covered the surface almost completely. At 673 K, the random deposition formed a heterogeneous structure of silica including thick layers and / or particles, which showed low activity.
2. Catalytic activity for isomerization of butene was observed over the monolayer deposited at 493 and 593 K. The samples deposited at low temperatures (≤ 423 K) showed almost no activity. It is suggested that Al-O-Si-OH in the network of Si-O-Si possesses the Brønsted acidity, whereas dispersed silica species has no acidity.

References

1. K. Tanabe, *Catalysis: Science and Technology, Vol. 2,* eds. J. R. Anderson and M. Boudart, Springer-Verlag, Berlin (1981) p. 231.
2. W. Grabowski, M. Misono and Y. Yoneda, *J. Catal.*, **61,** 103 (1980).
3. H. Kawakami, S. Yoshida and T. Yonezawa, *J. Chem. Soc., Faraday Trans. 2,* **80,** 205 (1984).
4. G. M. Zhidomirov, and V. B. Kazansky, *Adv. Catal.*, **34,** 131 (1986).
5. M. Niwa, Y. Kawashima, T. Hibino and Y. Murakami, *J. Chem. Soc., Faraday Trans. 1,* **84,** 4327 (1988).
6. T. Hibino, M. Niwa, A. Hattori and Y. Murakami, *Appl. Catal.*, **44,** 95 (1988).
7. T. Hibino, M. Niwa, Y. Kawashima and Y. Murakami, in *Chemistry of Microporous Crystals,* eds. T. Inui, S. Namba and Y. Murakami, Kodansha, Tokyo (1991) p. 151.

8. Y. Imizu, A. Tada and I. Toyoshima, *Shokubai (Catalyst),* **30,** 388 (1988).
9. Y. Imizu, K. Takahara, N. Okazaki, H. Itoh and A. Tada, in *Study in Surface Science and Catalysis Vol. 90: Acid-Base Catalysis II,* eds. H. Hattori, M. Misono and Y. Ono, Kodansha, Tokyo (1994) p. 339.
10. S. Sato, M. Toita, Y.-Q. Yu, T. Sodesawa and F. Nozaki, *Chem. Lett.*, **1987,** 1535.
11. S. Sato, M. Toita, T. Sodesawa and F. Nozaki, *Appl. Catal.*, **62,** 73 (1990).
12. S. Sato, T. Sodesawa and F. Nozaki, *J. Mol. Catal.*, **66,** 343 (1991).
13. T. Jin, T. Okuhara and J. M. White, *J. Chem. Soc., Chem. Commun.*, **1987,** 1248.
14. T. Jin and J. M. White, *Surf. Interface Anal.*, **11,** 517 (1988).
15. S. K. Jo, T. Jin and J. M. White, *Appl. Surf. Sci.*, **40,** 155 (1989).
16. H. Fukui, T. Ogawa, M. Nakano, M. Yamaguchi and Y. Kanda, in *Controlled Interphases in Composite Materials,* ed. H. Ishida, Elsevier Science Publishing, New York (1990) p. 469.
17. T.-C. Sheng and I. D. Gay, *J. Catal.*, **145,** 10 (1994).
18. T.-C. Sheng, S. Lang, B. A. Morrow and I. D. Gay, *J. Catal.*, **148,** 341 (1994).
19. B.-Q. Xu, T. Yamaguchi and K. Tanabe, *Chem. Lett.*, **1989,** 149.
20. N. Okazaki, T. Kohno, R. Inoue, Y. Imizu and A. Tada, *Chem. Lett.*, **1993,** 1195.
21. H. Knözinger and P. Ratnasamy, *Catal. Rev. -Sci. Eng.*, **17,** 31 (1978).
22. F. A. Cotton and G. Wilkinson, in *Advanced Inorganic Chemistry,* John Wiley & Sons, New York (1962) p. 93.
23. J. B. Peri, *J. Phys. Chem.*, **69,** 211 (1965).
24. J. E. Dabrowski, J. B. Butt and H. Bliss, *J. Catal.*, **18,** 297 (1980).
25. P. Sarrazin, S. Kasztelan, N. Zanier-Szyndlowski, J. P. Bonnelle and J. Grimblot, *J. Phys. Chem.* **97,** 5947 (1993).
26. Y. Tatsushima, Y. Morioka and A. Ueno, in *Proc. Heisei 6 Nendo Shokubai Kenkyu Happyou-kai* (1994) p. 554.

3-2 Generation of Acidity by Network of Siloxane

Synopsis

Structures of materials deposited from various Si alkoxides on alumina were determined based on gravimetry, product analysis and coverage measurement. The activity for double-bond isomerization of *1*-butene was observed over the silica monolayer with a network of siloxanes (Si-O-Si) deposited from $Si(OCH_3)_4$ at 493 - 593 K. However, the isolated silica species deposited from $Si(OCH_3)_4$ at low temperatures (≤ 423 K) and those deposited from $Si(OCH_3)_n(CH_3)_{4-n}$ (n = 1 - 3) showed almost no activity. Based on these findings, the species Al-O-Si(-O-Si)$_2$-OH in the network of Si-O-Si which mainly consists of Al-O-Si(-O-Si)$_3$ is proposed to be the Brønsted acid site, whereas the isolated species like (Al-O-)$_3$Si-OH has no acidity. The acidic property is supposed to be created by the structural stress of two-dimensional siloxane network due to the unfitness with support oxide.

Introduction

As described in Chapter 2, the CVD of $Si(OCH_3)_4$ formed silica monolayers on γ-alumina, titania and zirconia. In addition, a monolayer of germanium oxide was obtained by this method on alumina also. Weak Brønsted acidity was observed on all of these monolayers. A common rule for generation of acidity is therefore supposed on the hydroxyl species on the monolayer, M-O-T-OH (M = Al, Ti or Zr, and T = Si or Ge). Section 3 - 1 showed that the silica layer prepared from $Si(OCH_3)_4$ possessed a network structure consisting of siloxanes (Si-O-Si), because $Si(OCH_3)_4$ had four methoxy groups to form the siloxane bonds. A strong dependence of acidic property on structure was shown: since the activity for isomerization of *1*-butene was observed over the samples prepared at high temperatures (> 493 K) but not over those prepared at low temperatures, Brønsted acidity was indicated to depend on the degree of network of siloxanes. On the other hand, the acid strength of zeolite was found to depend on the crystal phase, and probably this shows the relationship between acidic property and micro structure (bond length and angle)[1, 2]. However, the reason of this phenomenon has not been understood well, because not only the structure but also pore-diameter and composition change with the crystal phase of zeolite. The most important purpose of the present thesis is to understand the origin of acidity, and so that, dependence of acidity on the structure should be clarified on the silica monolayer with simple structure.

In the present section, $Si(OCH_3)(CH_3)_3$ (monomethoxy-trimethylsilane), $Si(OCH_3)_2(CH_3)_2$ (dimethoxy-dimethylsilane) and $Si(OCH_3)_3(CH_3)$ (trimethoxy-monomethylsilane) were deposited on γ-alumina. It is suggested that the CVD of $Si(OCH_3)(CH_3)_3$ forms the isolated species of Al-O-Si-OH, because the methyl group is inactive to form Si-O-Si. It is also suggested that $Si(OCH_3)_2(CH_3)_2$ and $Si(OCH_3)_3(CH_3)$ form the species with the intermediate structure between those prepared from $Si(OCH_3)(CH_3)_3$ and $Si(OCH_3)_4$. The purpose of the present section is to show the dependence of acidity on the formation of Si-O-Si network, based on the relationship between the activity of deposited silica and the number of Si-O-Si bond.

Experimental

Chemical Vapor Deposition in Static System

Alumina was supplied from the Catalysis Society of Japan, as a reference catalyst, JRC-ALO4. The crystal phase was γ-Al_2O_3, and the surface area was 161 $m^2\ g^{-1}$.

According to Section 2 - 1, the sample was placed on a basket hung by a quartz spring in a vacuum line, and the change of weight was monitored by a transducer. Evacuation was carried out at 673 K until no change of the weight was observed. Vapor of Si alkoxide was then admitted onto the sample; the cycle of introduction of vapor and evacuation was repeated in order to allow the alkoxide vapor to be contacted with the sample. The vapor pressure of $Si(OCH_3)_4$, $Si(OCH_3)_3(CH_3)$, $Si(OCH_3)_2(CH_3)_2$ and $Si(OCH_3)(CH_3)_3$ was kept constant at *ca.* 2.5, 9.5, 21 and 74 Torr, respectively, by chilling the reservoir with an ice bath. The degree of evacuation was *ca.* 10^{-3} Torr. Finally, the sample was calcined with 200 Torr of oxygen at 673 K. The surface concentration of Si and organic materials were estimated from gravimetry and BET surface area.

Deposition in Pulse System

Alumina was set in a 4 mm i.d. Pyrex glass reactor. Helium was passed through a liquid nitrogen trap in order to remove the moisture and impurity oxygen, and fed onto the sample. After pretreatment at 673 K for 1 hour, 1 mm^3 (about $5 \cdot 10^{-6}$ mol) of liquid Si alkoxide was injected repeatedly. Products, methanol and dimethylether, were analyzed by GC which was directly connected with the reactor. The amount of deposited Si was estimated from the difference in the amounts between injected and eluted alkoxides.

Measurement of Coverage using Benzaldehyde-Ammonia Titration Method

Benzaldehyde is adsorbed on alumina (the saturated concentration, 1.8 nm^{-2}), but only little (< 0.01 nm^{-2}) on silica. On the basis of this finding, the coverage of alumina surface by the deposited materials was estimated by using the BAT method as shown in the previous sections. A sample was set in a Pyrex tube (i.d. 4 mm) connected with a GC. The carrier gas helium was purified by using a liquid nitrogen trap. After calcination at 673 K for 1 hour, 1 mm^3 ($9.8 \cdot 10^{-6}$ mol) of benzaldehyde was repeatedly injected onto the sample until no adsorption was observed. Finally, 10 cm^3 ($4.2 \cdot 10^{-4}$ mol) of gaseous ammonia was injected at 673 K, and the amount of desorbed benzonitrile was determined. Ammonia was repeatedly injected until no products were observed. The coverage by the deposited materials was calculated according to Section 2 - 1.

Test Reaction of Acidic Property

Isomerization of *1*-butene was chosen to test the acidic property of various species of SiO_2 under the conditions shown as (B) in Section 2 - 1. The catalyst was treated in a Pyrex reactor (4 mm i.d.) at 673 K for 1 hour in flowing helium which was purified with a liquid nitrogen trap. Then, 1 cm^3 ($4.2 \cdot 10^{-5}$ mol) of gaseous *1*-butene was injected onto the sample at 393 K. The flow rate of helium was 40 cm^3 min^{-1}, and the total pressure was 4 atm. The conversion was adjusted less than 5 % in order to measure the activity under differential reactor conditions. Products were analyzed using a column of VZ-7 at room temperature.

Results

Deposition in Static System

Table 3 - 2 - 1 shows the weight of materials deposited from various Si alkoxides in the static system until the saturation of deposition was observed. The deposition of $Si(OCH_3)(CH_3)_3$ was saturated at about 5 wt% of the deposited materials over the broad range of deposition temperature, 423 - 593 K. From $Si(OCH_3)_2(CH_3)_2$, the amount of deposited materials increased with the deposition temperature. As described in Section 3 - 1, the deposition behavior of $Si(OCH_3)_4$ was strongly dependent on the temperature. The saturation of deposition was observed at temperatures below 473 K, but not at higher temperatures.

Table 3 - 2 - 2 summarizes the weight, coverage and the Si concentration of materials deposited at 473 K from various alkoxides. The weight and coverage were decreased by the calcination following the deposition. The surface concentration of deposited silicon was determined based on

Table 3 - 2 - 1 : Deposition of various alkoxides in static system.

n of Source alkoxide $Si(OCH_3)_n(CH_3)_{4-n}$	Deposition temperature / K	Weight of materials deposited until deposition was saturated / wt%*
1	423	4.8
	473	5.2
	523	5.0
	593	5.2
2	423	5.1
	473	5.8
	523	6.5
	593	8.3
3	473	7.6
4	423	9.1
	473	11.9
	> 493	> 20**

*: Weight of deposited materials / weight of alumina. **: The deposition was not saturated.

Table 3 - 2 - 2 : Weight and coverage of materials deposited from various alkoxides until deposition was saturated at 473 K.

n of source alkoxide $Si(OCH_3)_n(CH_3)_{4-n}$	Before calcination		After calcination			a / b
	Weight of deposited materials* a	Coverage / %	Weight of deposited materials* b	Coverage / %	Si concentration / nm^{-2}	
1	5.2	61	3.4	38	1.9	1.53
2	5.8	60	3.9	41	2.2	1.47
3	7.6	70	5.6	64	3.1	1.36
4	11.9	80	8.1	68	5.2	1.47

*: wt% (Weight ratio of deposited materials / alumina).

the assumption that SiO_2 was formed after the calcination. The concentration of deposited Si and the coverage were increased with n of the source alkoxide $Si(OCH_3)_n(CH_3)_{4-n}$.

Deposition in Pulse System

The amount of deposited materials was determined until the deposition was saturated also in the pulse system. As shown in Table 3 - 2 - 3, the concentration of Si deposited from $Si(OCH_3)(CH_3)_3$ was 1.6 Si nm^{-2}, close to that observed in the static system, 1.9 Si nm^{-2}. Only dimethylether was observed in the products, the yield of which was 0.73 molecules per nm^2 of the alumina surface: it was about a half of the concentration of deposited Si. The concentration of Si was

Table 3 - 2 - 3 : Product analysis in pulse system. The deposition was carried out at 473 K.

n of source alkoxide $Si(OCH_3)_n(CH_3)_{4-n}$	Accumulated amount / (molecules / nm^2 of alumina surface) deposited alkoxide	formed dimethylether	formed methanol
1	1.6	0.73	not detected
2	1.6	0.63	0.80
3	2.1	0.50	1.93
4	2.6	0.42	3.8

lower than that obtained in the static system on the samples prepared from $Si(OCH_3)_n(CH_3)_{4-n}$ ($n \geq 2$).

Test Reaction

Figure 3 - 2 - 1 shows the change of catalytic activity for isomerization of *1*-butene by the CVD of silica. The activity was observed for the deposition of $Si(OCH_3)_4$ at 493 and 593 K. Only a small activity was observed for the deposition from $Si(OCH_3)_4$ at 473 K. Negligible activity was observed over the samples prepared from $Si(OCH_3)_4$ at 373 - 423 K, and those from $Si(OCH_3)_n(CH_3)_{4-n}$ (n = 1 - 3).

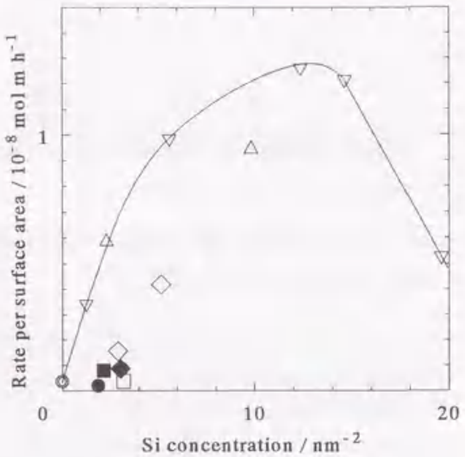

Figure 3 - 2 - 1 : Catalytic activity for isomerization from *1*- to *2*-butene at 393 K over the samples prepared from $Si(OCH_3)(CH_3)_3$ (●), $Si(OCH_3)_2(CH_3)_2$ (■), $Si(OCH_3)_3(CH_3)$ (◆) at 473 K and from $Si(OCH_3)_4$ at 373 (○), 423 (□), 473 (◇), 493 (△) and 593 K (▽).

Discussion

Structure of Deposited Species

Section 3 - 1 showed that the gaseous $Si(OCH_3)_4$ was quickly deposited to form the species

Al-O-$Si(OCH_3)_3$ over a broad range of temperature (373 - 673 K) and further reaction of the deposited species with gaseous $Si(OCH_3)_4$ was strongly dependent on the temperature. As a result, the saturation of deposition was observed in the low concentration of deposited Si at low temperature, whereas the deposition was not saturated at high temperature. On the other hand, the amount of materials deposited from $Si(OCH_3)(CH_3)_3$ was almost constant against the temperature. This indicates that the mechanism of deposition of $Si(OCH_3)(CH_3)_3$ was independent of the temperature. It is suggested that the surface species Al-O-$Si(CH_3)_3$ was formed from $Si(OCH_3)(CH_3)_3$ and was inactive for the reaction with gaseous alkoxide.

The findings that *ca.* 1/2 mol of dimethylether was obtained from 1 mol of $Si(OCH_3)(CH_3)_3$ in the pulse system lead us to propose the mechanism for deposition shown in Scheme 3 - 2 - 1. The formula weight of proposed species -O-$Si(CH_3)_3$ is 88, and that of SiO_2 is 60. The ratio of the formula weight before / after the calcination is thus 88 / 60 = 1.5, which agrees with the ratio shown by a / b in Table 3 - 2 - 2. In addition, the calculated and observed values of the surface area occupied by the proposed species agreed with each other as follows: for the area occupied by -O-$Si(CH_3)_3$, the calculated value was 0.38 nm^2 (Figure 3 - 2 - 2) and the observed one was 0.34 nm^2 (= coverage (61 %) / concentration (1.9 nm^{-2}) / 100) and after calcination, the calculated value was 0.19 - 0.20 nm^2 (Figure 3 - 2 - 3) and the observed one was 0.20 nm^2. These agreements support the validity for the proposed mechanism and indicate that no polymerization, migration or sintering of silica

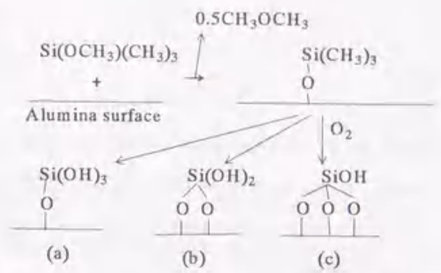

Scheme 3 - 2 - 1 : Proposed mechanism for deposition of $Si(OCH_3)(CH_3)_3$.

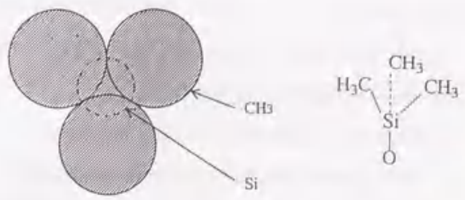

Figure 3 - 2 - 2 : Estimation of surface area occupied by the species O-$Si(CH_3)_3$. The Van der Waals radius of methyl group was assumed to be 0.20 nm[3]. The occupied are (////) was 0.38 nm^2.

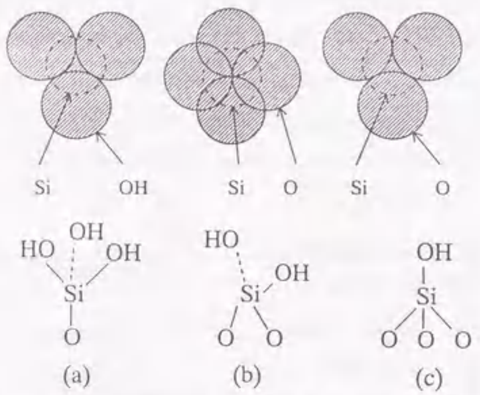

Figure 3 - 2 - 3 : Estimation of surface area occupied by the surface silica species, which were assumed to be formed from $Si(OCH_3)(CH_3)_3$ after the calcination. The Van der Waals radius of oxygen was assumed to be 0.17 nm[3]. The occupied area (/////) was 0.19 (a), 0.20 (b) and 0.19 nm^2 (c).

was caused by the calcination at 673 K. This will be supported by the next chapter also, because no sintering of silica monolayer at quite high temperature (1493 K) will be shown.

Scheme 3 - 2 - 2 shows the mechanism for the depositions of $Si(OCH_3)_2(CH_3)_2$ and $Si(OCH_3)_3(CH_3)$ based on the following assumptions: no methyl group was decomposed during the deposition; the methoxy groups were decomposed to form Si-O-Al and Si-O-Si bonds; the physical adsorption of products, the coke deposition and the change of amount of surface hydroxides were ignored. According to Scheme 3 - 2 - 2, the formula weight divided by the number

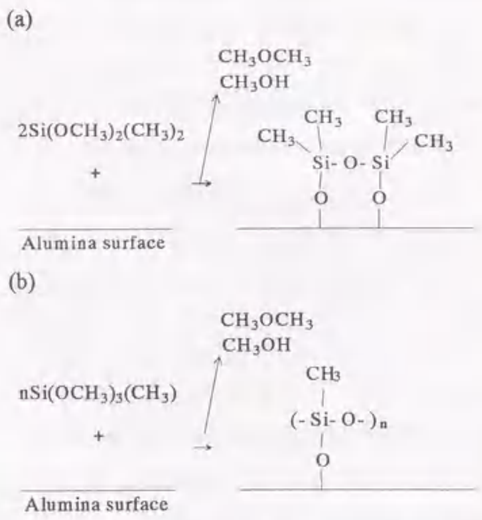

Scheme 3 - 2 - 2 : Proposed mechanism doe deposition of $Si(OCH_3)_2(CH_3)_2$ (a) and $Si(OCH_3)_3(CH_3)$ (b).

of Si atoms in the species from $Si(OCH_3)_2(CH_3)_2$ and $Si(OCH_3)_3(CH_3)$ is 82 and 75, and the ratio of weight before / after the calcination is thus calculated to be 1.4 and 1.3, respectively. The calculated ratios approximately agree with the observed ones at 473 K (a / b in Table 3 - 2 - 2). The small differences between the calculated and observed values were probably due to a minor fraction of methoxides remaining as $Si\text{-}O\text{-}CH_3$.

According to the proposed mechanisms, the surface species of silica with various degrees of network of siloxanes were obtained. The degree of network of siloxanes will be expressed by the ratio of the number of siloxane bonds to the number of silicon atoms (Si-O-Si / Si) in the following description. According to Scheme 3 - 2 - 1 and Scheme 3 - 2 - 2, the ratio of Si-O-Si / Si of materials deposited from $Si(OCH_3)_n(CH_3)_{4-n}$ with n = 1, 2 and 3 was 0, 0.5 and 1, respectively.

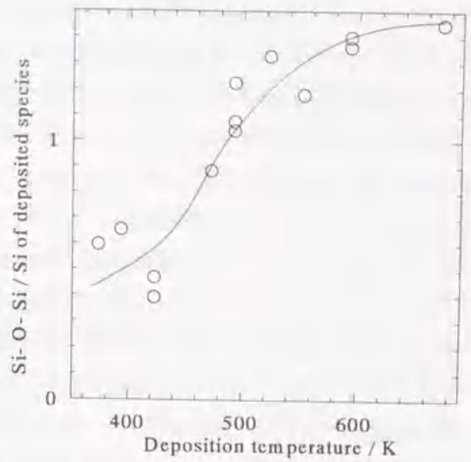

Figure 3 - 2 - 4 : Estimated ratio of Si-O-Si / Si of silica species prepared from $Si(OCH_3)_4$ as a function of temperature.

As shown in Figure 3 - 1 - 2, the composition of alkoxide deposited from $Si(OCH_3)_4$ was significantly affected by changing the deposition temperature. The ratio of Si-O-Si / Si is considered to be (3-x)/2 (x = CH_3O- / Si ratio), according to the structure proposed in Section 3 - 1 because one tetra-coordinated silicon atom had 1 of Al-O-Si, x of $Si\text{-}OCH_3$ and 3 - x of Si-O-Si bond, and the Si-O-Si bond was shared by two silicon atoms. Thus estimated Si-O-Si / Si ratio increased with the temperature as shown in Figure 3 - 2 - 4. The degree of development of siloxane network was thus quantified.

Origin of Brønsted Acidity

The activity for isomerization of *1*-butene was observed on the samples prepared from $Si(OCH_3)_4$ at 493 and 593 K. The activity showed the maximum at 13 Si nm^{-2}, where the silica monolayer covered the surface almost completely. As described in the previous chapter, these results indicate that the species Al-O-Si-OH on the silica monolayer has Brønsted acidity. On the

other hand, almost no activity was observed over the samples prepared from $Si(OCH_3)_4$ at low temperatures (373 - 423 K) and those from $Si(OCH_3)_n(CH_3)_{4-n}$ (n = 1 - 3). One may easily imagine that the interface between the two oxide, *i.e.* Al-O-Si, generates acidity, based on such electronic interactions as a charge transfer between two components. However, the lack of acidity on these isolated Al-O-Si-OH species clearly indicates that such an explanation is impossible. The structural property is presumed to induce the acidity.

In order to show the dependence of the activity on the network of Si-O-Si, the activity was divided by the number of Si atoms and plotted in Figure 3 - 2 - 5 against the ratio of Si-O-Si / Si. If the activity gradually increased, some other explanations are possible, but the activity was quite low below 1 of the Si-O-Si / Si ratio and jumped at *ca.* 1 of the Si-O-Si / Si ratio. It is therefore suggested that the Si species was isolated or bonded by an one-dimensional Si-O-Si chain below 1 of the Si-O-Si / Si ratio. The silica monolayer shown in Scheme 3 - 1 - 1 (c) which mainly consists of $Al\text{-}O\text{-}Si(\text{-}O\text{-}Si)_3$ containing a fraction of $Al\text{-}O\text{-}Si(\text{-}O\text{-}Si)_2\text{-}OH$ species has the Si-O-Si / Si ratio from 1 to 1.5. Therefore, the silica monolayer with a two-dimensional network of Si-O-Si is considered to be developed above 1 of the Si-O-Si / Si ratio. These findings indicate that the Brønsted acidity on the silica monolayer was created by the two-dimensional siloxane network on alumina. An oxide layer developed on another oxide is probably strained due to the difference in structures between the two oxides. It is suggested that such a stress due to unfitness is distinct on the two-dimensional network, while mono-dimensional chain and isolated species can relax it. Of course, the Brønsted acidity must be possessed by the hydroxyl species $Al\text{-}O\text{-}Si(\text{-}O\text{-}Si)_2\text{-}OH$. The strained structure is therefore speculated to give the acidity on $Al\text{-}O\text{-}Si(\text{-}O\text{-}Si)_2\text{-}OH$ species.

As shown in Chapter 2, the doublelayer had no acidity. It is suggested that

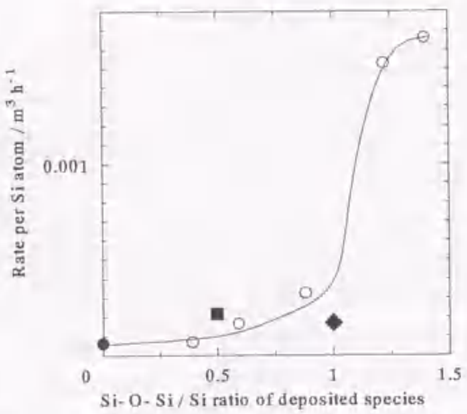

Figure 3 - 2 - 5 : Relationship between activity of Si atom and Si-O-Si / Si ratio over the samples with 1 - 3 nm² of silicon deposited from $Si(OCH_3)(CH_3)_3$ (●), $Si(OCH_3)_2(CH_3)_2$ (■), $Si(OCH_3)_3(CH_3)$ (◆) at 473 K and from $Si(OCH_3)_4$ (○) at various temperatures.

the structural stress is relaxed by a long distance between the interface and surface for the case of doublelayer. That chapter also shows the acid strength of monolayer is ordered as on alumina > titania > zirconia, and since silica is regarded as silica monolayer loaded on silica, silica is added after these oxides. This order is independent of the electronegativity, valence or coordination number of cation, as shown in Section 2 - 2. From alumina to zirconia, this corresponded to the concentration of silicon atoms on the monolayer, *i.e.* 13, 12 and 8 Si nm^{-2} on alumina, titania and zirconia, respectively. This indicates that well-developed network with high concentration of silicon atoms has relatively strong acid strength. As shown in Section 2 - 4, the germanium oxide monolayer loaded on alumina showed lower activity than that on silica monolayer. This also can be explained to be due to the less structural affinity of germanium oxide to alumina than silica, resulting in less developed network. Of course, silica has the highest concentration of surface silicon among the silica monolayers, but it possesses no acidity because there is no structural stress between surface and bulk. Thus, the explanation of generation of acidity by two-dimensional network is consistent with all the experimental results, and therefore, the species $M\text{-}O\text{-}T(\text{-}O\text{-}T)_2\text{-}Si\text{-}OH$ (M = Al, Ti or Zr, and T = Si or Ge) is generally concluded to possess weak Brønsted acidity due to a two-dimensional T-O-T network strained by the another oxide.

Fukui *et al.* reported a suppression of catalytic activity on titania by the CVD of polysiloxane[4]. The deposited silica is supposed to form a tetramer with 1 of the Si-O-Si / Si ratio based on the structure of precursor shown in Figure 3 - 2 - 6. So that the lack of acidity is predicted according to this study, and indeed, it showed neither acid nor redox catalytic function. Moreover, the property of isolated species must be related with the study carried out in the liquid phase as mentioned in Section 3 - 1. Sarrazin *et al.* reported no generation of acidity, while the basicity diminished with the loading of $Si(OC_2H_5)_4$ on alumina in ethanol[5]. These results support the lack of acidity on the dispersed Si species.

On the other hand, Imizu *et al.* reported the enhancement of activity for isotope exchange between D_2 and *1*-butene by such isolated silicon species as that deposited from $Si(OCH_3)(CH_3)_3$[6]. This reaction required a specific active site generated by the partial dehydration of alumina surface. The exchange activity was observed on the pure alumina, and was significantly enhanced by the low loading of $Si(OCH_3)_n(CH_3)_{4-n}$ (n =

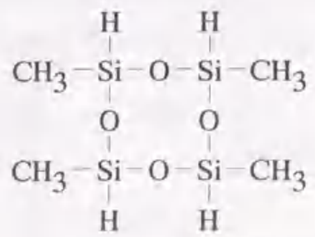

Figure 3 - 2 - 6 : Molecular used by Fukui *et al.* for CVD on titania[4].

1 to 3), $(CH_3)_6Si_2NH$ and $[(CH_3)_2SiOCH_3]_2O$. This was compared to the samples deposited from $Si(OCH_3)_4$ and $Si(OC_2H_5)_4$, which simply reduced the exchange activity, showing no exchange on a simple Brønsted acidic catalyst. It is suggested that the high dispersion of silicon species which is bonding to specific site on alumina gives the significant enhancement of exchange activity in the former cases.

The improvement of original catalytic activity was also reported recently for a interested reaction, the removal of nitrogen oxide from exhaust gas under the presence of oxygen and hydrocarbon[7]. The activity on the sample deposited from $Si(OC_2H_5)_2(CH_3)_2$ was quite higher than those of alumina and the conventional silica-alumina. Moreover, the same authors reported that the liquid phase loading of organometal complex $(CH_3)_3SiOAlCl_2$, which originally contained a specific Al-O-Si bond, showed a distinct modification effect for acid-base property[8].

The acid-base bifunctional activity was reported by Xu *et al.*[9] The selective decomposition of triethylamine into acetonitrile is known to proceed through the dealkylation of alkylamine catalyzed by an acid and the dehydrogenation from amine to nitrile on a base. So that, the total reaction requires both of acid and base sites, and zirconia, which is a typical acid-base bifunctional catalyst, therefore shows a high activity. The silica layer deposited from $Si(OC_2H_5)_4$ at room temperature on magnesia was as active as zirconia, while a simple acidic catalyst, *i.e.* silica-alumina, catalyzed only the dealkylation resulting in the low selectivity, and a typical basic catalyst, *i.e.* magnesia, showed no activity. This study suggests that the acid site is generated on the deposited silica layer and the basic site is remained on magnesia exposed surface with a distance between them enough to show a concerned effect.

These studies showed that a well-dispersed silica species creates no acidity but modifies the chemical property of support oxide by the strong interaction *via* the M-O-Si interface. In other words, a specific active site with a distinct structure is formed on the dispersed silica species. On the contrary, the homogeneous monolayer with simple Brønsted acidic property is characteristically obtained by the deposition of $Si(OCH_3)_4$ at 493 - 593 K. It should be noted that the structure and function of surface silicon species are controllable using the CVD method by selecting the Si reagent and conditions.

Conclusion

1. Deposition of $Si(OCH_3)_n(CH_3)_{4-n}$ (n = 1 - 3) proceeded *via* the expected reaction mechanism, and formed species with various degrees of siloxane network.

2. Catalytic activity for double-bond isomerization of butene showed one relationship against the ratio of Si-O-Si / Si over the samples prepared from various alkoxides or at various deposition temperatures. The activity was quite low at the Si-O-Si ratio below 1, and jumped at 1 of the ratio. This indicates the acidity requires a two-dimensional network of siloxanes which mainly consists of M-O-Si(-O-Si)$_3$ containing M-O-Si(-O-Si)$_2$-OH (M = Al, Ti or Zr, and T = Si or Ge) species.
3. The Brønsted acid site of silica monolayer loaded on metal oxide is proposed as the species M-O-T(-O-T)$_2$-Si-OH. The weak Brønsted acidity is considered to be due to a T-O-T network strained by the another oxide.

References

1. M. Niwa, N. Katada, M. Sawa and Y. Murakami, *J. Phys. Chem.*, **99,** 8812 (1995).
2. H. Igi, N. Katada, J.-H. Kim and M. Niwa, in *Proc. Heisei 7 Nendo Shokubai Kenkyu Happyoukai,* (1995) p. 185.
3. F. A. Cotton and G. Wilkinson, in *Advanced Inorganic Chemistry,* John Wiley & Sons, New York (1962) p. 104.
4. H. Fukui, T. Ogawa, M. Nakano, M. Yamaguchi and Y. Kanda, in *Controlled Interphases in Composite Materials,* ed. H. Ishida, Elsevier Science Publishing, New York (1990) p. 469.
5. P. Sarrazin, S. Kasztelan, N. Zanier-Szyndlowski, J. P. Bonnelle and J. Grimblot, *J. Phys. Chem.*, **97,** 5947 (1993).
6. Y. Imizu, A. Tada and I. Toyoshima, *Shokubai (Catalyst),* **30,** 388 (1988).
7. N. Okazaki, T. Kohno, R. Inoue, Y. Imizu and A. Tada, *Chem. Lett.*, **1989,** 149.
8. Y. Imizu, K. Takahara, N. Okazaki, H. Itoh and A. Tada, in *Study in Surface Science and Catalysis Vol. 90: Acid-Base Catalysis II,* eds. H. Hattori, M. Misono and Y. Ono, Kodansha, Tokyo (1994) p. 339.
9. B.-Q. Xu, T. Yamaguchi and K. Tanabe, *Chem. Lett.* **1989,** 149.

3-3 Micro Structure of Brønsted Acid Site on Silica Monolayer

Synopsis

Nuclear magnetic resonance (NMR) of ^{29}Si showed that the silica monolayer formed from $Si(OCH_3)_4$ at 593 K on alumina mainly consisted of $Si(OAl)_1(OSi)_3$ and $Si(OAl)_1(OSi)_2(OH)_1$ species. This confirms the proposal for structure of silica monolayer, and shows that the Brønsted acid site is the latter species. The change of concentration of the $Si(OAl)_1(OSi)_2(OH)_1$ species, which corresponds to the change of catalytic activity for isomerization of butene, supports that this species is the Brønsted acid site. The structure formed from $Si(OCH_3)(CH_3)_3$ is confirmed to be such an isolated species as $Si(OAl)_3(OH)_1$. The monolayer on titania is shown to possess a similar structure. The monolayer on zirconia has a less developed network of siloxanes caused by a lower concentration of silicon, and showed a weak acidity in comparison with the monolayers on alumina and titania. These findings indicate that the origin of acidity is the two-dimensional network containing the $Si(OAl)_1(OSi)_3$ and $Si(OAl)_1(OSi)_2(OH)_1$ species which is developed on the support oxide and is strained due to the structural unfitness.

Introduction

Among spectroscopic techniques, solid-state nuclear magnetic resonance (NMR) is one of the most useful analyses for studies on inorganic solids, because it can determine the micro structure of the observed element[1, 2]. This technique has been developed in the last decade, accompanying with progresses of ultra-conductive magnet and method for rotating the magic-angle spinning cell with ultra-high speed[3 - 13]. For silicate materials, ^{29}Si NMR can directly analyze to which atom Si is bonding, and this will show the structure of silica cluster or ultra thin layer in the atomic-order for the present catalysts.

Chemical shift in silicate, *i.e.* pure- or combined-silicon oxide, appears in the region from -60 to -120 ppm with respect to tetramethylsilane. Various aluminosilicates have been analyzed, and the chemical shifts of such species as $Si(OSi)_4$, $Si(OSi)_3(OAl)_1$ and $Si(OSi)_3(OH)_1$ have been determined[6, 8 - 13]. The chemical shift of silicon atom in a silica matrix, *i.e.* $Si(OSi)_4$, is observed in the range of -110 to -125 ppm, and is slightly changed by the crystal phase. The linear dependence of chemical shift on bond angle was pointed out as shown in Figure 3 - 3 - 1[14].

Substitution of silicon by aluminum makes the chemical shift larger (makes it to smaller negative value), and a linear dependence is obtained for $Si(OAl)_n(OSi)_{4-n}$ for each substitution number of n in various aluminosilicate compounds (Figure 3 - 3 - 2)[15]. The change of chemical shift induced by the substitution of one aluminum atom is almost 6 ppm: namely, $Si(OAl)_{n+1}(OSi)_{3-n}$ species shows the chemical shift 6 ppm larger (smaller in negative value) than that of $Si(OAl)_n(OSi)_{4-n}$, as shown in Figure 3 - 3 - 3[10].

Similar change in the chemical shift was observed with substitution of silicon by hydrogen. The chemical shift increases (becomes smaller negative value) approximately 10 ppm with isomorphous substitution of one hydrogen atom[16]. Identification of Si species can be made based on these phenomena, but the similar change of chemical shift by aluminum and hydrogen sometimes misleads the interpretation of spectrum.

Cross-polarization (CP) method, especially ^1H-CP method has been applied to study the physical and chemical behaviors of silanols on silica gel[17 - 20]. By this method, the resonance of silicon atom which locates near hydrogen atom, *e.g.* Si-OH, is enhanced by spin coupling between the two atoms. This confuses the quantitative analysis, but very rare surface species, which is often important to the chemical reaction, is emphasized.

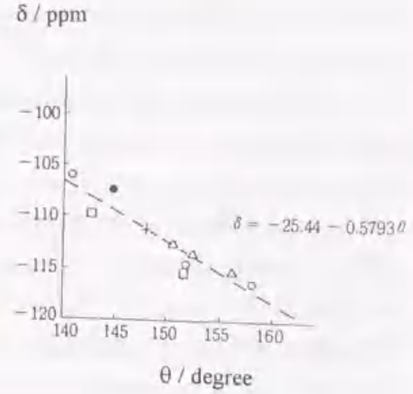

Figure 3 - 3 - 1 : Dependence of chemical shift of $Si(OSi)_4$ on bond angle of Si-O-Si (θ) in various silicate crystals[14].

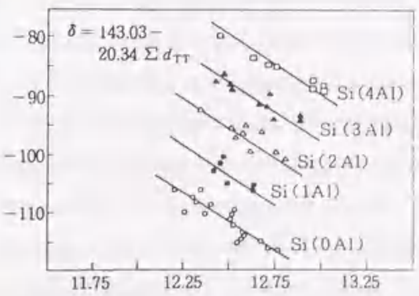

Figure 3 - 3 - 2 : Dependence of chemical shift of $Si(OAl)_n(OSi)_{4-n}$ [shown by Si(nAl)] on bond angle of Si-O-T (θ, T = Si or Al) in various aluminosilicate compounds[15].

In addition, the Si-OH species can be distinguished from Si-OAl by this technique.

The previous sections proposed that the silica monolayer mainly consists of M-O-Si(-O-Si)$_3$ and M-O-Si(-O-Si)$_2$-OH (M = Al, Ti or Zr). Weak Brønsted acid site is considered to be the latter. To prove these structures, NMR is promising. These technique will clarify the micro structure of silica monolayer, and will determine the structure of Brønsted acid site in the present section.

Sato *et al.*[21] and Sheng *et al.*[22] have already utilized the NMR to analyze the silica layers loaded on alumina by the CVD method. They reported different spectra for the silica layers prepared in oxygen and nitrogen. Sato *et al.* proposed a doubly-accumulated structure for the layer deposited from $Si(OC_2H_5)_4$ in oxygen, based on the spectrum showing a large amount of $Si(OSi)_4$ species (-107 ppm). Sheng *et al.* observed a relatively homogeneous and thin layer formed from $Si(OCH_3)_4$, but proposed a random build-up mechanism in flowing nitrogen. As shown in the previous sections, analyses other than NMR suggest a variation in the structure among the silica layers prepared under the different conditions. Therefore, this disagreement is probably due to the difference of preparation conditions.

Another disagreement is cited by these authors. Sato *et al.* measured the NMR without ^{1}H CP technique in a sufficient signal intensity mainly for the samples prepared in oxygen[21]. However, Sheng *et al.* reported that CP was necessary because the signal due to glass tube was intense[22], *i.e.* the sample showed too small peak and noise from the tube could not be ignored. This disagreement is possibly considered to be caused by the structural difference of samples prepared in different conditions. This section will solve these unexplained phenomena with the relationship between the NMR spectra and other characterization results observed for various samples.

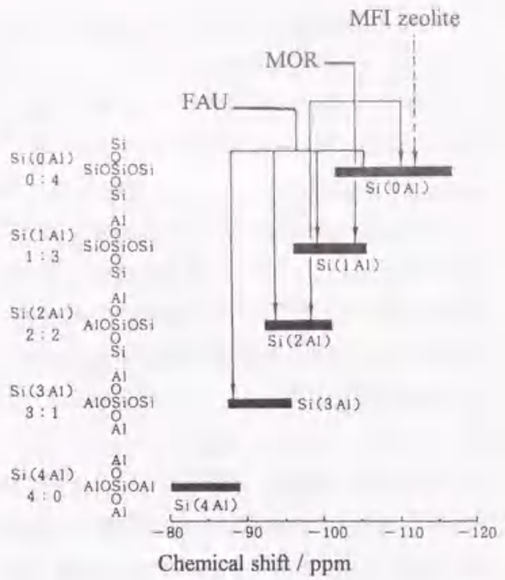

Figure 3 - 3 - 3 : Chemical shifts of various Si species in zeolites[10].

Experimental

Silica layers deposited from $Si(OCH_3)_4$ at 473 and 593 K, from $Si(OCH_3)(CH_3)_3$ at 473 K on alumina, and from $Si(OCH_3)_4$ at 593 K on titania and zirconia were analyzed in this section. The preparation was carried out according to the previous sections. The measurements were done after the sample was exposed to a humid atmosphere (relative humidity *ca.* 80 %) or was pretreated at 673 K in flowing nitrogen for 1 hour followed by quick transporting the sample into the NMR tube in atmosphere.

Magic-angle spinning (MAS) NMR spectra were observed for ^{29}Si on a Varian UNITY plus-400 spectrometer at 79.456 MHz of the magnetic field frequency, 5.5 μsec of the pulse width, 51 msec of the acquisition time, 4.0 sec of the relaxation time and about 4.2 kHz of the spinning rate. Cross-polarization (CP) spectra were measured with 0.5 - 6 msec of the contact time.

Results and Discussion

Influence of ^{1}H Cross-Polarization

Figure 3 - 3 - 4 (a) shows the NMR spectrum of silica monolayer on alumina (19.6 wt% of SiO_2, *i.e.* 11.4 Si nm^{-2} deposited from $Si(OCH_3)_4$ at 593 K as shown in Section 2 - 1; this sample will be termed as the full-coverage monolayer in the following description) measured without CP. The peak was observed a wide range from -80 to -120 ppm. The main peak seems to appear at -101 ppm, but so noisy spectrum is hardly analyzed, although the accumulation was carried out for more than 5 days to improve the signal to noise ratio. Under such conditions for NMR or even in a lower magnetic field, clear spectra were obtained in the cases of silica gel[17], zeolites[6, 8 - 16] and the silica layer prepared in oxygen[21]. The ^{29}Si NMR spectrum has been reported to be broadened by the presence of aluminum from the observations on zeolites with various aluminum contents[23]. This low signal to noise ratio, namely a large broadening of spectrum, is also supposed to be due to a polarization by aluminum atom which locates near the silicon atoms. In other words, almost all of silicon atoms of this sample reside close to aluminum, namely just onto the alumina surface, with distances enough short to induce the magnetic interaction. This behavior, obviously different from the cases of such bulky silica compounds as silica gel and zeolites, is strongly supports the ultra thin layer structure loaded on alumina.

This phenomenon also gives a possible explanation for disagreement between Sato *et al.* and Sheng *et al.* The former researchers measured the spectra without CP in satisfactory intensity[21],

while the latter observed a large signal due to glass tube, *i.e.* too small sample signal[22]. This disagreement suggest the difference in structure. The former sample prepared in oxygen is supposed to have a bulky structure like silica gel, whereas the latter prepared in nitrogen is an ultra thin layer like the present sample.

Anyway, detail cannot be discussed on such a noisy spectrum. So that, the ^1H cross-polarization (CP) technique was applied. As shown in Figure 3 - 3 - 4 (b) - (d), CP improves the signal to noise ratio, but seems not to change the peak shape and position. This is quite distinct from the cases of silica gel and zeolites; usually, the peak at large chemical shift (low negative value) is enhanced by CP because such a peak is connected with hydroxyl group while the peak at small chemical shift (high negative value) is due to the silicon atoms $Si(OSi)_4$ locate inside of bulk. The

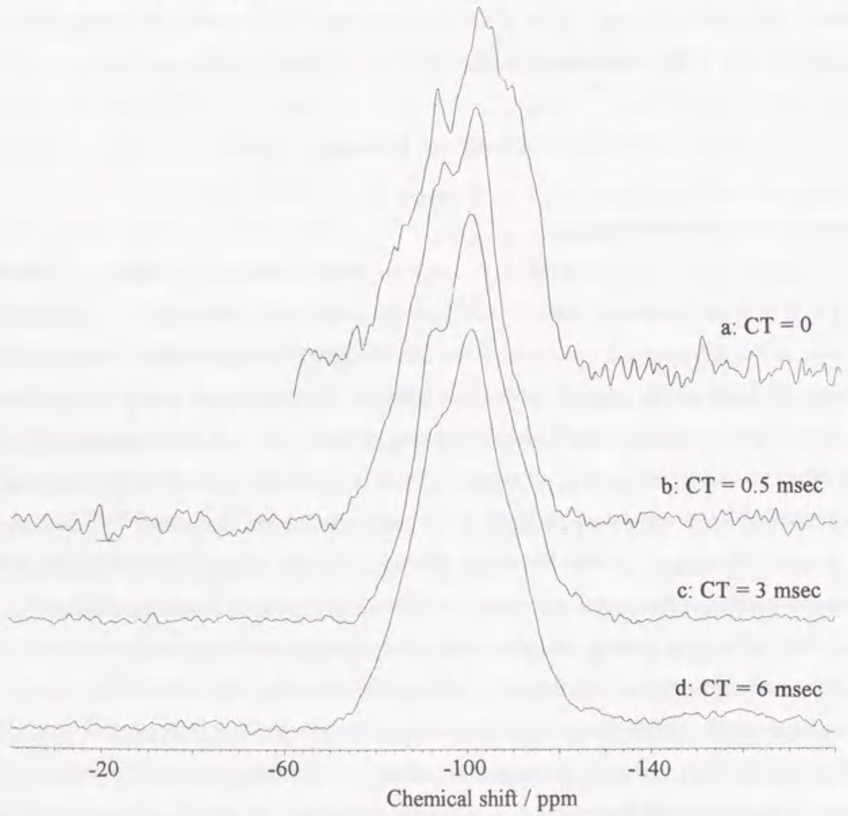

Figure 3 - 3 - 4 : ^{29}Si NMR spectra of sample with 11.4 nm^{-2} of Si deposited from $Si(OCH_3)_4$ at 593 K on alumina measured in humid conditions without CP (a), and with CP at 0.5 (b), 3 (c) and 6 msec (d) of the contact times.

simplest explanation for this phenomenon is that most of silicon atoms locate near the surface and are equally enhanced by surface hydroxide and / or adsorbed water. In other words, this supports the validity of monolayer structure. In the following description, the measurements were carried out with the CP technique at 3 msec of the contact time.

Silica Monolayer deposited from $Si(OCH_3)_4$ at 593 K on Alumina

Figure 3 - 3 - 5 shows the spectra of full-coverage monolayer under the dried conditions, *i.e.* after it was pretreated at 673 K for 1 hour. Deconvolution of spectrum showed four assignments,

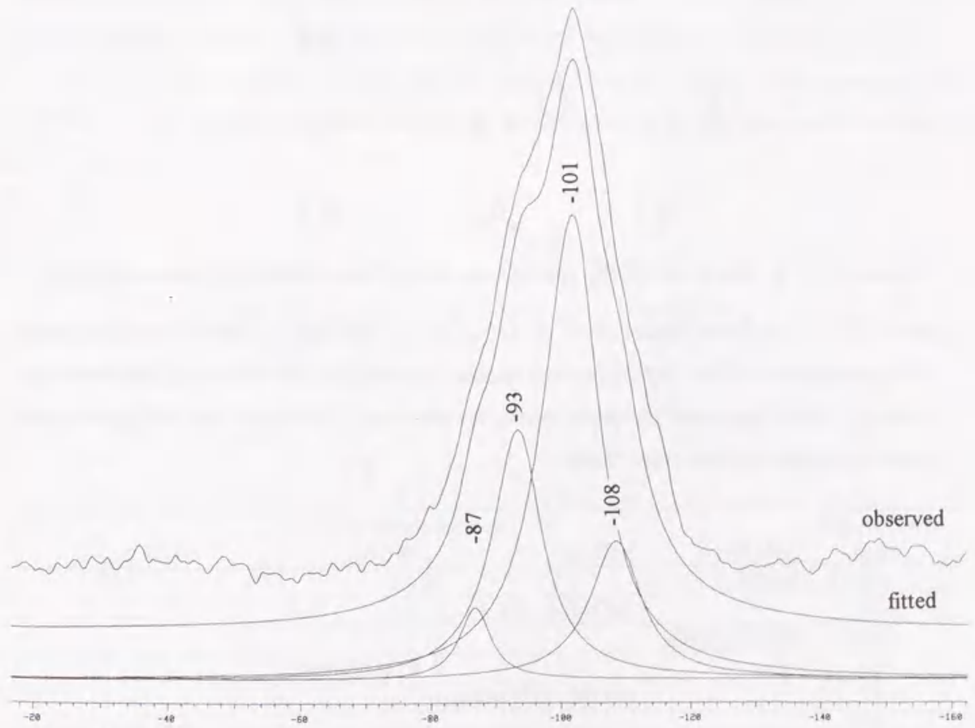

Figure 3 - 3 - 5 : Spectrum of full-coverage silica monolayer on alumina (11.4 Si nm^{-2} deposited from $Si(OCH_3)_4$ at 593 K) dried at 673 K and the best fitted curve synthesized from four Lorentzian functions.

-87 (A), -93 (B), -101 (C) and -108 (D) ppm. The peak (D) is clearly ascribable to $Si(OSi)_4$ species. At least, doubly accumulated layer is necessary to form such a $Si(OSi)_4$ species (Scheme 3 - 3 - 1). Since the peak intensity corresponds to *ca.* 10 %, it is pointed out that a small fraction of silicon formed such an accumulated layer with 11 Si nm^{-2}.

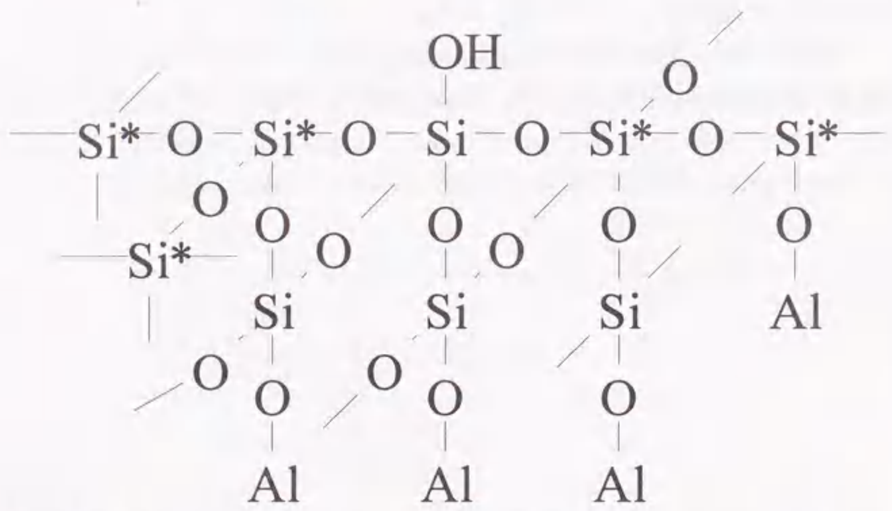

Scheme 3 - 3 - 1 : Model of $Si(OSi)_4$ species (marked by *) in a doubly-accumulated layer.

Table 3 - 3 - 1 : Predicted species at -80 to -110 ppm and their chemical shifts estimated from the assumptions that the $Si(OSi)_4$ species appears at -108 ppm, and one-atom substitution of silicon by aluminum and hydrogen makes the chemical shift into 6 and 10 ppm higher (smaller negative value), respectively.

Chemical shift / ppm	Species classified as $Si(OAl)_0$	$Si(OAl)_1$	$Si(OAl)_2$	$Si(OAl)_3$
-108	$Si(OSi)_4$			
-102		$Si(OAl)_1(OSi)_3$		
-98	$Si(OSi)_3(OH)_1$			
-96			$Si(OAl)_2(OSi)_2$	
-92		$Si(OAl)_1(OSi)_2(OH)_1$		
-90				$Si(OAl)_3(OSi)_1$
-88	$Si(OSi)_2(OH)_2$			
-86			$Si(OAl)_2(OSi)_1(OH)_1$	
-82		$Si(OAl)_1(OSi)_1(OH)_2$		
-80				$Si(OAl)_3(OH)_1$

In order to ascribe the other peaks, the predicted species and their chemical shifts estimated from that of $Si(OSi)_4$ species are summarized in Table 3 - 3 - 1. According to this table, the main peak (C, -101 ppm) has two possibilities; it can be ascribed to $Si(OAl)_1(OSi)_3$ or $Si(OSi)_3(OH)_1$.

The former $Si(OAl)_1(OSi)_3$ species is consistent with the proposal on structure of silica monolayer which consists of 1 : 1 bondings of Al-O-Si and a two-dimensional siloxane (Si-O-Si) network. Moreover, if the latter species was assumed, most of the surface of this sample should be covered by this hydroxyl species. Since this sample had been pretreated at 673 K, and the IR spectroscopy showed the silanols isolated from other hydroxyl groups (Figure 2 - 1 - 4), such an explanation is impossible. The peak (C), which seems most important for estimation of structure, is thus determined to $Si(OAl)_1(OSi)_3$ species.

The peak (B) is ascribable to $Si(OAl)_1(OSi)_2(OH)_1$ species. Because the Brønsted acid site is presumed to be te surface hydroxyl group, this hydroxyl species (B) is considered as the Brønsted acid site on the monolayer. The small peak (A) is probably due to $Si(OAl)_1(OSi)_1(OH)_2$ species.

Since the peak areas of (B) and (C) occupy more than 80 % of the whole peak area, the structure of silica monolayer with near 12 Si nm^{-2} of silicon, which fully covers the alumina surface, is

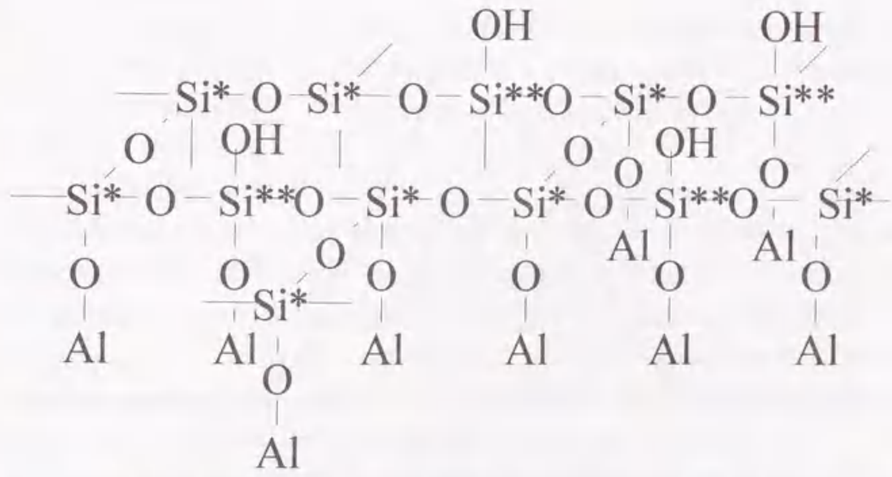

Scheme 3 - 3 - 2 : Model of silica monolayer fully covering alumina surface proposed from NMR spectroscopy. The symbol Si* shows the $Si(OAl)_1(OSi)_3$ species, and Si shows the $Si(OAl)_1(OSi)_2(OH)_1$ species. This model has 8 of the former species and 4 of the latter species on 12 Al atoms, which occupy approximately each 1 nm^2 of surface.**

concluded to mainly consist of a network containing $Si(OAl)_1(OSi)_3$ and Brønsted acidic $Si(OAl)_1(OSi)_2(OH)_1$ species. Ratio of peak area of (B) to (C) species is almost 1 : 2, and the concentrations of the (B) and (C) species is hence estimated to be approximately 4 and 8 nm^{-2}, respectively, although some uncertainties are supposed to be due to contaminated humidity after the pretreatment. These observations lead a model of monolayer as shown in Scheme 3 - 3 - 2 which consists of 4 and 8 of $Si(OAl)_1(OSi)_2(OH)_1$ and $Si(OAl)_1(OSi)_3$ species on 1 nm^{-2} of alumina surface, respectively, and it agrees well with the proposal from the growth mechanism shown in Scheme 3 - 1 - 1.

However, Sheng *et al.* presented a different interpretation for NMR spectra obtained on the silica layer deposited from $Si(OCH_3)_4$ at 593 K in flowing nitrogen as shown in Figure 3 - 3 - 6[22]. The disagreements are as follows:

1) Sheng *et al.* ascribed the -100 ppm peak to $Si(OSi)_3(OH)_1$ species, while the present author ascribed it to the $Si(OAl)_1(OSi)_3$ species.

2) They assumed three Gaussians including a quite broad $Si(OSi)_4$ peak, showing a formation of multiple layer, while the present author assumed four Lorentzians including a small (10 % in peak area) $Si(OSi)_4$ peak.

Figure 3 - 3 - 6 : Experimental spectrum and Gaussian fitting reported by Sheng *et al.*[22]

3) They implied the existence of further $Si(OSi)_4$ species because only hydroxyl species has a trend to be emphasized by CP, while the present author showed the similarity in peak shape between the spectra recorded with and without CP.

4) They assumed that at least three-atomic layers must be accumulated to form an $Si(OSi)_4$ species, probably based on the speculation as shown in Scheme 3 - 3 - 3, while the present author assumed that the doublelayer can form this species as shown in Scheme 3 - 3 - 1.

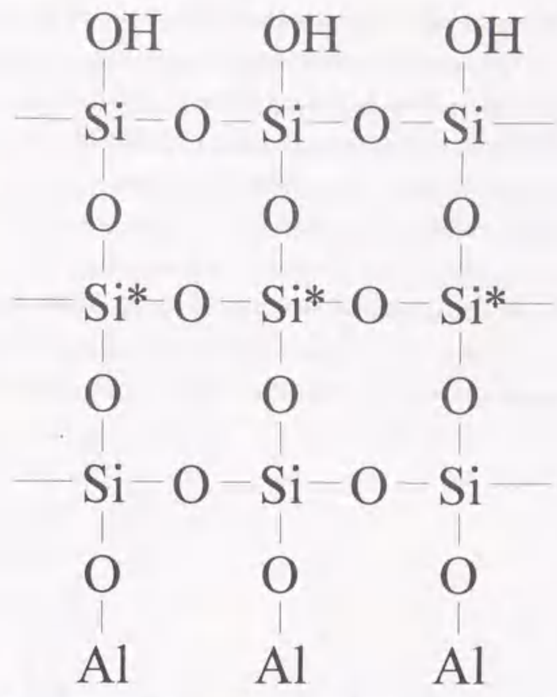

Scheme 3 - 3 - 3 : Assumption that $Si(OSi)_4$ species (marked by *) appears in the thirdly or further accumulated layer, but not in the doubly-accumulated layer.

As a result of these disagreements, Sheng *et al.* proposed a silica layer with heterogeneous thickness for the sample with *ca.* 12 Si nm^{-2}, while the present author proposes a homogeneous monolayer. One possible reason for this disagreement is the difference in structure between the samples prepared in the present static system and in their continuos-flow system. As shown in Section 3 - 1, such a random deposition can be proceed in the flow system due to the contamination of water vapor and / or some fluid mechanical factors. However, the spectra themselves are quite similar, so that further reasons are supposed about each four points shown above.

For the point 2), it cannot be judged whether deconvolution is right, because both are certainly possible. However, for the point 1), the explanation by Sheng *et al.* with high amount of $Si(OSi)_3(OH)_1$ species is unreliable, because the surface should be covered by hydroxyl groups according to this explanation. Both of Sheng *et al.* and the present author pretreated the sample at 673 K before the NMR measurement, and especially Sheng *et al.* completely sealed it in a glass tube.

The hydroxyl groups must be isolated from each other under such a situation.

For the point 3), all of silicon atoms can be emphasized by CP if the distance to hydrogen is less than about 0.4 nm, as Sheng *et al.* themselves estimated. It is supposed that the mono- and doublelayers are enough thin to interact with surface hydroxide with such a small distance, if several molecules of hydroxyl exists on each nm^2 of surface. About 30 % of $Si(OAl)_1(OSi)_2(OH)_1$ peak shows the existence of hydroxides with such a concentration according to the present explanation, or higher hydroxyl concentration is estimated in the case according to the proposal by Sheng *et al.* which ascribes the (C) peak to $Si(OSi)_3(OH)_1$. Addition with this, the similarity between spectra obtained with and without CP is originally shown by the present study. For the point 4), such a thick layer is unnecessary to explain the formation of $Si(OSi)_4$ species on dried surface.

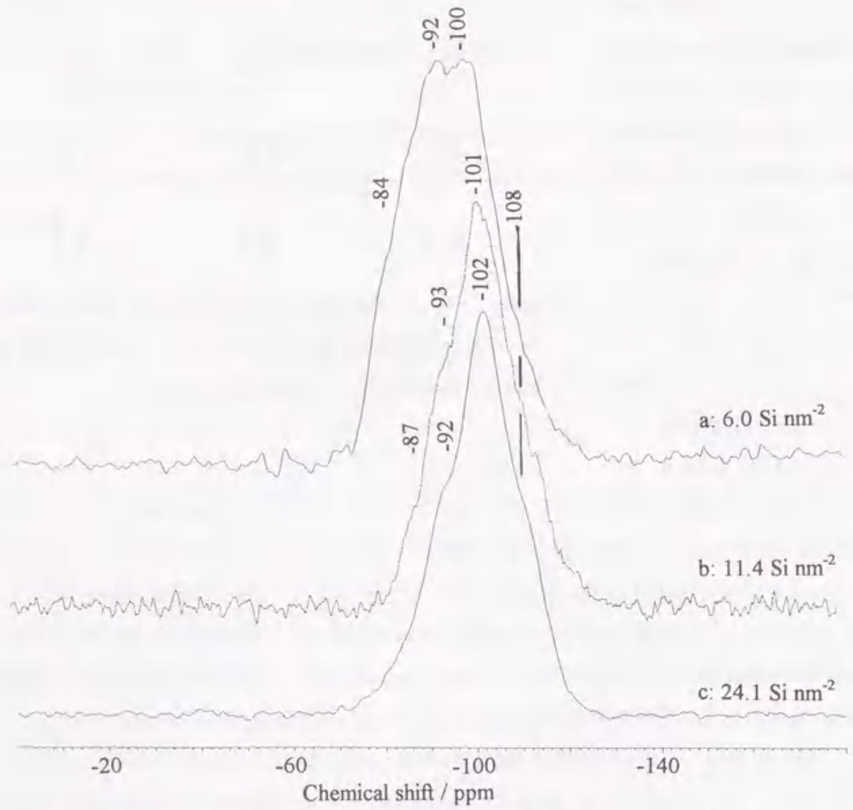

Figure 3 - 3 - 7 : Spectra of silica layer with 6.0 (a), 11.4 (b) and 24.1 Si nm^{-2} (c) deposited from $Si(OCH_3)_4$ at 593 K on alumina. The measurements were done after the pretreatment at 673 K.

The explanation by Sheng *et al.* is also based on the speculation that the monolayer of SiO_2 has 7 - 8 nm^{-2} of silicon, and further deposition forms the accumulated layer. However, this is based on findings by liquid phase loading method that the 7 - 8 nm^{-2} of silicon atoms are readily deposited on the solid surface, but further deposition is difficult[24]. According to the previous sections, this simply shows that the silicon atoms loaded at low temperature hardly form Si-O-Si bondings to concentrate. In conclusion, the present explanation is more reliable and agrees better with other experiments.

From the relationship between chemical shift of $Si(OSi)_4$ species and bond angle proposed by Thomas *et al.*[14], the bond angle Si-O-T (T = Al or Si) is estimated to be 143°. From the chemical shift of $Si(OAl)_1(OSi)_3$ species, the angle is estimated as 140°. These angles are similar to that of faujasite, and quite lower than those of mordenite and ZSM-5. This might show the dependence of acid strength on the bond angle; silicate with the lower bond angle seems to show the weaker acid site. It can be propose that the higher the bond angle, which is caused by the more tightly strained structure, induces the stronger the acid sites.

Figure 3 - 3 - 7 shows the spectra of samples with 6.0, 11.4 and 24.1 nm^{-2} of silicon dried at 673 K. From the deconvo-

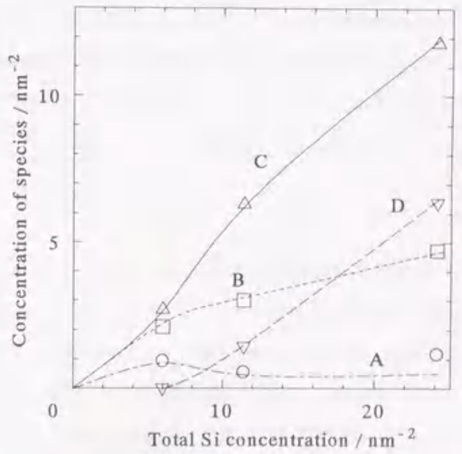

Figure 3 - 3 - 8 : Surface concentration of species (A) - (D) calculated from peak area in NMR spectrum and total Si concentration.

Table 3 - 3 - 2 : Activity for isomerization of *1*-butene at 393 K under the conditions shown as (C) in Section 2 - 1.

Concentration of total Si / nm^{-2}	(B) species	Activity for isomerization of *1*-butene per surface area 10^{-8} mol m h^{-1}	concentration of (B) 10^{-2} m^3 h^{-1}
6	2.10	4.75	1.36
11	3.01	6.17 - 6.45	1.24 - 1.29

luted peak areas and the Si concentration determined by gravimetry, the surface concentration of species (A) - (D) was plotted against the total Si concentration in Figure 3 - 3 - 8. The sample with 6.0 Si nm^{-2} shows the spectrum mainly consisting of (B) and (C) as well as the sample with 11.4 Si nm^{-2}., but the peak (B) is as large as (C) in the case of 6.0 Si nm^{-2}, while the peak (B) is relatively small on the sample with 11.4 Si nm^{-2}. This is also shown in Figure 3 - 3 - 8, because the concentration of species (B) quickly increased with the low concentration (0 - 6 Si nm^{-2}) of Si deposition, and continued to increase slowly in the region of 6 - 11 Si nm^{-2}. At the beginning of deposition, a small patch consisting of siloxane network is supposed; the size is not so small because too small silicon cluster may not show the acidity, as shown in Section 2 - 2. The smaller patch has the higher ratio of (B) to (C) species, because the hydroxyl (B) species is considered to be enriched at the edge of siloxane network.

The change of the species (B) with Si deposition is also consistent with the change of activity for double-bond isomerization of *1*-butene shown in Section 2 - 1. The activity significantly increased with the low concentration of silicon, and continued to increase slowly with the high concentration. From the peak intensity of (B), the concentration was calculated and the activity on one hydroxide (B) as shown in Table 3 - 3 - 2. It was similar on the samples with 6.0 and 11.4 Si nm^{-2}, and this supports that the Brønsted acid site is species (B).

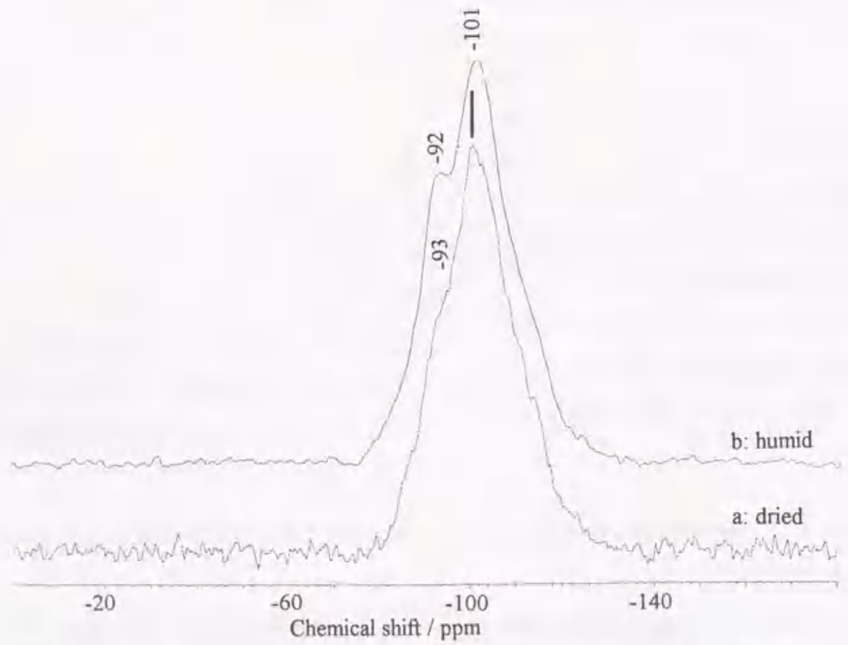

Figure 3 - 3 - 9 : Spectra of full-coverage monolayer sample (11.4 Si nm^{-2} deposited from $Si(OCH_3)_4$ at 593 K on alumina) under dried (a, pretreated at 673 K) and humid (b) conditions.

The sample with 24.1 Si nm^{-2} shows the spectrum mainly consisting of (B), (C) and additional (D). This clearly shows the formation of doubly or further accumulated layer. However, the concentration of (C) species looks as if it increases with the deposition of doublelayer. This is probably caused by less enhancement of $Si(OSi)_4$ species by CP in doublelayer and formation of $Si(OSi)_3(OH)_1$ species on the doublelayer, resulting in the enhancement of the peak at *ca.* -100 ppm.

The full-coverage monolayer sample showed a spectrum shown by (b) in Figure 3 - 3 - 9 under the humid conditions. The intensity of species (B) was enhanced, showing this species as the hydroxide. In conclusion, the structure proposed for silica monolayer on alumina was confirmed by the NMR spectroscopy.

Isolated Species on Alumina

Figure 3 - 3 - 10 shows the change of spectra by varying the deposition temperature and Si reagent in the low Si concentration region (2 - 6 Si nm^{-2}). The sample prepared from $Si(OCH_3)(CH_3)_3$ showed the peak at -70 to -90 ppm. Because the spectra were recorded under the humid conditions, some structural changes due to the surface hydration are possible. However, it is clear that silica deposited from $Si(OCH_3)(CH_3)_3$ mainly consists of the species with no or only one siloxane bonding, *i.e.* $Si(OAl)_3(OH)_1$, $Si(OAl)_3(OSi)_1$, $Si(OAl)_2(OSi)_1(OH)_1$ and / or $Si(OAl)_1(OSi)_1(OH)_2$, because only these species can show peaks in the region from -80 to -90 ppm; the $Si(OSi)_2(OH)_2$ is also possible to appear, but this species can be formed only on a doubly or further accumulated layer, and the possibility is therefore ignored. The sample deposited from $Si(OCH_3)_4$ at the low temperature (473 K) showed an spectrum probably containing the peaks due to the species both isolated and bonded by siloxanes. The difference of degree of siloxane network is thus clearly confirmed for the isolated species formed from $Si(OCH_3)(CH_3)_3$ and the silica monolayer formed from $Si(OCH_3)_4$ at 593 K. Because the acidity was observed only on the latter sample as described in the previous sections, it is pointed out that the Brønsted acidity requires the network consisted the $Si(OAl)_1(OSi)_3$ and $Si(OAl)_1(OSi)_2(OH)_1$ species.

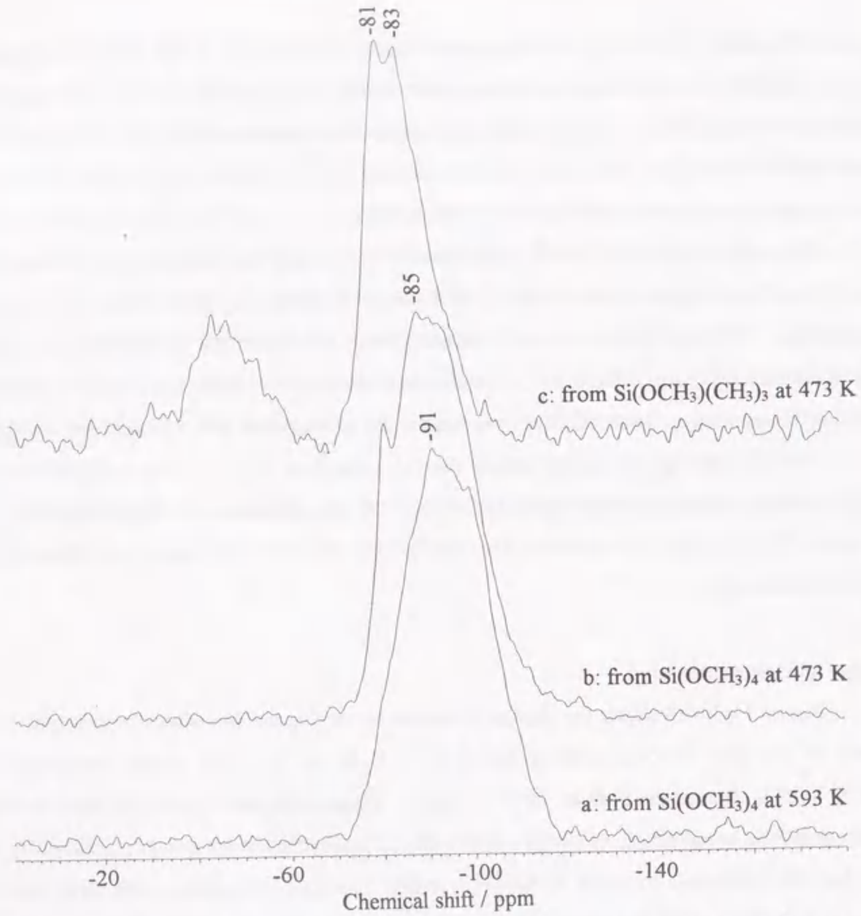

Figure 3 - 3 - 10 : Spectra of silica deposited from $Si(OCH_3)_4$ at 593 (a, 6.0 Si nm^{-2}) and 473 K (b, 3.0 Si nm^{-2}), and from $Si(OCH_3)(CH_3)_3$ at 473 K (c, 2.0 Si nm^{-2}).

Silica Monolayers on Titania and Zirconia

Figure 3 - 3 - 11 shows the spectra on silica monolayers loaded on various supports. Although some uncertainties are supposed because the measurements were carried out under the humid conditions, it is found that all of these monolayers mainly consist of the $Si(OM)_1(OSi)_3$ and $Si(OM)_1(OSi)_2(OH)_1$ (M = Al, Ti or Zr) species. This confirms a common structure of silica monolayers consisting of these species.

The peak positions are similar on those three monolayers; the $Si(OM)_1(OSi)_3$ peak appears

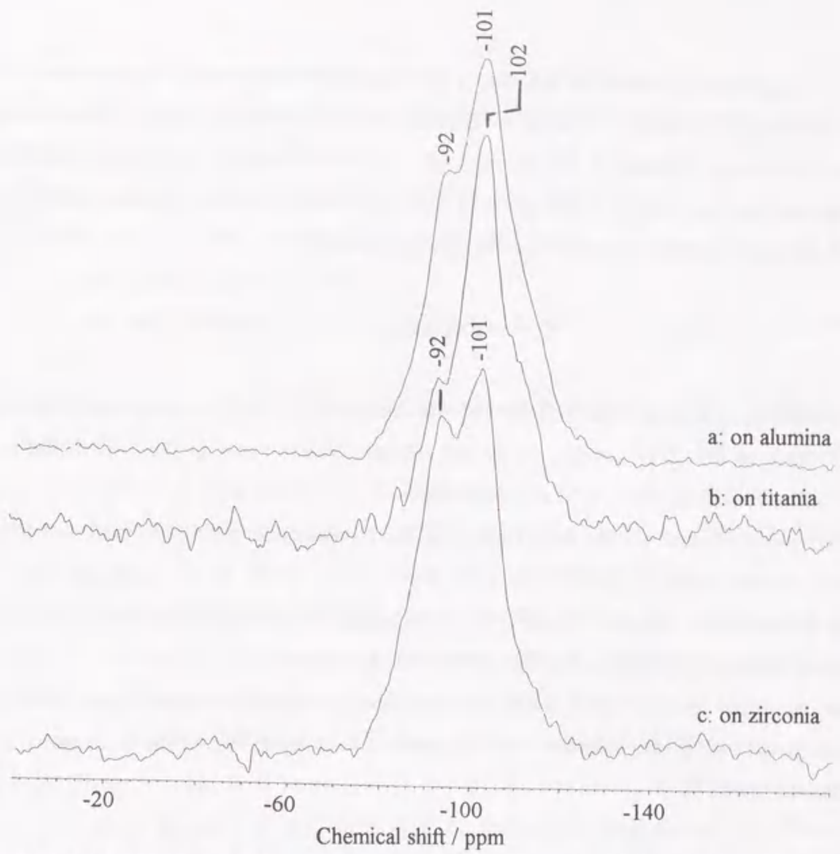

Figure 3 - 3 - 11 : Spectra of silica monolayers deposited from $Si(OCH_3)_4$ at 593 K on alumina (a, 11.4 Si nm^{-2}), titania (b, 11.9 Si nm^{-2}) and zirconia (c, 8.0 Si nm^{-2}).

at about -101 ppm, and the $Si(OM)_1(OSi)_2(OH)_1$ appears at -92 ppm in all the cases. Titano- and zirconosilicates (zeolite-like crystal consisting of Si, O and M in place of Al; M = Ti or Zr) with MFI structure were reported to show similar spectra that observed on the aluminosilicate with the same structure, *i.e.* ZSM-5, and hence the peak positions for $Si(OM)_1(OSi)_3$ species are still unclear, whereas germanosilicate showed a clear peak due to $Si(OGe)_1(OSi)_3$[25 - 27]. It is possibly considered that the $Si(OM)_1(OSi)_3$ (M = Ti and Zr) species show the same chemical shift as the $Si(OAl)_1(OSi)_3$ species, and this is consistent with the similar chemical shifts on the silica monolayers loaded on the three oxides.

The ratio of (B) to (C) species was higher on zirconia than on titania and alumina. This

behavior is considered to show the less degree of siloxane network formation on zirconia. The Si concentration on the monolayer is lower on zirconia than on alumina and titania. This is supposed to cause the less development of siloxane network. The NMR spectrum confirms this speculation, and supports that the relatively weak acidity of silica monolayer on zirconia is owing to the less degree of siloxane network, as speculated in the previous sections.

Conclusion

1. ^{29}Si NMR spectroscopy confirmed the proposal for structure of silica monolayer deposited from $Si(OCH_3)_4$ at 593 K on alumina, titania and zirconia, which consist of the $Si(OM)_1(OSi)_3$ and $Si(OM)_1(OSi)_2(OH)_1$ (M = Al, Ti or Zr) species.
2. The isolated structure formed from $Si(OCH_3)(CH_3)_3$ is also confirmed by the peak ascribable to such a species as $Si(OAl)_3(OH)_1$.
3. The Brønsted acid site of monolayer is shown to be the $Si(OM)_1(OSi)_2(OH)_1$ (M = Al, Ti or Zr) species connected by the two-dimensional network of siloxane.
4. The monolayer on zirconia was shown to possess less developed monolayer caused by the lower concentration of silicon, consistent with the weaker acidity than those of the monolayers on alumina and titania.

References

1. M. Mehring, *Principles of High Resolution NMR in Solids, 2nd ed.*, Springer Verlag, Berlin (1983).
2. C. A. Fyfe, *Solid State NMR for Chemists*, C. F. C. Press, Guelph (1983).
3. E. Lippmaa, M. Mägi, A. Samoson, G. Engelhardt and A. R. Grimmer, *J. Am. Chem. Soc.*, **102,** 4889 (1980).
4. M. Mägi, E. Lippmaa, A. Samoson, G. Engelhardt and A. R. Grimmer, *J. Phys. Chem.*, **88,** 1518 (1984).
5. L. B. Welsh, J. P. Gilso and M. J. Gattuso, *Appl. Catal.*, **15,** 327 (1985).
6. J. M. Thomas and J. Klinowski, *Adv. Catal.*, **33,** 199 (1985).
7. S. Komarneni, R. Roy, C. A. Fyfe, G. J. Kennedy and H. Strobl, *J. Am. Ceram. Soc.*, **69,** C42 (1986).
8. K. Segawa, Y. Nakajima, S. Nakata, S. Asaoka and H. Takahashi, *J. Catal.*, **101,** 81 (1986).

9. G. Engelhardt and D. Michel, *High-Resolution Solid-State NMR of Silicates and Zeolites*, John Wiley & Sons, New York (1987).
10. S. Nakata and S. Asaoka, *Shokubai (Catalyst)*, **29,** 634 (1987).
11. S. Asaoka and S. Nakata, *Hyomen (Surface)*, **26,** 133 (1988).
12. S. Nakata, *Kagaku Kogyo*, **41,** 354 (1990).
13. S. Hayashi and S. Nakata, *Chart de miru Zairyo no Kotai NMR*, Kodansha Scientific, Tokyo (1993).
14. J. M. Thomas, C. A. Fyfe, S. Ramdas, J. Klinowski and G. C. Gobbi, *J. Phys. Chem.*, **86,** 3061 (1982).
15. J. Klinowski, *Prog. NMR Spectrosc.*, **16,** 268 (1984).
16. T. Bein, R. F. Carver, R. D. Farlee and G. D. Stucky, *J. Am. Chem. Soc.*, **110,** 4546 (1988).
17. G. E. Maciel and D. W. Sindorf, *J. Am. Chem. Soc.*, **102,** 7606 (1980).
18. D. W. Sindorf and G. E. Maciel, *J. Phys. Chem.*, **86,** 5208 (1982).
19. D. W. Sindorf and G. E. Maciel, *J. Am. Chem. Soc.*, **105,** 1487 (1983).
20. D. W. Sindorf and G. E. Maciel, *J. Am. Chem. Soc.*, **105,** 3767 (1983).
21. S. Sato, T. Sodesawa, F. Nozaki and H. Shoji, *J. Mol. Catal.*, **6,** 343 (1991).
22. T.-C. Sheng, S. Lang, B. A. Morrow and I. D. Gay, *J. Catal.*, **148,** 341 (1994).
23. C. A. Fyfe, H. Strobl, G. T. Kokotailo, G. J. .Kennedy and G. E. Barlow, *J. Am. Chem. Soc.*, **110,** 3375 (1988).
24. G. E. Berendsen and L. de Galan, *Liq. Chromatogr.*, **1,** 403 (1978).
25. A. Tuel and B. B. Taarit, *J. Chem. Soc., Chem. Commun.*, **1992,** 1578.
26. S. A. Axon and J. Klinowski, *Appl. Catal., A: General*, **81,** 27 (1992).
27. R. Fricke, H. Kosslick, V. A. Tuan, I. Grohmann, W. Pilz, W. Storek and G. Walther, in *Zeolites and Microporous Materials*, eds. T. Hattori and T. Yashima, Kodansha, Tokyo (1994) p. 57.

Chapter 4. Thermal Stability and Heat-Resisting Acidity of Silica Monolayer on Alumina

Synopsis

Chemical vapor deposition of silica improved the thermal stability toward sintering and loss of surface area of alumina; these observations are similar to the other reports. Benzaldehyde-ammonia titration showed that the samples with high stabilities were covered by silica almost completely. From these observations, the origin of stabilization is proposed. The ultra thin silica layer, probably the monolayer, is suggested to give the thermal stability to the covered surface to protect the alumina particle like an egg shell. The stability was supposed to be owing to the predicted tight Al-O-Si bond and specific property of monolayer. This stabilization mechanism is considered commonly for vapor and liquid phase modifications of alumina with silica, and the proposal is the first one that explains the origin of stabilization of alumina by silica. The Brønsted acidity was observed even after calcination at 1493 K: it was once diminished by the calcination, but readily recovered by exposure to a humid atmosphere, while the conventional solid-acids were irreversibly deactivated *via* complete sintering. The silica monolayer on alumina was thus found to be a heat-resisting acid catalyst, namely the material with heat-durability extremely higher (of course the highest) than those of other acid catalysts.

Introduction

Solid-acid catalysts such as silica-alumina and zeolites have been used at temperatures below ca. 1000 K because of the loss of surface area by the sintering of solid and / or the destruction of active sites. Because the conventional catalytic processes have been operated under the mild conditions, no utilization of acid catalyst has been required at such a high temperature as > 1000 K. Recently, a novel use of solid-acid catalysts has been focused with the recognition of the importance to protect the global environment: the metal-loaded[1 - 4] and H-form[5] zeolites, alumina[6] and sulfur-promoted oxides[7] have been found to catalyze the removal of nitrogen oxide from the exhaust gas in the presence of oxygen and hydrocarbon. Although the relationships between the acidic properties and the catalytic activities have not been clarified yet, the acid sites probably play some roles for this reaction. However, the thermal instability of solid-acid catalysts will be a fatal problem for the practical use[8] because the temperature of exhaust gas often exceeds above 1000 K. It is therefore considered that the material which possesses both of the high thermal stability and the acidity, namely the heat-resisting acid catalyst, is promising.

The solid-acid catalysts, especially the zeolites[9] have become to be utilized also for the organic synthesis. The deactivation is sometimes caused by the deposition of the heavy molecules and/or the materials containing such hetero elements as nitrogen, sulfur and halogens. Since the combustion at such a high temperature as > 1400 K will completely remove these deposited materials to regenerate the catalyst, a number of applications to the organic syntheses will be anticipated by using the heat-resisting acid catalyst. From these view points, we tried to find the material with both of the high thermal stability and the acidity.

Alumina lost the surface area with the phase-transformation from metastable phases (γ, η and θ-Al_2O_3) into α-Al_2O_3 by the heating at 1300 - 1500 K[10, 11], and the thermal stability was improved by the addition of alkaline[12] and rare earths[13, 14]. These studies aimed the improvement of catalyst support for the catalytic combustion, and no acidity has been found on the improved catalysts, presumably these stabilizers decreased the acidity.

Silica has also been reported to give the thermal stability[15 - 19]. As described in the previous chapters, the silica monolayer prepared by the CVD (chemical vapor deposition) on γ-alumina showed the Brønsted acidity. Acid strength of the silica monolayer was relatively weak compared with the conventional silica-alumina and zeolites. The difference in acidic property clearly indicates that the acid site on monolayer was not the tetra-coordinated aluminum cation substituted in a silica matrix, which might give strong Brønsted acidity, and Chapter 3 showed the weak Brønsted acid site is the species Al-O-Si(-O-Si)$_2$-OH in a two-dimensional network consisting of siloxanes. From these findings, the silica monolayer is concluded to possess the physical and chemical properties quite different from those of the pure oxides and the conventional combined catalysts, and is therefore expected to have both of the acidity and the thermal stability. The present chapter will show the acidic property over the thin silica layer which was prepared by the CVD method and then calcined at 1493 K.

The sintering of alumina proceeded *via* the formation of grain boundary and the neck growth, which were caused by the surface- and bulk-diffusion of aluminum and oxygen ions[20]. The alkaline, alkaline earths and rare earths stabilized the alumina by formation of stable hexaaluminate compounds[11 - 13]. On the contrary, the silica-modified alumina with the high thermal stability showed no X-ray diffraction other than that of alumina. Therefore, the glassy structure of the loaded silica has been proposed[15]. The origin of stabilization with silica is however confused, because the amorphous compounds are usually unstable. The analysis of the surface structure will clarify the mechanism of suppression of sintering by the added silica. The present thesis deals with the simple surface

structure on monolayer analyzed by the benzaldehyde-ammonia titration (BAT) method. Therefore, the mechanism for stabilization will be also discussed on the basis of the observations by the BAT.

Experimental

Catalyst Preparation

γ-Alumina was supplied from Catalysis Society of Japan as a reference catalyst, JRC-ALO4, and the surface area was 161 $m^2 g^{-1}$. The CVD of silica was carried out according to Section 2 - 1. The sample was put in a quartz basket hung by a quartz spring in order to monitor the weight, and it was evacuated at 673 K until no change of the weight was observed. Vapor of $Si(OCH_3)_4$ (tetramethoxysilane) was then admitted on the sample at 593 K. The cycles of the introduction of vapor and the evacuation were repeated in order to avoid the vapor lock by the products. The degree of evacuation was *ca.* 10^{-3} Torr (1 Torr = 133.3 Pa), and the vapor pressure was kept at 2.5 Torr by chilling the reservoir with an ice bath. The sample was then treated at 673 K under the presence of 200 Torr of oxygen. It is assumed that the treated material had the composition of SiO_2, and the loading was determined from the weight gain based on the assumption. The present chapter will show the loading in the unit of wt% (SiO_2 / Al_2O_3 weight ratio) but not in Si nm^{-2}, because the surface area changes during calcination and this will confuse the surface concentration.

Silica gel (N602A) and silica-alumina (N631L, containing 13 wt% of Al_2O_3) were obtained from Nikki Kagaku Co. Ltd. A H-ZSM5 sample with 76 of the SiO_2 / Al_2O_3 molar ratio was obtained from Nippon Mobil Catalysts Co. Ltd. A sulfur-promoted zirconia super-acid catalyst (SO_4^{2-}/ZrO_2) was prepared according to the literature[21] as follows. Zirconium hydroxide was precipitated by addition of ammonia into a solution of $ZrO(NO_3)_2$, followed by drying the obtained solid at 383 - 393 K for 24 hours. This dried solid was then put into a diluted sulfuric acid (about 1 N), and washed with water followed by calcination at 923 K in flowing oxygen for 4 hours.

The sample was heated in an electric furnace with < 10 K min^{-1} of the heating rate up to 1373 - 1573 K and then kept for 24 hours under the atmospheric conditions.

Characterization

The total surface area was determined on the basis of the BET equation from the nitrogen adsorption at 77 K and p/p_0 = 0.3 on the sample pretreated at 673 K.

In order to show which surface of silica or alumina was lost by sintering, the BAT (benzaldehyde-ammonia titration) measurements were carried out according to Section 2 - 1. The sample was set in a 4 mm i.d. Pyrex reactor and pretreated at 673 K for 1 hour in 50 cm^3 min^{-1} of flowing helium which was purified by passing a liquid nitrogen trap. Then, 1 mm^3 of benzaldehyde was injected on the sample at 523 K, and the eluted benzaldehyde was detected by a GC (gas chromatography) connected after the reactor. The injections of benzaldehyde were repeated until the saturation of adsorption was observed. Ammonia was finally introduced at 673 K, and the formed benzonitrile (BN) was quantified. This chapter shows the results of exposed surface area of alumina, determined as follows: exposed area ($m^2 g^{-1}$) = amount of BN (mmol g^{-1}) / amount of BN on the support JRC-ALO4 (0.48 mmol g^{-1}) × surface area of the support (161 $m^2 g^{-1}$). The area of surface covered by silica was determined from the difference between the total and the alumina exposed surface areas.

X-ray powder diffraction (XRD) was recorded by a Rigaku diffractometer with Cu-k radiation at 30 kV of the acceleration voltage and 15 mA of the tube current. ^{29}Si NMR spectra were recorded according to Section 3 - 3.

Tests for Acidic Property

The sample was exposed to an atmosphere with *ca.* 80 % of the relative humidity kept by the presence of a solution saturated with ammonium chloride for several days before the tests for acidity as described in the previous chapters. The purpose of this procedure was to avoid the uncertainties during the weight measurements in the previous chapters, but there is an additional purpose in this chapter. The acidic property of solid is strongly affected by humid conditions. This procedure will avoid uncertainties due to difference in the degree of rehydration after high temperature calcination,

The double-bond isomerization of *1*-butene to *2*-butene was carried out by the pulse technique under the conditions (C) shown in Section 2 - 1. The sample (5 mg) was set in a 4 mm i.d. Pyrex- or quartz-glass reactor and pretreated at 673 K for 1 hour in 40 - 45 cm^3 min^{-1} of flowing helium which was purified by passing a liquid nitrogen trap. At 393 K, a pulse of *1*-butene (1.3 cm^3) was introduced on the sample from a sampling loop, and the products were analyzed by a VZ-7 column. The activity was shown by the yield of *2*-butene (mol) × the flow rate of carrier (m^3 h^{-1}) / the amount (g) or surface area (m^2) of catalyst. In order to show the influence of degree of dehydration of surface, the pretreatment temperature was varied, or 10 mm^3 of liquid water was injected into the sample in several experiments. The cracking of cumene (isopropylbenzene) into benzene and pro-

pylene (propene) was also carried out on the sample (5 mg) pretreated at 673 K for 1 hour in 25 cm^3 min^{-1} of flowing helium. At 623 K, 1 mm^3 of cumene was injected, and the products were analyzed by a SE-30 column operated at 403 K.

IR spectrum was recorded in an *in-situ* cell by using a JASCO FT/IR-5300 spectrometer on the evacuated self-supporting disk (1 cm in diameter) which was molded from 7 mg of the sample powder. The spectrum of adsorbed ammonia was recorded on the sample evacuated at 373 K after the adsorption of 50 Torr of ammonia at 373 K.

Results

Characterization

Figure 4 - 1 shows the total surface area of silica layer on alumina before and after the calcination at 1373 - 1573 K. The surface area / weight of catalyst before the calcination decreased with the deposition of silica, but this was caused by the increment of weight: the surface area / weight of alumina slightly increased as described in Chapter 2. The deposition of silica obviously improved the thermal stability of alumina, because the surface area after the calcination at 1373 - 1573 K increased with the loading of SiO_2. The surface area showed the maximum at *ca.* 15 wt% of the SiO_2 loading, and it decreased with more than 20 wt% of the loading. Specifically at 1493 K, the surface areas of the samples with 15 - 20 wt% of SiO_2 were quite higher (50 - 60 m^2 $g\text{-}cat^{-1}$) than that of the unmodified sample (4 m^2 g^{-1}). At 1573 K, all the samples showed the low surface areas (< 6 m^2 g^{-1}).

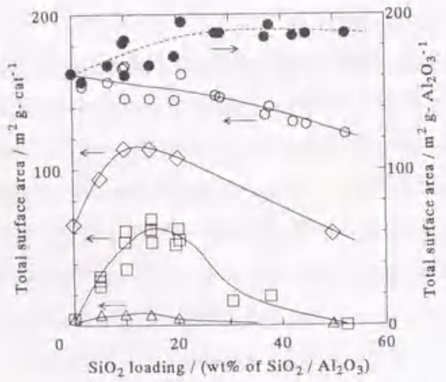

Figure 4 - 1 : Total surface area measured by the BET method before (● : divided by the weight of alumina and ○ : divided by the weight of catalyst) and after the calcination at 1373 (◇), 1493 (□) and 1573 K (△) for 24 hours.

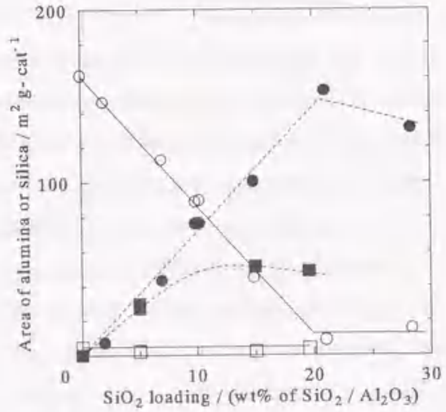

Figure 4 - 2 : Areas of exposed surface of alumina (○ and □) and surface covered with silica (● and ■) measured by the BAT method before (○ and ●) and after (□ and ■) the calcination at 1493 K.

Figure 4 - 2 shows the changes of alumina exposed and silica covered surface areas by the calcination at 1493 K. The exposed surface area of alumina decreased linearly with the SiO_2 loading before the calcination and arrived at almost zero with 20 wt% of SiO_2, which corresponded to 13 silicon atoms on 1 nm^2 of the surface: the area of surface covered by silica increased, and the surface was covered by silica almost completely at > 20 wt% of the loading. The concentration of aluminum cations on the surface of γ-Al_2O_3 was reported to be 9 - 14.5 nm^{-2} [22]. As described in Section 2 - 1, this shows that the silica monolayer, which consisted of 1 : 1 bonding of Al-O-Si, covered the surface almost completely with 13 nm^{-2} of the silicon atoms. Therefore, the sample with 20 wt% of the SiO_2 loading will be termed as a full-coverage monolayer in the following description. By the calcination at 1493 K, the exposed area was suppressed down to only 2 - 4 m^2 $g\text{-}cat^{-1}$ over the broad range of SiO_2 loading. On the contrary, no (at 5 wt% of the loading) or relatively small decrement (15 - 20 wt%) was shown in the area of surface covered by silica.

The XRD pattern was shown in Figure 4 - 3, and the crystal phase was determined according to the literature[10]. The support alumina showed the diffraction due to the γ-Al_2O_3 before the calcination, and the

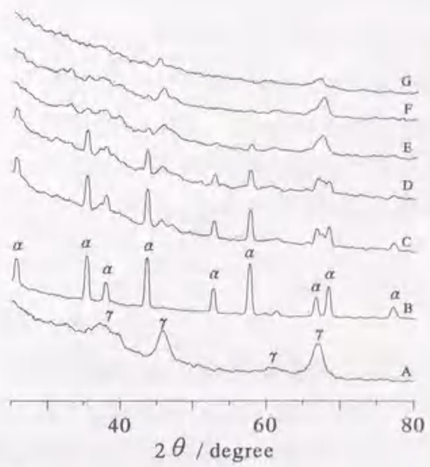

Figure 4 - 3 : X-ray diffraction pattern of alumina (A : before and B : after the calcination) and silica-covered alumina after the calcination at 1493 K (C : SiO_2 5 wt%, D : 10 wt%, E : 15 wt%, F : 20 wt% and G : 52 wt%). α and γ shows the diffraction due to α- and γ-Al_2O_3, respectively.

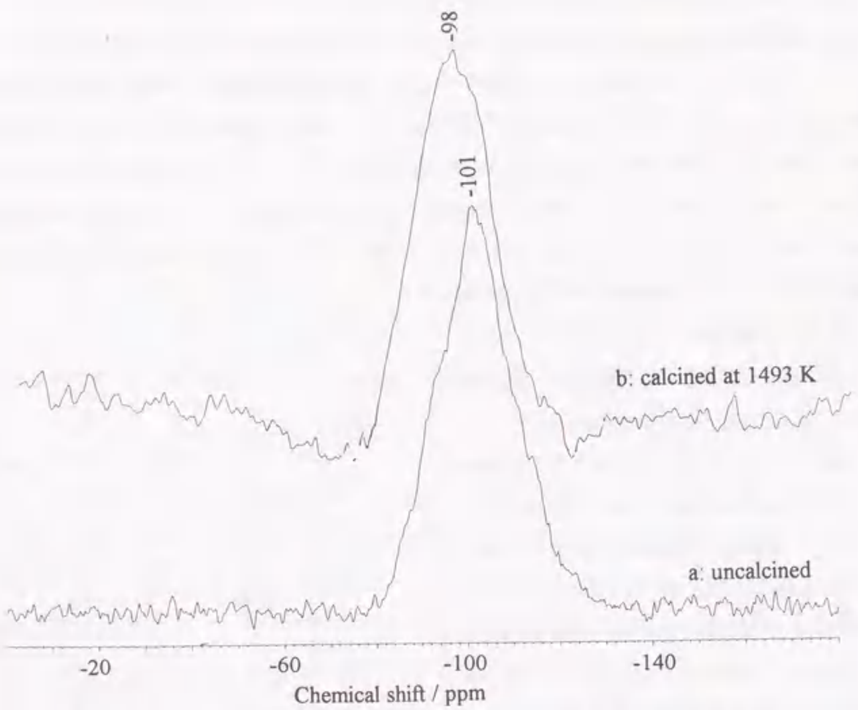

Figure 4 - 4 : ^{29}Si NMR spectra of full-coverage monolayer sample (a, SiO_2 20 wt%) and sample with 15 wt% of SiO_2 calcined at 1493 K followed by exposure to humid atmosphere (b). The spectra were recorded after the drying at 673 K for 1 hour in flowing nitrogen.

formation of α-Al_2O_3 was observed after the calcination at 1493 K. The formation of α phase was weakened by the CVD of SiO_2, and almost no diffraction due to the α phase was observed on the samples with more than 20 wt% of SiO_2. The crystal phases of the samples with more than 20 wt% of silica could not be determined because of the weak diffraction which was close to those of the γ, η and θ phases. These results indicate that the CVD of SiO_2 prevented from the transformation of the metastable phases (γ, η and θ) into α-Al_2O_3.

Figure 4 - 4 shows the ^{29}Si NMR spectra. The sample calcined at 1493 K showed a spectrum similar to that obtained on the full-coverage monolayer sample before calcination. The main peak was shifted by the calcination from -101 to -98 ppm.

Acidic Property

Figure 4 - 5 shows the catalytic activity for the double-bond isomerization of *1*-butene on the catalysts pretreated at 673 K after the exposure to the humid atmosphere. The activity increased with the SiO_2 loading and showed the maximum at 20 wt% before the calcination, because 20 wt% of the loading corresponded to 12 nm^{-2} of Si concentration with which the monolayer fully covered the surface as shown in Section 2 - 1. The further deposition decreased the activity. The activity was observed even after the calcination at 1493

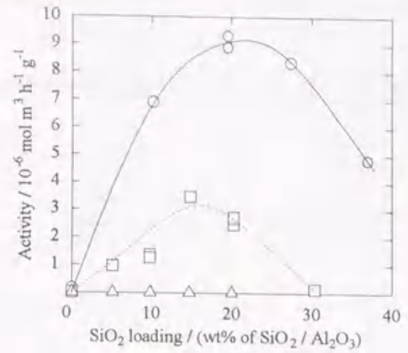

Figure 4 - 5 : Catalytic activity for isomerization from *1*- to *2*-butene at 393 K under conditions (C) shown in Section 2 - 1 before (○) and after calcination at 1493 (□) and 1573 K (△) followed by exposure to humid atmosphere and pretreatment at 673 K. The activity was shown by the yield of *2*-butene (mol) × flow rate of carrier gas (m^3 h^{-1}) / catalyst amount (g).

Table 4 - 1 : Comparison of surface areas and activities among various catalysts calcined at 1493 K*.

Catalyst	SiO_2 loading / wt%	Total surface area / m^2 $g\text{-}cat^{-1}$	Activity for isomerization from *1*- to *2*-butene / weight**	/ surface area***	*cis*- / *trans*-*2*-butene
Silica layer	15	54	3.5	5.1	1.0
	20	52	2.5 - 2.7	4.5 - 5.0	1.0
Silica gel	-	<1	no products		-
Silica-alumina	-	*ca.* 1	no products		-
H-ZSM5	-	<1	no products		-
SO_4^{2-}/ZrO_2	-	2	no products (pretreated at 823 K)		-
Silica layer (uncalcined)	20	144	9.3	6.5	1.6

*: After the calcination at 1493 K followed by the exposure to the humid atmosphere and the pretreatment at 673 K. **: 10^6 × yield of *2*-butene (mol) × flow rate of carrier gas (m^3 h^{-1}) / catalyst amount (g). ***: 10^8 × yield of *2*-butene (mol) × flow rate of carrier gas (m^3 h^{-1}) / surface area (m^2).

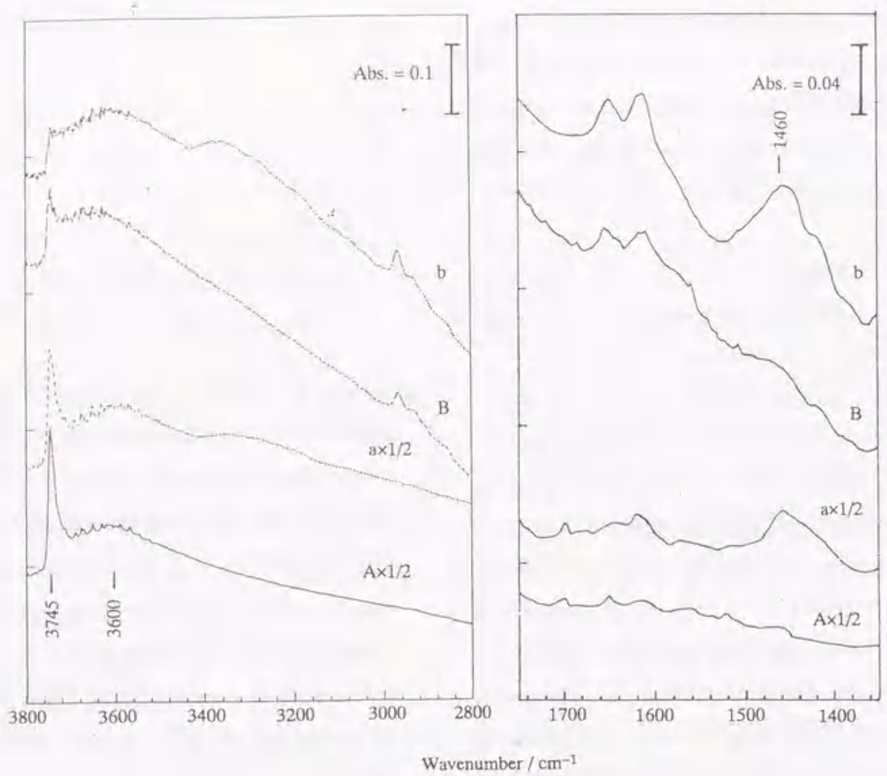

Figure 4 - 6 : IR spectra of the full-coverage monolayer evacuated at 673 K (A : SiO_2 20 wt%) and the sample with 15 wt% of the SiO_2 loading calcined at 1493 K (B), and those recorded after the adsorption of ammonia followed by the evacuation at 373 K (a and b).

K, and it showed the maximum at 15 - 20 wt% of the SiO_2 loading. The further deposition also decreased the activity. The activity was completely diminished after the calcination at 1573 K.

Figure 4 - 6 shows the IR spectra of the full-coverage monolayer evacuated at 673 K and the sample with 15 wt% of SiO_2 calcined at 1493 K. Both samples showed two absorptions of hydroxides at 3745 and 3600 cm^{-1}. The former sharp absorption was ascribable to the isolated silanol. The former was decreased and the latter was slightly increased by the adsorption of ammonia. Simultaneously, the absorption ascribable to ammonium cation appeared at 1450 cm^{-1} on both samples.

Table 4 - 1 compares the activities per total surface areas on the full-coverage monolayer

sample before the calcination and the samples after the calcination at 1493 K. After the calcination, the samples with 15 - 20 wt% of SiO_2 showed the similar activities per surface areas, and these were slightly lower than that over the full-coverage monolayer before the calcination. The ratios of *cis*- to *trans*-2-butene in the products were in the range from 1 to 2 over both of the calcined and uncalcined silica layers. Table 4 - 1 points out that only the thin silica layers possessed the high surface areas and activities after the calcination at 1493 K, while the conventional solid-acids, *i.e.* silica-alumina, H-ZSM5 and SO_4^{2-}/ZrO_2, lost the surface areas and showed no activity.

Table 4 - 2 shows the activity for the cracking of cumene. As described in Section 2 - 1, the activity on silica monolayer uncalcined at high temperature was small for this reaction. Very low activity, similar to that found before calcination, was observed on the silica layers after calcination at 1493 K.

The temperature of pretreatment strongly affected the activity of sample which had been calcined at 1493 K and then exposed to the humid atmosphere as shown

Table 4 - 2 : Catalytic activity for cracking of cumene (isopropylbenzene) at 623 K.

	SiO_2 loading (wt%)	Activity / surface area*
Before calcination at 1493 K	10	0.7
	20	1.5
After calcination at 1493 K	10	0.05
	20	0.5

* 10^{10} × yield of benzene (mol) × flow rate of carrier gas ($m^3\ h^{-1}$) / surface area of catalyst (m^2)

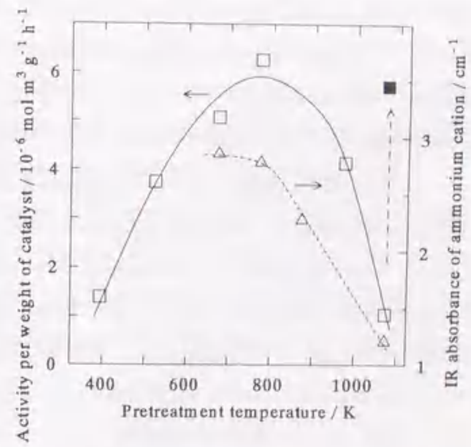

Figure 4 - 7 : Activity for double-bond isomerization of *1*-butene (□ and ■) and IR peak area of adsorbed ammonium cation (△) over the sample with 15 wt% of SiO_2 calcined at 1493 K followed by exposure to humid atmosphere. The activity and IR spectrum were measured after the pretreatment at various temperatures (□ and △), and followed by the injection of 10 mm^3 of liquid water at 773 K (■).

in Figure 4 - 7. The activity increased with increasing the pretreatment temperature at 393 - 773 K, but it decreased above 773 K. The IR peak area of adsorbed ammonium cation also decreased with the pretreatment temperature in the range between 773 and 1073 K. However, the injection of water at 773 K after the pretreatment at 1073 K regenerated the activity (■ in Figure 4 - 7)

Discussion

Improvement of Thermal Stability by Thin Layer of Silica

The mechanism of sintering of alumina has been explained as shown in Figure 1 - 6. The unmodified alumina readily sintered *via* the formation of grain boundary between two particles (a) followed by the neck growth (b), and the particles shrank to form a large particle with low surface area (c)[23]. The neck growth is suggested to be caused by the surface and bulk diffusions of aluminum and oxygen ions at *ca.* 1400 K[20]. The X-ray diffraction showed that the phase-transformation from γ- into α-Al_2O_3 was accompanied with the sintering.

The CVD of silica obviously improved the thermal stability of alumina and prevented the formation of α-Al_2O_3. The total surface area arrived at the maximum with 15 - 20 wt% of the SiO_2 loading, which approximately corresponded to that of the full-coverage monolayer, and decreased with the further loading at 1493 K. The thermal stability seemed to be improved only by the surface thin layer, but not by the bulky silica. The BAT experiments showed that the exposed surface area of alumina was only 2 - 4 m^2 $g\text{-}cat^{-1}$ after the calcination at 1493 K, while the relatively small decrement of the area of surface covered by silica was shown. Thus, the calcined samples with the high stabilities were indicated to be covered by silica almost completely. It is therefore considered that only the area covered by silica possessed the high thermal stability, whereas the uncovered area of alumina readily sintered. In order to estimate the thickness of surface layer after the calcination at 1493 K, the surface concentration of Si was calculated from the number of Si atoms divided by the total surface area after the calcination: it was in the range between 10 and 30 Si nm^{-2} on the sample with 5 - 20 wt% of the SiO_2 loading. This concentration approximately corresponded to 1 - 2.5 times as much as that on the full-coverage silica monolayer. The surface is therefore considered to be covered by the ultra thin layer of silica, *i.e.* mono- or doublelayer, or by the ultra thin layer of an aluminosilicate compound like mullite, which can be assumed to be formed *via* the migration of aluminum cation into the silica layer at the high temperature. Horiuchi *et al.* however reported that too much loading of silica reduced the stability of alumina, and simultaneously formed a bulky solid of

mullite phase[19]. Therefore, the mullite itself probably gives no stability. Although it is still possible to propose a surface layer consisted of an unknown aluminosilicate phase, it probably has a highly siliceous composition, because the BAT experiments showed little exposure of aluminum cations on the surface. The lack of strong Brønsted acidity, which will be described in the following section, is also consistent with no or little migration of the aluminum cation into the silica layer. Moreover, the thickness is presumably ultra thin, because it fully covered the surface with only 10 - 30 silicon atoms. So that, the surface layer can be called as the thin silica layer, namely the layer with the highly siliceous composition and the atomic order thickness. It is thus concluded that the ultra thin layer of silica stabilized the surface.

The maintenance of morphology is supported by almost no change of ^{29}Si NMR spectrum with calcination; this confirms the maintenance of monolayer structure consisted of $Si(OAl)_1(OSi)_3$ and $Si(OAl)_1(OSi)_2(OH)_1$ species. Small shift of the peak suggests a change of structure, probably some rearrangements of ions during calcination. As shown above, this rearrangement is considered not to occur between the surface layer and substrate alumina. It can be explained that the arrangement of silicon was modified by the transformation from γ- to other metastable phase of Al_2O_3.

From these observations, the mechanism for the sintering of samples with both areas covered and uncovered by the silica monolayer, *i.e.* with 5 - 20 wt% of the SiO_2 loading, at 1493 K is proposed as shown in Scheme 4 - 1; two particles bonded only on the uncovered surfaces of alumina, but not on the surface covered by the monolayer (a); the dispersion of oxygen anions could consequently proceed, but the surface layer prevented the dispersion on and near the surface covered by the layer (b); as a result of this, the surface layer moved on the surface like a raft, and the crystallite was reconstructed to be completely covered by the surface thin layer like an egg shell (c).

The thick layer and bulk of silica are presumed to be thermally unstable, because the silica-based catalysts, *i.e.* silica gel, silica-alumina and the highly siliceous H-ZSM5, lost the

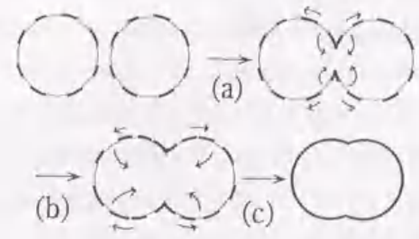

Scheme 4 - 1 : Proposed scheme for sintering of sample with both of silica monolayer and alumina surfaces, *i.e.* with 5 - 20 wt% of SiO_2.

surface areas with the calcination at 1493 K. The serious sintering is therefore suggested with the SiO_2 loading of more than 20 %. However, the sintering is probably caused only by melting of surface SiO_2 even in these cases, and the inner small particle of alumina must be protected by the hard shell of silica monolayer (Scheme 4 - 2). This is consistent with no formation of α-Al_2O_3 in these samples in spite of the serious sintering.

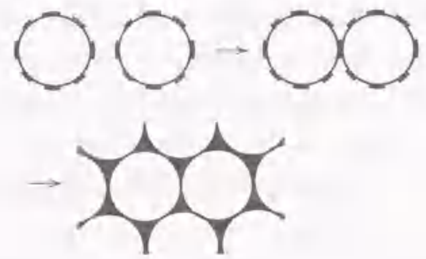

Scheme 4 - 2 : Proposed scheme for sintering of sample with SiO_2 loading > 20 wt%.

Because no diffraction other than those of alumina was found on the XRD of the silica-modified alumina with the high stability in the previous studies, the added silica has been proposed to form a glassy phase[15]. However, no explanation has been made for the stabilizing mechanism with the glassy silica. The present author supposes that the glassy silica never stabilizes the surface, because amorphous materials are usually unstable, and in fact, the amorphous silica gel and silica-alumina showed almost no surface areas after the calcination at 1493 K. No explanation has been made also for the volcano-shape relationship between the thermal stability and the loading of SiO_2, although this relationship has already been found[16]. Thus, the origin of thermal stabilization by silica has not been understood well. The present results clearly show that the surface thin layer improved the stability, and on the contrary, the thick layer of silica, which probably had an amorphous like structure, caused the serious sintering.

According to Scheme 4 - 1, the stabilization of surface by the thin silica layer is explained from the two phenomena, *i.e.* the surface of silica layer is inactive to bond with other particles, and the silica layer prevents the dispersion of ions on and near it. The particular chemical and physical properties of surface thin layer developed on another oxide, which are quite distinct from those of silica, alumina and the conventional binary catalysts, is presumed to give these phenomena. A possible explanation is proposed on the basis of the probable structure of surface thin layer as follows.

The surface concentration of silicon atoms on the silica monolayer, *i.e.* 13 Si nm^{-2}, agreed with the concentration of aluminum cations on the surface of alumina. The structure of monolayer,

i.e. the arrangement of cations, is therefore suggested to be similar to that of alumina. The agreements between the concentrations of silicon atoms on the monolayer and the cations of support oxides were observed also on titania and zirconia, and these agreements support the structural similarity between the substrates and the monolayers on them. Hence, the previous chapters proposed that the silica monolayer on alumina possessed the composition of SiO_2 but the structure like Al_2O_3, *i.e.* the composition different from Al_2O_3 and the structure different from SiO_2. This probably caused the difficulty of the crystallite growth of both of SiO_2 and Al_2O_3 on the monolayer surface. It is therefore suggested that the monolayer surface was inactive to bond with other particles.

In addition, tight Si-O-Al bondings are suggested between the silica monolayer and alumina support, because the homogeneous monolayer must be formed due to such strong bondings between the promoter and support. This tight bond is considered to be caused by difference in electronegativity between Al and Si, as suggested in Section 2 - 2. The tight bond is suggested to prevent the moving of ions on and near it, resulting in the maintenance of the morphology of monolayer, which gave the thermal stability of surface covered by the silica monolayer. Prevention from phase-transformation was also reported on sulfur-, boron-, tungsten- and molybdenum-loaded zirconia, titania and iron oxide catalysts with super acidity[24]. All of these combinations are supposed to form tight M_1-O-M_2 bondings due to large difference in electro-negativity between the promoter and substrate. Thus proposed mechanism for the improvement of thermal stability is quite different from the stabilization with alkaline and rare earths which formed the bulk hexaaluminate compounds[11 - 14], and it should be noted that the surface modification in the atomic order thickness controlled the sintering of solid; the present study is the first one which experimentally exhibited such a controlling effect.

The surface modification with silicon alkoxide has also been reported in the liquid phase[18, 19]. Especially Beguin *et al.* tested the stability of the silica-loaded alumina under the conditions similar to the present study (1493 K, 24 hours)[18], and the relationship between the surface area and the SiO_2 loading was almost the same as the present results (Figure 4 - 8). However, it was reported that the liquid phase preparation gave only the low loading of silica: only 2 wt% of the Si atoms, corresponding to 4 wt% of SiO_2 and *ca.* 20 % of the coverage, was deposited by one-step impregnation of $Si(OC_2H_5)_4$ (tetraethoxysilane), and repeating of the operation was needed to load the larger amount of silica. Section 3 - 1 also pointed out that the CVD of $Si(OCH_3)_4$ at the low temperature (< 473 K) was saturated at the low coverage although the alumina surface was still exposed, because the deposited alkoxide Al-O-$Si(OCH_3)_n$ covered the surface, but did not polymerize into siloxanes

(Si-O-Si) at such a temperature: on the contrary, the CVD at 493 - 593 K formed a network of polymerized siloxanes, resulting in the high coverage (> 90 %); too high temperature (673 K) gave the heterogeneous thickness of silica deposited randomly. Probably, only the deposition of alkoxide in the temperature range of 493 - 593 K can form the thin layer of silica covering the surface completely. The present catalysts, prepared in the gas phase at 593 K, thus showed the clear stabilizing effect by the silica layer with the high coverage.

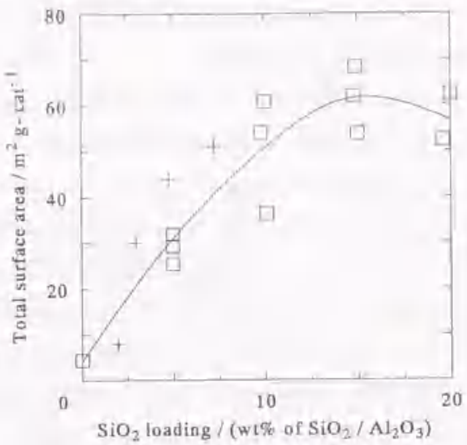

Figure 4 - 8 : Relationship between the total surface area and the SiO_2 loading on SiO_2 / Al_2O_3 calcined at 1493 K for 24 hours obtained from the present results (□) and calculated from ref. 18 (+).

Acidity on Silica Layer calcined at 1493 K

Alumina showed the Lewis acidity, and it was diminished with the coverage by silica. On the other hand, the silica monolayer possessed the Brønsted acidity to catalyze the double-bond isomerization of *1*-butene, as shown in the previous chapters. Before the calcination, the activity therefore showed the maximum at 20 wt% of the SiO_2 loading, where the silica monolayer covered the surface completely. The activity was observed even after the calcination at 1493 K followed by the exposure to the humid atmosphere. The maximum was observed at 15 wt% of the SiO_2 loading, and the further loading decreased the activity; this almost agreed with the change of surface area. The activity per surface area on the sample with 15 - 20 wt% of the SiO_2 loading calcined at 1493 K were slightly lower than that on the full-coverage monolayer before the calcination. This shows that the activity on the surface of silica monolayer was almost maintained. The ratio of *cis*- to *trans*-*2*-butene in the products, which was in the range from 1 to 2 showing the Brønsted acidity[25], was also maintained. The ammonium cation observed by the IR measurements also showed the Brønsted acidity on both silica layers before and after the calcination. Therefore, the nature of the Brønsted acid sites on the silica monolayer is concluded to be maintained, while the conventional solid-acids, *i.e.* silica-alumina, H-ZSM5 and SO_4^{2-}/ZrO_2, lost the surface areas during the calcination and therefore showed no activity.

The cracking of cumene requires strong Brønsted acid sites[26]. The lack of activity for this reaction on the silica monolayer before the calcination suggests that the acid strength of the monolayer was relatively weak compared with the conventional silica-alumina. Also after the calcination, few activity was observed. This supports the maintenance of the acidic property of the silica monolayer, and the lack of strong Brønsted acidity, *i.e.* the lack of tetra-coordinated aluminum cations on the surface, is consistent with no or little migration of aluminum cation into the silica layer to form an aluminosilicate compound.

The pretreatment temperature strongly affected the activity for the isomerization of butene, and this indicates that the rehydration after the calcination at 1493 K changed the acidic property. The low pretreatment temperature gave the low activity. This was probably due to the strong adsorption of water molecular on the acid site, like as observed on various solid-acid catalysts. Too high pretreatment temperature reduced the activity also. In addition, the IR spectroscopy showed that the amount of adsorbed ammonium cations decreased after the pretreatment at too high temperature. The previous chapters proposed that the Brønsted acid site on the monolayer was the hydroxyl group like Al-O-Si(-O-Si)$_2$-OH located in the network of siloxanes (Si-O-Si). The active hydroxyl species seems to be once decomposed during the calcination at high temperature. However, this deactivation process was presumably different from the irreversible deactivation of conventional catalyst due to the complete sintering, because it is speculated that the hydroxide on the silica monolayer was decomposed *via* the dehydration from a pair of silanols to form a water molecule and a siloxane bond, and then regenerated by the rehydration in the humid atmosphere; the dehydration-rehydration process was reversible. The reversibility is clearly shown by the fact that the injection of water at 773 K regenerated the activity after the pretreatment at 1073 K. It is concluded that the acidic hydroxyl group on the silica monolayer was readily regenerated by the exposure to humid atmosphere although it was decomposed by the calcination at high temperature. This reversibility gives the distinct and novel function heat-resisting acidity to the silica monolayer.

Conclusion

1. The chemical vapor deposition of silica improved the stability of alumina.
2. The origin of stabilization was experimentally shown. The ultra thin silica layer, probably the monolayer, is suggested to give the thermal stability to the covered surface to protect the alumina particle like an egg shell. The stability seems owing to tight Al-O-Si bonds and specific property

of monolayer.

2. The acidic hydroxyl species Al-O-Si-OH was once decomposed by the calcination at the high temperature, but readily regenerated by the rehydration. As a result, the Brønsted acidity was observed even after the calcination at 1493 K, while the conventional solid-acids lost the acidities. A heat-resisting acid catalyst, namely the acidic material with heat-durability extremely higher (of course the highest) than those of other acid catalysts, was thus found.

References

1. W. Held, A. König, T. Richter and L. Puppe, *SAE Tech. Paper,* **1990,** 900496.
2. S. Sato, Y. Yu-U, H. Yahiro, N. Mizuno and M. Iwamoto, *Appl. Catal.,* **70,** L1 (1991).
3. E. Kikuchi, K. Yogo, S. Tanaka and M. Abe, *Chem. Lett.,* **1991,** 1063.
4. M. Misono and K. Kondo, *Chem. Lett.,* **1991,** 1001.
5. H. Hamada, Y. Kintaichi, M. Sasaki and T. Ito, *Appl. Catal.,* **64,** L1 (1990).
6. Y. Kintaichi, H. Hamada, M. Tabata, M. Sasaki and T. Ito, *Catal. Lett.,* **6,** 239 (1990).
7. H. Hamada, Y. Kintaichi, M. Tabata, M. Sasaki and T. Ito, *Chem. Lett.,* **1991,** 2179.
8. M. Iwamoto, *Stud. Surf. Sci. Catal.,* **84,** 1395 (1994).
9. J. Weitkamp, *Stud. Surf. Sci. Catal.,* **65,** 21 (1991).
10. H. C. Stumpf, A. S. Russell, J. W. Newsome and C. M. Tucker, *Ind. Eng. Chem.,* **42,** 1398 (1950).
11. H. Arai and M. Machida, *Catal. Today,* **10,** 81 (1991).
12. M. Machida, K. Eguchi and H. Arai, *J. Catal.,* **103,** 385 (1987).
13. S. Matsuda, A. Kato, M. Mizumoto and H. Yamashita, in *Proc. 8th International Congress Catalysis, Vol. 4,* Verlag Chemie, Weinheim, (1984) p. 879.
14. J. S. Church, N. W. Cant and D. L. Trimm, *Appl. Catal., A: general,* **101,** 105 (1993).
15. I. Amato, D. Martorama and B, Sliengo, in *Sintering and Catalysis,* ed. G. C. Kuczynski, Plenum Press, New York (1975) p. 187.
16. B. E. Yoldas, *J. Mater. Sci.,* **11,** 465 (1976).
17. M. F. L. Johnson, *J. Catal.,* **123,** 245 (1990).
18. B. Beguin, E. Grabowski and M. Primet, *J. Catal.,* **127,** 595 (1991).
19. T. Horiuchi, T. Sugiyama and T. Mori, *J. Mater. Chem.,* **3,** 861 (1993).
20. D. L. Johnson and L. Berrin, in *Sintering and Related Phenomena,* eds. G. C. Kuczynski, N. A. Hooton and C. F. Gibbon, Gordon and Research, New York (1967) p. 445.
21. M. Hino and K. Arata, *J. Chem. Soc., Chem. Commun.,* **1979,** 1148.
22. H. Knözinger and P. Ratnasamy, *Catal. Rev.-Sci. Eng.,* **17,** 31 (1978).
23. E. Katoh, in *Muki Zairyo Kagaku I, 6th edition,* ed. I. Noda, Corona Publishing, Tokyo (1977). p. 158.
24. K. Arata, *Adv. Catal.,* **37,** 165 (1990).
25. J. W. Hightower and W. K. Hall, *Chem. Eng. Prog. Symp. Ser.,* **63,** 122 (1967).
26. A. Corma and B. W. Wojciechowski, *Catal. Rev.-Sci. Eng.,* **24,** 1 (1982).

Chapter 5. Conclusions and Future Prospects

Summery of Each Chapter

The author has investigated chemical vapor deposition (CVD) method of silicon alkoxide on several metal oxides, and has clarified the structure, formation mechanism, acidic and thermal behaviors and origin of the created functions on the obtained novel material, silica monolayer catalyst. The important results are summarized as follows.

Chapter 2 demonstrated the formation of silica monolayer with an atomic-order thickness. The characterization was carried out mainly from the view point of coverage and spreading of surface layer by means of BAT (benzaldehyde-ammonia titration) method. Acidic property was also characterized with various test reactions in order to obtain a novel model solid-acid with a well-defined structure.

Section 2 - 1 showed the generation of silica monolayer on γ-alumina until it almost completely covered the surface, and found Brønsted acidity on it. The monolayer, *i.e.* the surface layer consisted of 1 : 1 of Al-O-Si bondings, was formed from $Si(OCH_3)_4$ at 593 K with 13 nm^{-2} of concentration of silicon atoms, and showed catalytic activities for double-bond isomerization of olefin and dehydration of *tert*-butyl alcohol, but not for cracking of cumene and dehydration of ethanol. These findings showed the acid strength was weak and therefore homogeneous based upon the simple structure of proposed acidic species Al-O-Si-OH, while a conventional silica-alumina catalyst possessed a wide distribution of acid strength.

Similar observations were given on titania and zirconia as described in Section 2 - 2. The deposited silica formed a monolayer, and showed weak Brønsted acidity also on these oxides. The concentration of Si on the monolayer was shown to depend on the surface concentration of metal cation of support oxide; the Si concentration was 8, 12 and 13 Si nm^{-2} on the monolayer loaded on zirconia, titania and alumina, respectively. The acid strength of M-O-Si-OH was estimated to be M = Al > Ti > Zr > Si from the comparison of activities for isomerization of *1*-butene and dehydration of *tert*-butyl alcohol.

Section 2 - 3 exhibited an application of silica monolayer as a model acid catalyst with a simple property to an industrially important reaction, Beckmann rearrangement of cyclohexanone oxime. The activity was observed on the monolayer; this showed that Brønsted acid site catalyzed this reaction, while original active sites on support, *e.g.* Lewis acid site, causes side-reactions and deactivation. The monolayers loaded on the three oxides showed similar activities. This shows that the rearrangement is insensitive to the acid strength.

In Section 2 - 4, $Ge(OCH_3)_4$ was used in place of $Si(OCH_3)_4$, and the formation of germanium oxide monolayer and the generation of Brønsted acid site on it were confirmed. The thin layer structure was confirmed by EXAFS (extended X-ray absorption fine structure).

In summery, Chapter 2 showed that the CVD of $Si(OCH_3)_4$ and $Ge(OCH_3)_4$ formed monolayers of silicon or germanium oxide on alumina, titania and zirconia, and created weak Brønsted acid sites on them. This material is the first one as a model catalyst for mixed-oxide solid-acids with weak acid sites, whereas model compounds with strong acid sites have already been found.

In Chapter 3, the micro structure and origin of acid site were investigated.

At first, elementary steps of CVD of $Si(OCH_3)_4$ on alumina were studied in Section 3 - 1. The mechanism of growth of silica monolayer was proposed based on the gravimetry and product analysis during the CVD operation at various conditions, and computer graphics. Gaseous $Si(OCH_3)_4$ was readily reacted with alumina exposed surface, but this reaction was quickly saturated because the surface was occupied by alkoxides anchored on surface. Only at high temperature (493 - 593 K), the successive reaction to form siloxane bond (Si-O-Si) could proceed. As a result, the isolated Si species was formed at lower temperatures < 473 K, while a two-dimensional network of siloxane was developed at higher temperatures. Too high temperature caused the random deposition forming a heterogeneous structure. The Brønsted acidity seemed to generate only on the monolayer deposited at 493 - 593 K. Not only the temperature but also the co-presence of reactive gas was shown to affect the structure. Comparison among the results reported by several authors on thin silica layers deposited from silicon alkoxides were dealt with on the basis of these observations.

Section 3 - 2 related the acid property with the degree of siloxane network, using the samples with various degrees of network deposited from various silicon alkoxides $Si(OCH_3)_n(CH_3)_{4-n}$ (n = 1 - 4). The completely or relatively isolated structure was shown to be formed from $Si(OCH_3)_n(CH_3)_{4-n}$ (n = 1 - 3). The activity obviously required the network with the Si-O-Si / Si ratio higher than 1, namely a two-dimensional network.

Section 3 - 3 determined the micro structure of silica monolayer by means of NMR (nuclear magnetic resonance) of ^{29}Si. The spectrum showed $Si(OAl)_1(OSi)_3$ and $Si(OAl)_1(OSi)_2(OH)_1$ species on the silica monolayer prepared from $Si(OCH_3)_4$ at 593 K on alumina. The change of catalytic activity for isomerization of *1*-butene corresponded to the change of concentration of the latter species. Therefore, the Brønsted acid site was considered to be the $Si(OAl)_1(OSi)_2(OH)_1$ species connected with the two-dimensional network consisting of $Si(OAl)_1(OSi)_3$ species. The structures of isolated species formed from $Si(OCH_3)(CH_3)_3$ and from $Si(OCH_3)_4$ at the low temperature were also

confirmed. The monolayers on titania and zirconia had similar structures, but the difference in degree of network was shown. Since the monolayer on zirconia had low concentration of Si, the network developed in relatively low degree, probably resulting in the weak acid strength.

The structure of acid site on the silica monolayer thus became clear in Chapter 3. From the observations in this chapter, the origin of acidity was concluded to be a strained structure of two-dimensional network consisting of siloxane bonds developed on another oxide. Thus, the character of silica monolayer as a catalyst or model compound with a uniform acid strength was related with the simple structure and its formation mechanism.

Chapter 4 dealt with the thermal behavior of silica monolayer on alumina. As well as the previous reports, the deposited silica showed a high thermal stability. The observations by BAT method clarified that the ultra thin layer of silica covered the surface of calcined samples whereas the alumina exposed area was lost by sintering. This pointed out that the monolayer gave the thermal stability to the covered surface to protect the alumina particle like an egg shell. The stability was supposed to be owing to the predicted tight Al-O-Si bond and specific property of monolayer. This stabilization mechanism is considered common for vapor and liquid phase modifications of alumina with silica, and the proposal is the first one that explains the origin of stabilization of alumina by silica. The Brønsted acid site on the monolayer was once diminished during the calcination at high temperature, but readily recovered by contacting with water vapor. The silica monolayer was thus shown to be a heat-resisting acid catalyst durable at 1493 K, namely the acid catalyst with extremely high thermal stability.

General Conclusions

Silica monolayer solid-acid catalyst was prepared by chemical vapor deposition of silicon alkoxide on alumina, titania and zirconia. The silica monolayers on these three oxides have a distinct catalytic function, *i.e.* Brønsted acidity with weak and homogeneous strength based upon the simple structure. The acid strength is ordered as on alumina > titania > zirconia. Germanium oxide monolayer was also prepared. The structure of silica monolayer was clarified to consist of a two-dimensional siloxane network which contained $Si(OM)_1(OSi)_3$ species and Brønsted acidic $Si(OM)_1(OSi)_2(OH)_1$ species (M = Al, Ti or Zr). The formation of siloxane network can proceed under suitable conditions. Otherwise, isolated species or heterogeneous multiple layer is formed. Only the monolayer with the two-dimensional siloxane network showed the Brønsted acidity. The

origin of acidity is the siloxane network strained by structural unfitness with another oxide surface. Another important feature of the silica monolayer on alumina is an extremely high thermal stability compatible with the acidic property. The silica monolayer was found to be the heat-resisting acid catalyst durable at 1493 K. The mechanism for stabilization of surface by silica was also clarified; the monolayer stabilized the surface covered by it to protect the crystallite like an egg shell. Thus, the preparation, mechanism of formation, functions (acidity and thermal stability) and origin of the functions of this novel material were investigated and related with each other. An application as a model acid catalyst was also made to Beckmann rearrangement of cyclohexanone oxime to clarify the role of acid site for this complex reaction.

Future Prospects

The novel functionalized material, silica monolayer catalyst can be used as a model catalyst to understand the reaction mechanism of complex reaction, as used for Beckmann rearrangement. High selectivity and long catalyst life owing to the weak and homogeneous acid strength are expected for various reactions.

However, the most promising field to utilize this material is the environmental catalysis, which significantly interests scientists all over the world. Such acidic solids as zeolites and metals loaded on solid-acids have been reported to be active for removal of nitrogen oxide, but it quickly loses the activity under thermal or hydrothermal conditions. Conventional application of catalyst has been done under mild conditions in chemical plant. However, the lack of stability will be a fatal problem for environmental catalyst because the catalyst must be used in a high-temperature exhaust gas under humid conditions. Catalytic combustion is one more promising field of environmental catalysis to use the silica monolayer as a catalyst support. The monolayer is itself enough durable, and is expected to inhibit the sintering of loaded metal. Some positive interactions between acid site and the loaded metal are also supposed; at least, the relationship between activity and acidity must be shown by using this catalyst with a simple acidic property. The investigation for this field has been started by the present author and co-workers, and the catalyst life of palladium catalyst has been improved by using the silica monolayer as the support[1]. The silica monolayer itself is thus promising as a new heat-resisting material.

The present thesis clarified that the structure of deposited silica is controllable by procedure and conditions of CVD. In other words, a well-defined surface species can be formed homogene-

ously over the surface. The specific catalytic activity shown by Imizu and co-workers[2, 3] and Xu *et al.*[4] suggest such a uniform surface structure different from the monolayer shown by this thesis. The studies are being continued in this field.

The present study utilized the stable chemisorption of benzaldehyde to measure the coverage. Another evolution of research is considered by combination of the chemisorption of this organic material and CVD of silica. The CVD on the surface which adsorbs benzaldehyde will form a thin silica layer with the micro pores of which the size and shape were controlled by the aldehyde. This method is promising as a novel surface design to be classified as a nano-technology. Such a silica layer formed on alumina, titania and zirconia is promising as a molecular-sieving adsorbent, catalyst and catalyst support. Not only these purpose, a shape-selective sensor can be considered because both of the chemisorption of aldehyde and deposition of silica will readily proceed on tin oxide possessing a sensing function. An attempt has been made, and an adsorbent with molecular-sieving function has been obtained on tin oxide[5]. Thus, the development of CVD method will become more important to design a functionalized surface, and the present author believes that the knowledge about the mechanism of CVD shown by this thesis will contribute to evolve the CVD method.

The present thesis showed the origin of acidity on the weak Brønsted acid site generated on the silica monolayer. The monolayer can be a model of one type of acid site in binary oxide catalyst. Various other kinds of acid catalysts with uniform structures will give a general rule for generation of acidity on interface between two oxide. For this purpose, CVD methods to load various elements on various supports are promising. The progress in this field will make it enable to research on the mechanism of generation of acidity, and in addition, basicity or some other catalytic properties.

Thus, the silica monolayer catalyst and the CVD method can be applied to various fields in functionalized material as well as catalysis chemistry. For these purposes, some unknown phenomena should be clarified. Especially, determining the concentration of surface hydroxides will directly clarify the micro structure of monolayer and Brønsted acid site on it. Exact determination of acid amount and strength also must be important. However, it is difficult even for strong acid catalyst, and such a facial acidity as that of silica monolayer often amazes the analysis. The recent progress to measure the acidic property, *e.g.* theoretical analysis of TPD[6], will make it clear. A general understanding about the generation of acidity also will be given from this information. Further research on these details will contribute to the development of design of functionalized surface, and will make new applications of the CVD method and the materials prepared by it.

References

1. K. Muto, N. Katada and M. Niwa, *Appl. Catal., B: Environmental,* in press.
2. Y. Imizu, A. Tada and I. Toyoshima, *Shokubai (Catalyst),* **30,** 388 (1988).
3. N. Okazaki, T. Kohno, R. Inoue, Y. Imizu and A. Tada, *Chem. Lett.,* **1993,** 1195.
4. B.-Q. Xu, T. Yamaguchi and K. Tanabe, *Chem. Lett.,* **1989,** 149.
5. N. Kodakari, N. Katada and M. Niwa, *J. Chem. Soc., Chem. Commun.,* **1995,** 623.
6. M. Niwa, N. Katada, M. Sawa and Y. Murakami, *J. Phys. Chem.,* **99,** 8812 (1995).

List of Publications

Location in this thesis

1. **A Silica Monolayer on Alumina and Evidence of Lack of Acidity of Silanol Attached to Alumina** — Section 2 - 1
   Miki Niwa, Takashi Hibino, Haruhiko Murata, Naonobu Katada and Yuichi Murakami
   J. Chem. Soc., Chem. Commun., **1989,** 289

2. **Thin Silica Layer on Alumina: Evidence of the Acidity in the Monolayer** — Section 2 - 1
   Miki Niwa, Naonobu Katada and Yuichi Murakami
   J. Phys. Chem., **94,** 6441 (1990)

3. **Generation of Acid Sites by SiO_2 Deposition on Groups IVB Metal Oxides** — Section 2 - 2
   Miki Niwa, Naonobu Katada and Yuichi Murakami
   J. Catal., **134,** 340 (1992)

4. **Mechanism of Growth of Silica Monolayer and Generation of Acidity by Chemical Vapor Deposition of Tetramethoxysilane on Alumina** — Section 3 - 1, Section 3 - 3
   Naonobu Katada, Takuya Toyama and Miki Niwa
   J. Phys. Chem., **98,** 7647 (1994)

5. **Vapor-Phase Beckmann Rearrangement over Silica Monolayers prepared by Chemical Vapor Deposition** — Section 2 - 3
   Naonobu Katada, Takahiro Tsubouchi, Miki Niwa and Yuichi Murakami
   Appl. Catal. A: General, **124,** 1 (1995)

6. **Generation of Acidity on Silica Monolayer by Network of Si-O-Si on Alumina** — Section 3 - 2, Section 3 - 3
   Naonobu Katada, Takuya Toyama, Miki Niwa, Takahiro Tsubouchi and Yuichi Murakami
   Res. Chem. Intermed., **9,** 137 (1995)

7. **Germanium Oxide Mono-Atomic Layer prepared by Chemical Vapor Deposition Method on γ-Alumina: the Structure and Acidic Property** — Section 2 - 4
   Naonobu Katada, Miki Niwa and Mitsuru Sano
   Catal. Lett., **32,** 131 (1995)

8. **A Heat-Resisting Acid Catalyst: Thermal Stability and Acidity of a Thin Silica Layer on Alumina calcined at 1493 K** — Chapter 4
   Naonobu Katada, Hideaki Ishiguro, Koh-ichi Muto and Miki Niwa
   Adv. Mater., CVD, **1,** 54 (1995)

Other Publications

Acidic Property of Silica Monolayers on Metal Oxides prepared by CVD Method

Naonobu Katada, Miki Niwa and Yuichi Murakami

in *Study in Surface Science and Catalysis Vol. 90: Acid-Base Catalysis II,* eds. H. Hattori, M. Misono and Y. Ono, Kodansha, Tokyo (1994) p. 333

Molecular Sieving Silica Overlayer on Tin Oxide prepared using an Organic Template

Nobuaki Kodakari, Naonobu Katada and Miki Niwa

J. Chem. Soc., Chem. Commun., **1995,** 623

Temperature-Programmed Desorption of Ammonia with Readsorption Based on the Derived Theoretical Equation

Miki Niwa, Naonobu Katada, Masahiko Sawa and Yuichi Murakami

J. Phys. Chem., **99,** 8812 (1995)

Complete Oxidation of Methane on Supported Palladium Catalyst: Support Effect

Koh-ichi Muto, Naonobu Katada and Miki Niwa

Appl. Catal., B: Environmental, in press.